REMOTE SENSING OF ST. AUGUSTINE DECLINE (SAD) DISEASE

By

William Claude Odle
Robert W. Toler
James C. Harlan

August 1976

Supported by
National Aeronautics and Space Administration
Grant NGL 44-001-001

TEXAS A&M UNIVERSITY
REMOTE SENSING CENTER
COLLEGE STATION, TEXAS

Technical Report RSC-

REMOTE SENSING OF ST. AUGUSTINE DECLINE (SAD) DISEASE

by

William Claude Odle

August 1976

Supported by

National Aeronautics and Space Administration

Grant NGL 44-001-001

ABSTRACT

Remote Sensing of St. Augustine Decline (SAD) Disease.

Laboratory and field spectral reflectance measurements of healthy and SAD-infected St. Augustine grass were made using several different instruments. Spectral differences between healthy and infected grass occurred in the visible (0.38 - 0.70 μm) and near infrared (0.70 - 1.30 μm) regions.

Multiband and color infrared photographs were taken of healthy and diseased turf from ground-based platforms and low altitude aircraft. Qualitative (density slicing) and quantitative (transmission densitometry) analyses revealed distinct tonal differences between healthy and SAD-infected grass.

Similar experiments were done to determine if healthy and diseased grass could be distinguished from water-stressed grass and grass deficient in either nitrogen or iron.

Using spectral reflectance measurements and photographic techniques, healthy grass could be distinguished

from SAD-infected, nutrient-deficient and water-stressed grass. However, these techniques were not adequate to distinguish the various stress factors from one another.

Outdoor reflectance measurements in four broad spectral bands were made from container-grown plants using an ERTS-band radiometer. A computerized, pattern recognition analysis, known as transformed divergence, was carried out using reflectance data from various two-band combinations to determine the ability to discriminate among different treatments. Results showed a discriminability of over 90% for healthy and diseased grass. Unlike photographic techniques, this analysis also indicated a high percent discrimination for non-infected and infected grass in the presence of nutritional deficiencies and water stress.

Using a portable infrared thermometer, temperature differences in the range of 0.5 - 1.5°C were shown to exist among some of the fully watered treatments. Large temperature differences occurred between fully watered and water-stressed treatments.

ACKNOWLEDGEMENTS

First of all, I would like to express my sincere gratitude to Dr. Robert W. Toler who has served as a continuous source of encouragement, advice and friendship.

I would also like to express my deepest thanks to Dr. J. C. Harlan of the Texas A&M Remote Sensing Center for his personal, as well as professional, interest in this research. On numerous occasions, Dr. Harlan contributed valuable suggestions and assistance.

I also appreciate the help and encouragement provided by Drs. R. S. Halliwell, W. R. Jordan and R. H. Haas, during this research and manuscript preparation.

This study was made possible through National Aeronautics and Space Administration Grant NGL 44-001-001. I am grateful to the many people at the National Aeronautics and Space Administration/Johnson Space Center and the Texas A&M Remote Sensing Center who contributed their time and effort in data acquisition and analysis during this research.

TABLE OF CONTENTS

LIST OF FIGURES

LIST OF TABLES

INTRODUCTION

Although the process of remote sensing often involves sophisticated techniques and instrumentation, it can ultimately be reduced to a few basic concepts. Remote sensing can simply be defined as the recording and interpretation of information about an object by a distant sensor. An illustration from Hoffer and Johannsen (39) showing the major subdivisions of the electromagnetic spectrum utilized for remote sensing purposes is presented in Fig. 1. This wide array of sensing capabilities, coupled with appropriate data analysis techniques, makes possible the monitoring of many agricultural crop problems, including plant diseases.

Plant diseases constitute a serious limiting factor in the production of agricultural and ornamental crops amounting to an annual average loss of near $3.7 billion for major U.S. crops during the period 1951-60 (77). Due to tremendous increases in crop values, current losses would probably be substantially higher. Disease-related losses for field

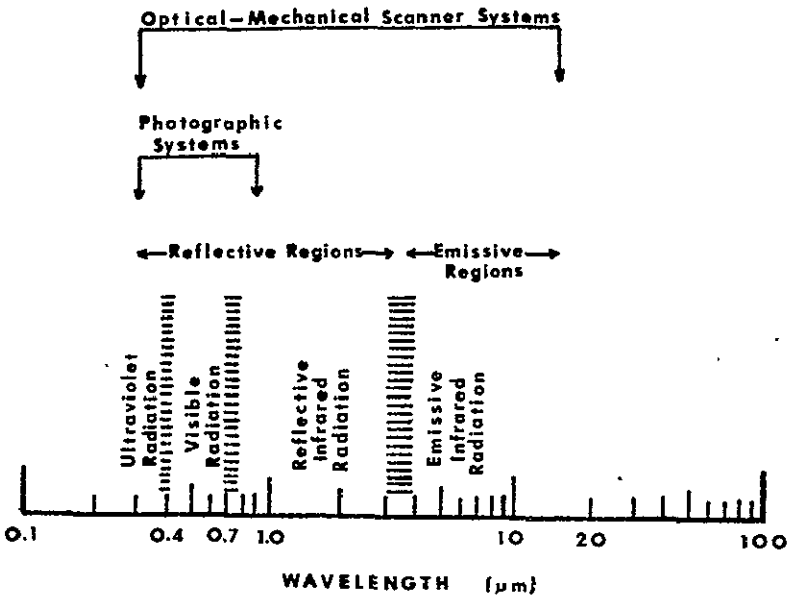

Fig. 1. Regions of the electromagnetic spectrum used for remote sensing. (From Hoffer and Johannsen, 1969)

crops (cotton, grain sorghum, peanuts, etc.) in Texas alone were estimated at over $104 million in 1969 (66). Rapid, efficient, and economical methods of disease monitoring would aid control programs and be valuable in efforts to meet the world's demand for food, fiber, oil, and ornamental crops.

Previous research on remote sensing of plant diseases has largely centered on diseases caused by fungi. Substantially less information exists on the remote sensing of plant virus diseases. St. Augustine Decline (SAD), a virus disease of St. Augustine grass (Stenotaphrum secundatum (Walt.) Kunze), was selected for a remote sensing study of plant virus diseases for several reasons.

First of all, SAD is an economically important disease in Texas. In 1964 turf and lawn maintenance costs were estimated to be about $212 million (40). St. Augustine grass constitutes 56% of the lawns in Texas and 96% within the Gulf coast area of the state (53). The disease was first found in the Rio Grande Valley of Texas in 1966, and has since spread throughout the Gulf coast area of the state and into Louisiana and Mexico. In 1971, only five years after its dis-

covery, SAD-related losses within the Corpus Christi area alone were estimated at $18 million (42).

Certain characteristics of the SAD host-pathogen combination were advantageous for a study of this type. St. Augustine grass is genetically stable and produces a perennial turf which can be vegetatively propagated. The virus, which is the St. Augustine Decline strain of Panicum Mosaic Virus (50), is mechanically transmissable, has a 3-4 week incubation period, and produces a typical mosaic symptom (53). Various degrees of the foliar symptom are shown in Fig. 2.

As its name implies, the disease causes a gradual decline of infected grass. The weakened grass results in an unthrifty turf which is sensitive to stresses such as nutritional deficiencies, drought, insects, and other diseases. Thinning of the St. Augustine truf allows invasion by weeds and other grasses such as Bermuda grass. Fig. 3 shows the severe yellowing present in a heavily infected St. Augustine lawn.

The Texas Department of Agriculture currently maintains a quarantine program for SAD which includes an annual ground survey of all commercial grass farms

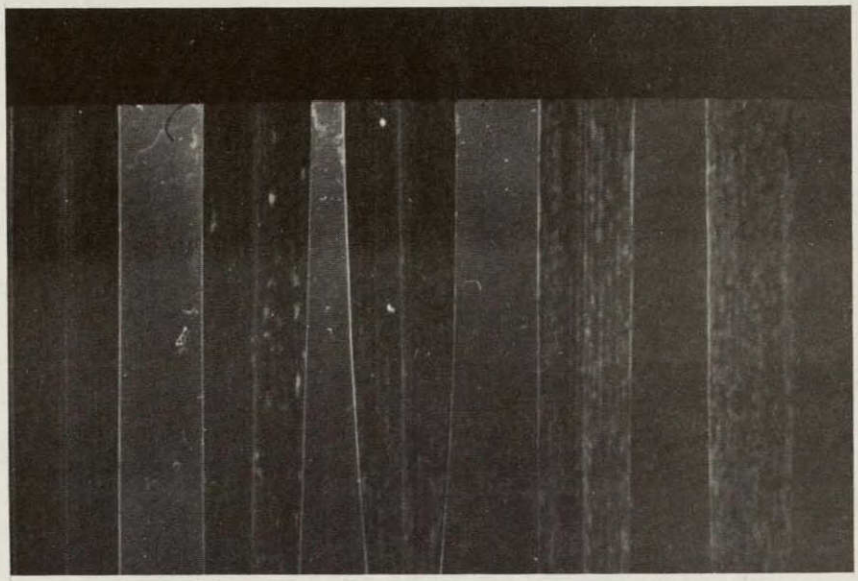

Fig. 2. Progressive symptoms of St. Augustine Decline from a healthy leaf (left) to a severely diseased leaf (right).

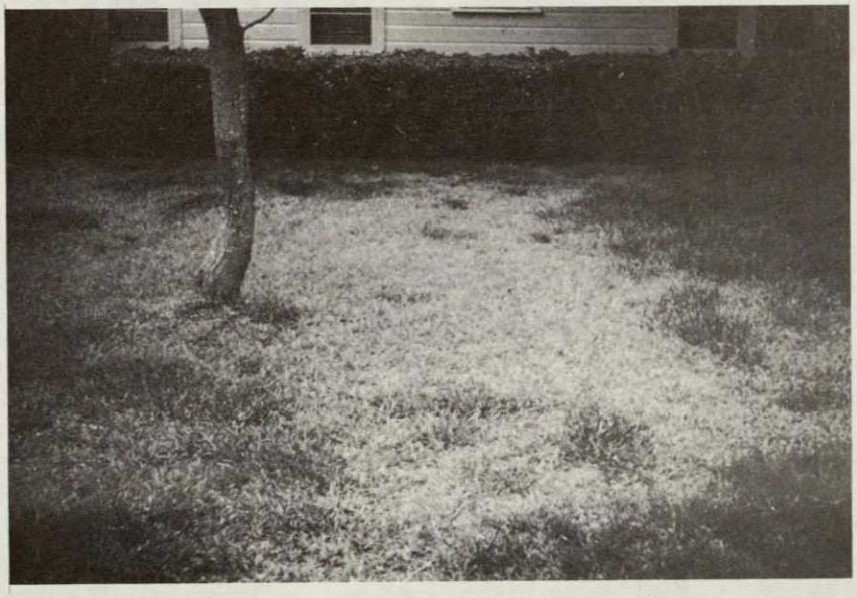

Fig. 3. Severe yellowing of St. Augustine grass turf caused by St. Augustine Decline.

in the state. If SAD could be adequately detected using remote sensing techniques, more frequent, efficient, and rapid surveys would be possible. A study of this type also has potential value for developing techniques applicable to other remote sensing problems in plant pathology and related areas.

The specific objectives of this study included the following:

1. Determine reflectance properties of healthy St. Augustine grass and St. Augustine grass infected with the SAD strain of Panicum Mosaic Virus.
2. Determine the effectiveness of selected photographic films and filters for SAD detection in ground-based experiments.
3. Investigate effects of selected nutritional deficiencies and water stress on reflectance characteristics of St. Augustine grass.
4. Attempt to determine the effectiveness of selected films and filters for aerial detection of SAD-infected grass from various altitudes.

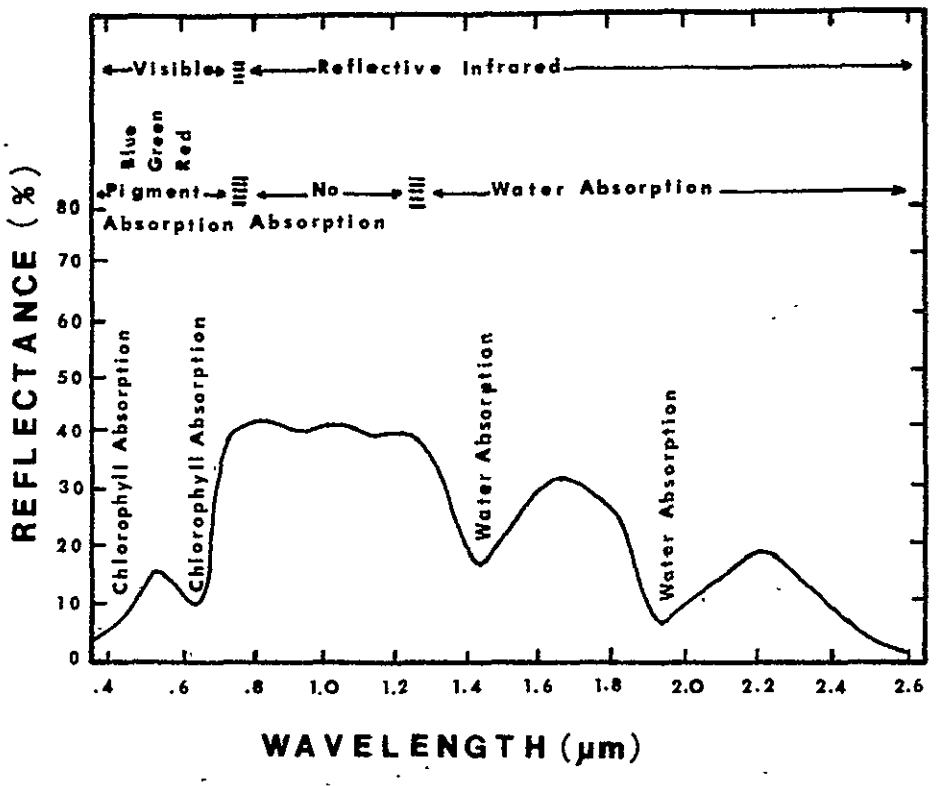

Fig. 4. Reflectance properties of a typical green leaf. (From Hoffer and Johannsen, 1969)

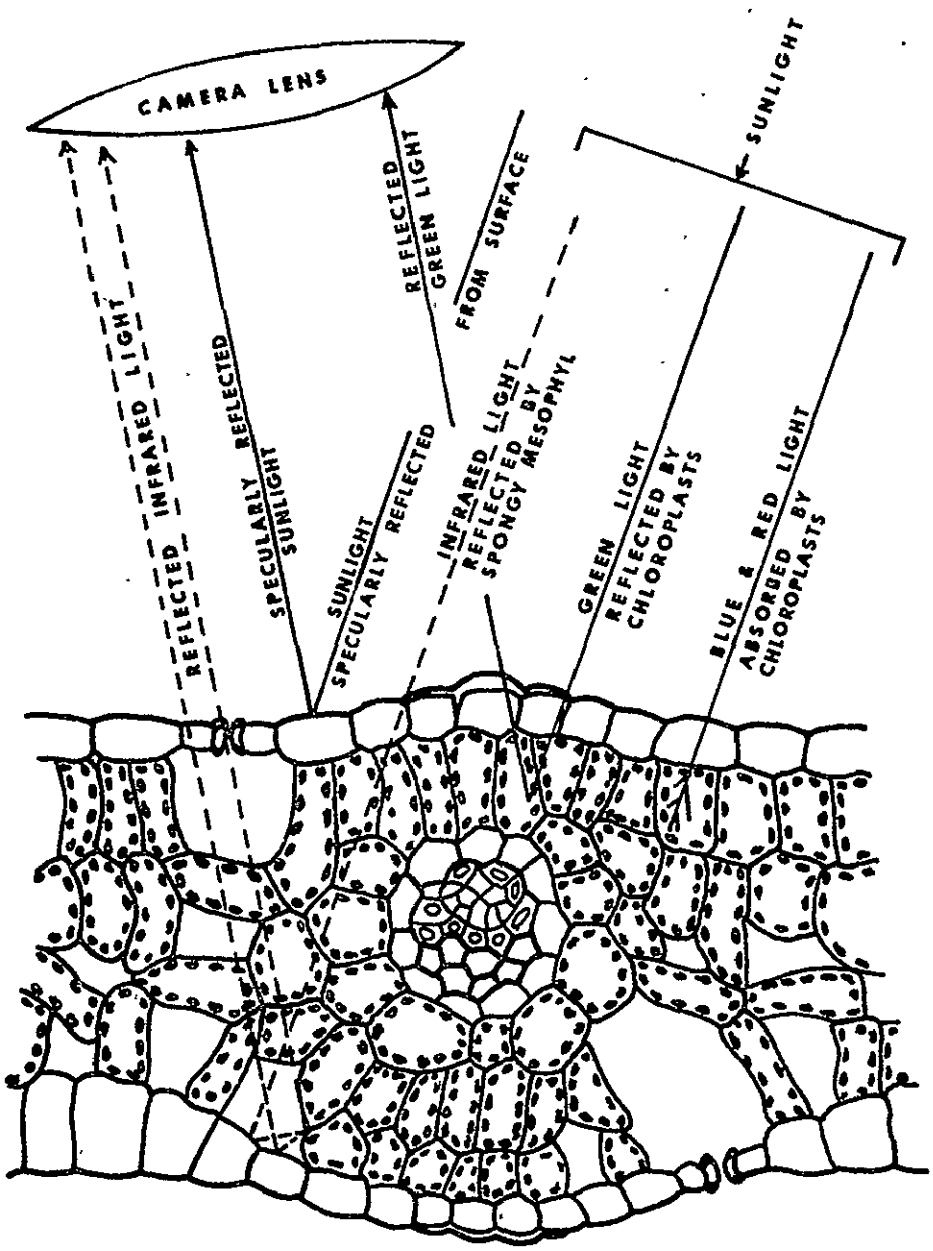

Fig. 5. Light interaction with various leaf components. (From Colwell, 1956)

Some of the radiation striking a leaf is specularly reflected from the surface, while the remainder penetrates the cutical and epidermis (32). Visible wavelengths are reflected and transmitted (green) or absorbed (red and blue) by the plant pigments. Near infrared energy is diffused and scattered primarily by its interaction with cell wall-air space interfaces within the palisade and spongy mesophyll tissues (29, 31, 49, 54, 68). Some of the radiation is scattered upward (reflected), while some is scattered downward (transmitted). This refractive scattering of near infrared energy is the result of refractive index differences between hydrated cell walls and adjacent free air spaces. Therefore, the number of cell wall-air interfaces has more influence than the total amount of free air space present in the leaf (3, 33, 68).

Optical properties of individual leaves roughly correspond with those of plant canopies. However, factors such as plant geometry, soil reflectance, and attenuation of certain wavelengths by various atmospheric conditions produce some differences between laboratory and field reflectance patterns (57). Several mathematical models have been developed to account

for canopy reflectance and transmittance (5, 2, 25, 44, 58, 63). Allen and Richardson (4) found that canopy reflectance of cotton (Gossypium hirsutum L.) is a function of total leaf area, an absorption coefficient, a scattering coefficient, and background reflectance. The coefficients are related to crop geometry and to optical properties of individual leaves. Spectrophotometric studies have shown that the ratio of infrared to visible reflectance for vegetation canopies is about double that for individual leaves. Howard (44) found that stacks of up to eight Eucalyptus leaves had a visible reflectance value similar to that of a single leaf. Infrared reflectance, however, increased from 50% for one leaf up to 80% for an eight-leaf stack. Similar results have been reported for cotton leaves (59).

Another interesting aspect involved in the optical properties of plants concerns polarization characteristics. Some of the incident radiation striking a leaf is specularly reflected from the surface and is seen as "glare". The majority of this radiation is polarized in a plane parallel to the principle plane (source, target, sensor plane) (H. Soule', personal communication). A polarizing filter can screen out much of this "noise", which contains very little useful in-

formation. Use of this technique insures that most of the radiation entering the sensor will consist of radiation diffusely reflected from the interior leaf structure. Radiation reflected from the interior is largely polarized in a plane perpendicular to the principle plane, and it contains most of the important information concerning the leaf's internal characteristics (H. Soule', personal communication).

Coulson and his co-workers (21, 22) have determined polarization characteristics of many types of natural surfaces (sand, soil, water, vegetation, etc.) under laboratory and field conditions. For green grass turf, measurements were made to determine the effects of illumination angle, look angle, and wavelength on the degree of polarization of incident radiation. At a wavelength of 0.492 μm, the degree of polarization increased from a negative value at a nadir illumination angle of 0° (directly overhead) to over 40% as the nadir illumination angle increased to 78.5°. With the illumination angle fixed at 53.1°, maximum polarization for wavelengths of 0.492 μm and 0.643 μm occurred at about 35° from nadir. At a look angle of 0°, these wavelengths exhibited about 10% polarization.

Similar measurements have shown that very little polarization occurs in the near infrared wavelengths. Wavelengths which are strongly absorbed by the leaves (blue and red) are reflected with the highest degree of polarization. Polarization of those wavelengths selectively absorbed by the plant pigments may be due to alignment of chloroplasts or to some characteristics of highly absorbing dielectrics such as plant leaves (22, 30).

It is apparent that polarization characteristics, in addition to spectral reflectance measurements, could be useful in gaining information about remotely sensed objects. Since diseases have profound effects upon the physical and physiological conditions of plants, they may also alter polarization characteristics enough to allow discrimination between healthy and diseased plants using remote sensing techniques.

Although no previous investigations have been done to determine the effects of plant diseases on polarization characteristics, it is well-known that diseases cause significant alterations in normal optical properties of plants. Reflectance characteristics of individual leaves may vary with changes in cell arrangement, cell morphology and cell contents.

Studies of plant canopies indicate that reduction of near infrared reflectance can result from changes in leaf area (76), leaf density (76), and leaf orientation (49), as well as changes in optical properties of individual leaves. An increase in visible reflectance, usually associated with reduction in chlorophyll content, often results from plant diseases, but changes in near infrared reflectance are more variable. For this reason, detection of changes in visible reflectance is sometimes more beneficial than detection of changes in infrared reflectance.

Taubenhaus, Ezekiel and Neblette (72) were among the first to utilize aerial photography for surveying plant disease damages. Using black and white panchromatic film and a light yellow filter from an altitude of 75-150 m, they recorded and assessed cotton root rot damage caused by Phymatotrichum omnivorum (Shear) Dug.

Not until 1956 did Colwell publish the first major study concerning remote sensing of plant diseases (19). He theorized that for any particular film/filter combination, the photographic tone or color of an object can be predicted provided the following are known: 1. spectral reflectance of the object

being photographed, 2. spectral sensitivity of the film, 3. spectral scattering by atmospheric haze, and 4. spectral transmission of the filter.

Spectrophotometric analysis of detached leaves showed that wheat (Triticum aestivum L.) infected with Puccinia Graminis Pers. reflected less red and near infrared radiation than did healthy wheat. Similar findings were reported for rusted wheat and rye (Secale cereale L.) by Keegan, Schleter, and Hall (47). Colwell was able to differentiate healthy and rusted wheat and oats (Avena sativa L.) on black and white infrared film at a much earlier stage than with panchromatic or color films.

During the twenty years since Colwell's basic investigations, remote sensing capabilities have been developed for diseases on a variety of agricultural crops. Brenchley and Dadd (13) used black and white aerial infrared photography to detect late blight (Phytophthora infestans (Mont.) d By.) of potato (Solanum tuberosum L.) and subsequently revealed some interesting aspects of disease initiation and spread over the course of a growing season. They were also able to detect halo blight (Pseudomonas phaseolicola (Burkh,) Dows) of bean (Phaseolus

vulgaris L.) using infrared photography. With close-up photography in the laboratory, Jackson (46) readily detected foliar symptoms of two bacterial pathogens, Xanthamonas phaseoli (E. F. Sm.) Dows and Pseudomonas glycinea Coerper, on soybean (Glycine max (L.) Merr.) leaves using black and white infrared film. Black and white panchromatic film did not detect early symptoms. Manzer and Cooper (51) reported previsual detection of potato late blight on infrared film. They were also able to correlate disease ratings from ground surveys with film densities measured by a densitometer.

Color infrared film has proven to be a valuable tool for disease detection in several important field crops. Cercospora leaf spot of sugar beets (Beta vulgaris L.) was found by Meyer and Calpouzos (55) to produce a distinct tonal signature on color infrared transparencies. Monitoring of disease development in this manner enabled more timely fungicide applications. Jackson and Wallen (45) recently reported that late stages of bacterial blight on field beans could be detected on color infrared film using microdensitometry.

Because of its important economic impact in 1970, southern corn leaf blight (Helminthosporium maydis, Nisik. and Miyake) has been the subject of extensive remote sensing efforts (7, 10, 18, 62). Coffman (18) reported that various levels of blight severity could be distinguished on color infrared aerial photographs as a progressive loss of near infrared reflectance. Safir and his colleagues (62), on the other hand, determined that blighted leaves exhibit an increased near infrared reflectance compared to healthy leaves. Their spectrophotometric measurements of individual corn leaves indicated that blighted leaves first exhibit an increased reflectance in the chlorophyll absorption regions of the spectrum. These first changes occurred about 40 hours after inoculation, when the lesions became visible. At a later stage, an increased reflectance was noted in the water absorption regions (1.45 and 1.95 μm). Factors such as reductions in leaf density and area and leaf reorientation due to wilting may combine to lower canopy reflectance and increase soil reflectance. These factors were mentioned by Safir and his colleagues as possible explanations for the discrepancy between their report and that of Coffman con-

cerning blight-induced changes in near infrared reflectance.

Efforts have also been made to remotely sense diseases of several orchard crops. Brodrick and his co-workers (14) used multispectral photographic techniques to detect and rate avocado trees (Persea americana Mill.) suffering from root rot (Phytophthora cinnamoni Rands.). Disease signatures were initially established using field spectroradiometers. Selected spectral filters were then used on a four-lens multispectral camera to photograph orchards from an altitude of 1500 meters. Analysis of the film with color enhancement techniques enabled identification of 100% of the trees shown to be diseased by ground truth surveys. Color infrared film demonstrated an 80% accuracy, while conventional color film was very ineffective.

A similar disease, citrus footrot (Photophthora parasitica Dast.), was reported by Gausman and his colleagues (34) to exhibit a very distinct tonal signature on color infrared film. Spectrophotometric analysis revealed that infected plants reflected significantly more green and red light, and to a lesser extent more blue light.

Edwards and his co-workers (26, 27) have tested the effectiveness of remote sensing techniques to detect another citrus disease, Young Tree Decline. At present, the cause of the decline has still not been determined. Using a portable infrared thermometer, temperature measurements of healthy and diseased tree canopies were made 9 times over a 24-hour period. No differences were detected between healthy trees and trees in early or moderate stages of decline. Maximum differences (1.3°C) between healthy and severely declined trees occurred around 1:30-3:00 p.m. Aerial photography using color infrared film was also only effective in identifying severely declined trees. The investigators stated that these two remote sensing techniques were no more reliable than ground surveys. Another study was done using an aerial 24-channel spectral analyzer (28). This instrument records quantitative reflectance data in narrow bands over a range of 0.34-13 μm. Reflectance data in the 0.82-0.88 μm band, which was collected from an altitude of 458 m and analyzed by a computer, gave an overall accuracy of 89% for differentiation of trees in various stages of decline.

As previously mentioned, only a relatively small amount of research on remote sensing of plant virus diseases has been reported. Several laboratory investigations have demonstrated the superiority of infrared films for detection of virus symptoms on individual leaves. In one of the earlier studies, Bawden (11) found that black and white infrared film was more effective than conventional panchromatic film for detection of Tobacco Necrosis Virus symptoms on potato leaves. However, he found the reverse to be true for detection of the virus in tobacco leaves (Nicotiana tobacum L.). More recent investigations using Tobacco Ringspot Virus (15) and Watermelon Mosaic Virus (17) have shown that symptoms caused by these pathogens can be detected better, and at an earlier stage, with color infrared than with conventional color film or visual observation.

In his classic report of 1956, Colwell mentioned that wheat infected with Yellow Dwarf Virus produced a tonal signature on black and white infrared film similar to that produced by rusted wheat (19). Since that time, only a few reports dealing with aerial detection of virus diseases have been published.

Hill and his co-workers (37) used low altitude color infrared photography to detect Tobacco Ringspot Virus on soybeans. This disease causes the plants to become dwarfed and retain their foliage longer than mature, healthy plants. Because of this unique situation whereby mature, healthy plants become defoliated and diseased plants remain green, aerial detection was readily attained. Study of photographs revealed that disease severity was highest in field areas nearest to native vegetation. Spread of the disease in the direction of prevailing winds suggested the possibility of a wind-borne vector.

Remote sensing of Maize Dwarf Mosaic Virus on corn (Zea mays L.) has been studied by Ausmus and Hilty (7). Spectrophotometric measurements revealed that healthy and infected leaves exhibited no significant reflectance differences in visible wavelengths. However, infected leaves with various degrees of symptoms exhibited a significantly lower near infrared reflectance than healthy leaves. Ausmus and Hilty (8) also used scanning microdensitometry to analyze color infrared aerial photographs of corn infected with this same virus. Percentages of each disease rating were determined within the area scanned. Although advanced

disease stages were detected with conventional panchromatic and color films, early stages could only be detected by color infrared film.

The primary symptom of SAD, like most virus diseases, is a chlorotic mottling of the host plants's leaves. However, other problems which also produce leaf yellowing commonly occur in field situations. Nutritional deficiencies can result in various patterns of chlorosis and discoloration which are visible because of alterations in the plant's normal optical properties. One of the earliest mentions of deficiency detection with aerial photography was by West (78), who found that potassium-deficient strawberry plants (Fragaria chiloensis Duchesne) could be differentiated from healthy plants using conventional color film and a deep blue filter.

Several investigators have examined the effects of nitrogen (N) deficiency on reflectance properties of plants. McClellan, Meiners, and Orr (52) reported increased infrared reflectance for wheat grown under low fertilization. Thomas and his co-workers (74), however, found that N-deficient cotton exhibited a reduced near infrared reflectance. Both studies reported a high visible reflectance, probably re-

sulting from reduced chlorophyll content. Myers (57) observed that N-deficient sweet pepper leaves (Capsicum frutescens L.) had an increased water content and an increased thickness, which accounted for a higher near infrared reflectance. Thomas and Oerther (73) reported that spectrophotometric reflectance measurements could be used to estimate the nitrogen status of sweet peppers. They found an increased reflectance from N-deficient sweet peppers in the 0.7-1.3 μm range and a decreased reflectance in the 1.3-2.5 μm range. They suggested that the increased reflectance could have been due to an increase in the number of intercellular air spaces, while decreased reflectance may have resulted from higher water content. Increased reflectance in the visible region around 0.55 μm was due to the reduction of chlorophyll and carotenoids.

Gausman, Cardenas, and Gerbermann (35) have carried out an investigation concerning photographic detection of iron-deficient sorghum (Sorghum bicolor (L.) Moench). They were able to correlate chlorophyll concentration to density readings from aerial color infrared photographs. Deficient leaves were thinner, contained 6-10 times less chlorophyll, and had fewer

intercellular spaces than healthy leaves. Spectrophotometric analysis showed that deficient leaves reflected 10% more energy at 0.55 μm and 8% less energy at 1.0 μm.

Gausman, Escobar, and Rodriguez (36) carried out reflectance studies on several nutritional deficiencies of squash (Cucurbita pepo (L.) Alef. var. melopepo). They were able to distinguish potassium-, iron-, and magnesium-deficient leaves from healthy, phosphorous-, and sulfur-deficient leaves in the 0.55-0.65 μm range. Magnesium and iron deficiencies exhibited different reflectance values in the 0.65-0.75 μm range (chlorophyll absorption band). Nitrogen deficiency had a unique reflectance pattern in the 0.75-0.9 μm range (near infrared).

Al-Abbas and his colleagues (1) conducted similar investigations with deficiencies in corn. Reflectance, transmittance, and absorption spectra were determined for normal leaves and leaves deficient in nitrogen, phosphorous, potassium, sulfur, magnesium, and calcium. Chlorophyll content was reduced by all deficiency treatments. An increased moisture content was observed in sulfur-, magnesium-, and nitrogen-deficient leaves, and percent moisture was positively correlated with

percent absorption at 1.45 and 1.93 μm. Phosphorous and calcium deficiencies caused less absorption in the near infrared when compared to healthy controls. In contrast, sulfur-, magnesium-, potassium-, and nitrogen-deficient leaves absorbed more than normal at these wavelengths.

A plant's optical properties can also be significantly influenced by soil-water stress, another problem which is commonly encountered. It is generally agreed that temporary soil-water stress causes an increased visible reflectance; however, there is some confusion concerning infrared reflectance. Some investigations have indicated a decreased near infrared reflectance (20, 57), while some have shown little or no change (4, 68). The majority of such studies, however, have revealed that near infrared reflectance increases with increased water stress (23, 52, 59, 74).

Early stages of soil-water stress manifests itself as a wilting symptom. This reorientation of the leaves may alter certain reflectance properties of the canopy. Severe stress results in additional loss of turgor and the ultimate collapse of leaf mesophyll tissues. This may reduce the number of reflective

cell wall-air interfaces and cause a reduction in near infrared reflectance (19). On the other hand, such mesophyll changes may cause the reflective surfaces to become reoriented in a way which causes increased reflectance. Cell protoplasts may also plasmolyze and draw away from the cell walls, creating additional reflective surfaces (49). Thomas and his colleagues (74) suggested that concentration of cell solutes and subcellular particles may also contribute to changes in reflectance.

Reduced water content directly affects reflectance in the infrared water absorption bands and may also result in chemical changes which alter reflectance in other regions. Increased transmission and reflectance of water-stressed cotton may be attributed to a decreased absorption by certain leaf compounds other than water (74). Myers (57), working with individual cotton leaves, reported an increased reflectance and decreased transmission over a range of 0.75-1.3 μm. However, he also stated that physiological changes resulted in reduced near infrared reflectance from the plant canopy. Smaller changes occurred in the visible region, possibly due to changes involving chlorophyll. Addition of water to

the soil restored original reflectance values in the visible region but not in the infrared regions. An increased visible reflectance (0.5-0.6 μm) from water-stressed oaks was also reported by Dadykin and Bedenko (23).

Thomas and his co-workers have also explored effects of soil-water stress on cotton (74, 75). Reflectance and transmission measurements were made over a 24-hour period as individual leaves dried from a fully turgid condition. Reflectance generally increased over a range of 0.4-2.5 μm as relative leaf turgidity decreased. Relative turgidity was defined as the field moisture content of plants expressed as a percentage of their turgid water content. Extensive reflectance changes did not occur until leaves had reached 70% relative turgidity and were visibly wilted. Smallest effects were detected in the visible region, while the greatest change occurred at the 1.45 μm water absorption band. Original reflectance values returned as leaf turgidity was restored. Absolute water content influenced reflectance more than relative leaf turgidity. A 10% increase in water content decreased reflectance values by 5.2, 4.5, 1.9, and 4.5% at 1.45, 1.75,

1.93, and 2.2 μm, respectively. Photographic studies revealed that soil-water stress significantly affected the densities of black and white and color infrared films.

Reflectance of wheat grown under different irrigation regimes has been investigated by Stanhill and his colleagues (69). From field radiometric measurements, they found that visible and infrared reflectance (0.28-2.8 μm) increased as soil-water stress increased. Similar changes were also apparent in reflectance data taken from individual leaves with a laboratory spectrophotometer.

Soil-water stress has also been remotely detected using various types of thermal sensors. Bartholic and his co-workers (9) reported that cotton affected by various levels of stress could be detected from an altitude of 600 meters using a thermal scanner. Ground truth information was obtained with a portable infrared thermometer and an infrared camera. Canopy temperatures were also determined using an array of thermocouples, and the levels of water stress were assessed from pressure bomb measurements and percent moisture content of leaves. At midday, fully watered plots exhibited a temperature of about 30°C, a leaf

water potential of -14 bars, and a water content of 80%. The driest plots had a temperature of 37°C, a water potential of -19 to -24 bars, and a water content of 72 to 66%. Results indicated that an aerial thermal scanner could be used to determine relative plant-water stress, and therefore could be used as an aid in irrigation management. Investigations using various types of plants and techniques have shown that leaf temperatures are dependent upon a wide array of factors including solar energy influx, convective cooling from air movement, plant respiration, and water stress (71, 79).

MATERIALS AND METHODS

Spectral and Tonal Signatures of Healthy and SAD-infected St. Augustine Grass

Initial studies consisted of spectrophotometric reflectance measurements of healthy and SAD-infected plants. Plants used for this study were grown under controlled greenhouse conditions at Texas A&M University. Sod pieces (8 cm^2) of healthy St. Augustine grass were placed in one-quart (0.946 ℓ), plastic pots containing a mixture of peat moss and perlite. Plants were watered daily and given complete Hoagland and Arnon's nutrient solution (38) once a week. Over a period of two months, four different plants were inoculated with SAD Virus every fourth day in order to obtain plants in various stages of disease development. Inoculum was prepared by macerating infected tissue using a mortar and pestle and 0.01 M potassium phosphate buffer (pH 7.4). Plants were dusted with 500 mesh carborundum prior to inoculation to insure adequate abrasive action as the inoculum was rubbed onto the leaves by hand. Eight plants were inoculated with buffer solution and maintained as healthy controls. All plants were arranged

randomly on the greenhouse bench, and all received identical treatment concerning watering, nutritional supplements, and trimming.

The plants were transported to the National Aeronautics and Space Administration/Johnson Space Center (NASA/JSC) in Houston, Texas where a Cary 14 RI spectrophotometer (Fig. 6) was used to make laboratory reflectance measurements. Using a tungsten light source and a magnesium oxide standard, diffuse spectral reflectance was recorded over a range of 0.35-0.9 μm for healthy and diseased excised leaves. Various leaf orientations were used in the spectrophotometer's sample cup in an effort to determine any sensitivity to sample configuration.

Polarization spectral reflectance of the samples was also determined using a modified Cary 14 RI spectrophotometer with a Cary model 50-400-000 gonioreflectometer. This gonioreflectometer employs a 25 cm diameter integrating sphere with a tiltable sample holder in the center of the sphere. The sphere is illuminated with light from a quartz-iodine lamp. Polarization spectra of healthy and diseased grass were measured and recorded on punched paper tape using a Datex model CV-702-0 data logger. This tape

Fig. 6. Cary 14 RI spectrophotometer used to make laboratory reflectance measurements from detached St. Augustine grass leaves.

was analyzed by an XDS Sigma 7 computer to give average reflectance and percent polarization. Polarization values from +100 percent to -100 percent were plotted by an X-Y recorder.

On the basis of these laboratory reflectance measurements, several film/filter combinations were selected for photographic studies. Wratten filters 25 (red), 47 (blue), and 58 (green) were used in combination with polarizing filters and plus-X type black and white panchromatic film to take indoor and outdoor multiband photographs. The red, blue, and green filters transmitted wavelengths in the following spectral bands: above 0.58 μm, 0.38-0.48 μm, and 480-600 μm, respectively. Multiband photographs were taken without use of polarizing filters, and they were also taken using polarizers at minimum and maximum polarization settings. Minimum and maximum polarization settings were determined by viewing a specularly reflecting object through the filter as it was rotated. The position at which the least glare appeared was designated as maximum polarization; and likewise, the position in which the most glare appeared was designated as minimum polarization. Plants which had previously been used for laboratory

reflectance measurements were photographed indoors using photoflood lighting.

Multiband photographs were also taken of 2.5 m^2 field plots, half of which consisted of healthy grass and half of which consisted of naturally infected grass exhibiting moderate to severe symptoms. The plots were replicated 12 times. An array of 4 Nikon-F cameras equipped with 50 mm lenses was mounted on a specially made frame which was supported by a heavy-duty tripod. Three of the cameras were used for the selected film/filter combinations, and the fourth camera was loaded with conventional Ektachrome color film. Photographs were made at various sun angles with and without polarizing filters. To photograph the field plots, this multiband camera apparatus was elevated to a height of 12 m using a cherry picker crane as a platform (Fig. 7).

A tripod-mounted field instrument, model 580/585 EG&G spectroradiometer, was used to make quantitative spectral reflectance measurements from the field plots over a range of 0.35-0.80 μm (Fig. 8). High-order interference was eliminated with prefilters. Reflectance values from grass samples were compared to reflectance values from a barium sulfate reference

Fig. 7. Multiband camera apparatus and cherry picker crane used to make overhead photographs of St. Augustine grass field plots

Fig. 8. EG&G spectroradiometer utilized for outdoor reflectance measurements of field plots.

target to determine percent reflectance at each wavelength. The hemispherical radiation flux input at ground level was monitored using an ISCO radiometer. Data from this instrument were used to supply corrections to the EG&G measurements.

The containers of healthy and diseased grass grown under greenhouse conditions, described above, were photographed outdoors at close range with color infrared film and a Wratten 12 (yellow) filter. The yellow filter screens out blue light to which all three of the film's emulsion layers are sensitive. Color infrared film is known as a "false color" film because colors of light which expose it are represented as different colors in the resulting photograph. Green, red, and near infrared wavelengths produce various shades of blue, green, and red, respectively. Because of these spectral shifts, near infrared radiation, which is invisible to the human eye, can be recorded on photographic film. Because the film is known as color infrared film, there is a tendency to attribute its tonal characteristics primarily to effects of near infrared. However, under most circumstances, tonal characteristics are determined by interaction of the film with both visible and near infrared radiation.

Black and white multiband negatives of field plots were qualitatively analyzed using color density contouring and slicing techniques. An I^2S Corporation multiband TV display unit, housed at NASA/JSC, was utilized for this purpose (Fig. 9). This analysis involved color enhancement techniques by which different colors could be assigned to the various film densities within each photograph. This allows discrimination among objects which reflect significantly different amounts of radiation within a particular spectral band. Quantitative densitometric analysis of color infrared transparencies from closeup photographs of healthy and diseased grass was accomplished with a Macbeth TD-504 transmission densitometer. Density measurements were made utilizing a 2 mm aperture in conjunction with Wratten filters 92 (red), 93 (green), 94 (blue), and 106 (visual). These filters transmit light in the following spectral bands: above 0.62 μm, 0.52-0.57 μm, 0.43-0.48 μm, and above 0.42 μm, respectively. Digital readings from the instrument indicate the level of film opacity (density) for each band on a scale of 0.0-4.0. Qualitative density analysis of color infrared photographs was done with an Antech Inc. Densicolor A12 density slicing instrument.

Fig. 9. I^2S (International Imaging Systems) color density contouring and slicing unit used to qualitatively analyze multiband photographs.

Aerial Photography

Multiband photographs were made of healthy and SAD-infected St. Augustine grass using the film/filter combinations previously discussed. Lawns on the campus of Pan American University in Edinburg, Texas served as the target area. Ground truth surveys of the campus revealed areas of healthy grass and areas of grass exhibiting a wide range of disease symptoms. Other conditions such as weed cover, nutritional deficiencies, and turf thinning due to water stress and pedestrian traffic were also noted.

The aerial photography was performed by a remote sensing group from the USDA Citrus Insect Investigations Laboratory in Weslaco, Texas. Black and white multiband photographs were taken with a 4-lens camera manufactured by Spectral Data Corporation (Fig. 10). Each of the f 2.8, 150 mm lenses have a focal length of 6 inches (15.2 cm), and each is equipped with a different filter (25-red, 57A-green, 47B-blue, or 89B-infrared). The camera takes four photographs simultaneously and records them on one 9 x 9 in. (15.24 cm^2) area of film (in this case, Plus X Aerographic 2402 film). Multiband photographs were

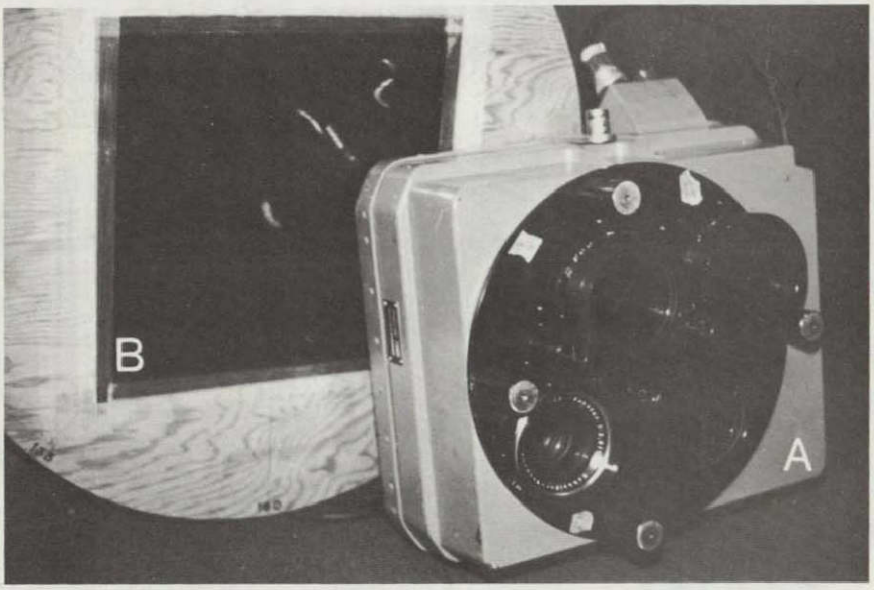

Fig. 10-(A,B). Multiband photography equipment. A) Spectral Data 4-lens camera used to take aerial multiband photographs. B) Large polarizing filter mounted in a wooden frame which could be placed over the camera lenses and be rotated to any desired position.

taken from altitudes of 150 and 300 m. Camera shutter speed was set at 1/350 second.

A large sheet of Kodak polarizing material was mounted in a wooden frame so it could be placed in front of the camera lenses and rotated to any desired position (Fig. 10). Minimum and maximum polarization positions of the filter were determined by viewing the sky through the filter as it was rotated. The position at which the sky appeared darkest was designated as maximum polarization; and likewise, the position at which the sky appeared brightest was designated as minimum polarization. Multiband photographs were taken using the polarizing filter in each of these positions. When minimum polarization was desired, the filter was rotated until the mark designated as minimum polarization was pointing directly at the sun. This position was maintained until maximum polarization was desired, at which time the frame was rotated 90° to point the maximum polarization mark toward the sun. For minimum polarization, the f-values used for the red, blue, and green filters were 6.3, 5.6, and 5.6, respectively. For maximum polarization these values were 4.9, 4.5, and 4.5, respectively. Photographs were made

between 9:30 a.m. and 10:00 a.m. CDT to insure a low sun angle and to enhance polarization differences between healthy and diseased grass.

Color infrared photographs were also made of the same areas from altitudes of 150 and 200 m. A modified K22 camera with a 12 inch (30.5 cm) focal length and a 9 x 9 in. (15.24 cm^2) format was utilized for this purpose. The camera was equipped with Kodak Aerochrome Infrared 2443 film and Wratten 15 (yellow) and CC40 (blue) filters. Camera settings of 1/350 and f 6 were used. Photographs were made between 11:30 a.m. and 12:00 noon CDT.

Positive transparencies of multiband photographs were qualitatively analyzed in the laboratory at Weslaco, Texas using a Spectral Data Corporation multispectral viewer and a Densicolor A12 density slicing apparatus manufactured by Antech Inc. (Fig. 11).

The multispectral viewer is capable of superimposing images of up to four different photographs taken of the same scene using multiband photographic techniques. Different colors and intensities of light can then be projected through each photograph to produce a composite color image in which different

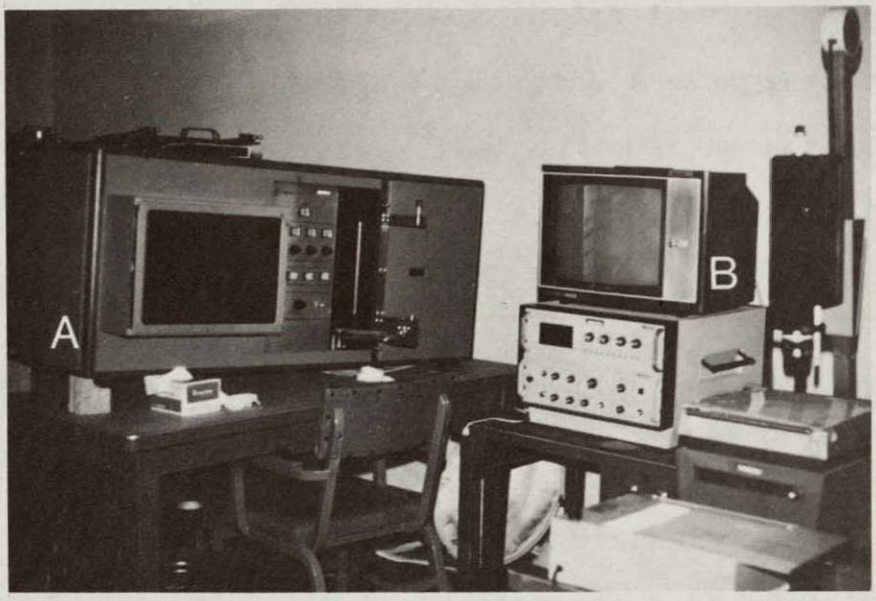

Fig. 11 - (A,B). Film analysis equipment. A) Spectral Data multispectral viewer unit used to analyze multiband photography. B) Antech density slicing unit used to analyze multiband and color infrared photographs.

film densities appear as different colors or intensities of colors. Because the optical properties of most objects differ widely from one region of the spectrum to another, their tonal signatures are usually enhanced by simultaneous analysis of photographs from two or more spectral bands.

In contrast to the multispectral viewer, the density slicing apparatus was only capable of analyzing one photograph at a time. For this analysis, white light is projected through the transparency which is then viewed on a TV screen. Different film densities, which appear as various shades of black, white, and gray on the transparency, are seen as distinctly different colors with no gradual transitions in color intensities or hues.

Color infrared transparencies were also analyzed using the Antech density slicing apparatus. Additional density analysis was done with the Macbeth transmission densitometer. For this analysis, densities were measured of specific areas on the photograph for which ground truth data had been collected. Density readings were then compared to disease ratings obtained by the ground surveys.

Effects of Selected Nutritional Deficiencies on Optical Properties of St. Augustine Grass

Two common nutritional deficiencies of St. Augustine grass, nitrogen and iron, cause leaf chlorosis. Nitrogen deficiency results in a gradual, overall yellowing, while iron deficiency manifests itself as an interveinal yellowing which results in a longitudinal striping (Fig. 12). Chlorosis patterns produced by nitrogen and iron deficiencies and SAD can be easily distinguished by close-up examination However, a remote sensor viewing these conditions from a distance might confuse them because the gross effect of all three would be an overall yellowing of the grass canopy.

A study was undertaken to determine if these three abnormalities of St. Augustine grass could be distinguished using remote sensing techniques. Healthy and SAD-infected grass was initially grown hydroponically under controlled environmental conditions in a growth chamber. A 15 hr. daylength (22,000 lux light intensity) was used during which a temperature of 30°C and a humidity of 70% was maintained. Temperature during periods of darkness was lowered to 22°C.

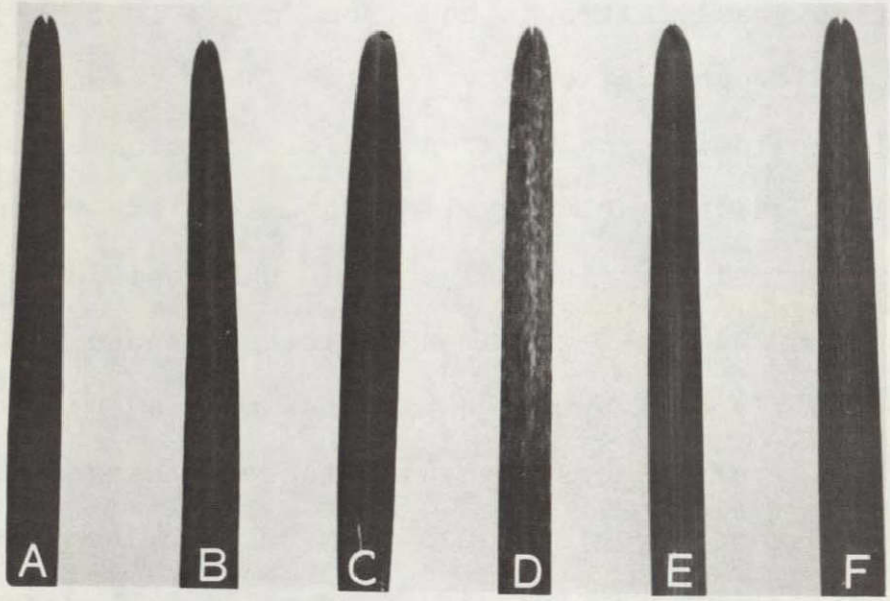

Fig. 12 (A-F). Nutrient deficiency and St. Augustine Decline symptoms on St. Augustine grass leaves. A) Healthy (dark green). B) Infected. C) Nitrogen-deficient (slight yellowing). D) Infected, nitrogen-deficient. E) Iron-deficient (interveinal chlorosis). F) Infected, iron-deficient.

Healthy and diseased grass sods, which had been grown in containers of peatmoss and perlite in the greenhouse, were separated into individual stolons while disrupting the root systems as little as possible. Soil-free roots of the individual plants were placed in one-quart (0.946 ℓ) glass containers filled with nutrient solutions. Each container was equipped with a styrofoam lid, and each lid had three holes through which single stolons were placed and secured with cotton (Fig. 13). Each container of three plants (healthy or diseased) constituted one treatment replication. Complete Hoagland and Arnon's nutrient solution and solutions deficient in either nitrogen or iron were the three treatments used (38). Each treatment was replicated four times for healthy plants and SAD-infected plants, and all replications were randomly arranged on metal carts in the growth chamber. Solutions were aerated by continuously pumping filtered air through a network of plastic tubing and into each container at a rate of 1.4 liters/min. Nutrient solutions were prepared with distilled, deionized water, and were adjusted to a pH of 5.8-6.2 using either 1.0 M HCl or 1.0 M NaOH. Solutions in each container were replaced periodically to maintain this pH range.

Fig. 13. St. Augustine grass grown hydroponically using complete, nitrogen-deficient, and iron-deficient nutrient solutions.

of each deficiency as compared to control values. Healthy and diseased control plants grown in complete nutrient solutions were analyzed for both nitrogen and iron content, while other plants were tested only for the element in which they were deficient. Nitrogen content was determined using the Kjeldahl method, and iron determination was done with an atomic absorption method (43).

Following this initial study, similar experiments were done using plants grown in sand culture. Healthy and diseased grass sods from the greenhouse were again broken up into individual stolons, and the roots were washed free of soil. Several stolons from either healthy or diseased plants were planted in each of 40 one-gallon (3.79 ℓ) crocks containing acid-washed quartz sand. Plants were distributed uniformly throughout each container to facilitate rapid, complete coverage of the sand surface by the developing grass. Plants were watered three times a week with the same type of nutrient solutions used for the hydroponic experiment. Each treatment was replicated four times for both healthy and diseased grass, resulting in a total of 24 containers. Each container

was thoroughly watered with distilled, deionized water once a week to help leach out any accumulated salts. All plants, which were maintained in random arrangement on carts in the growth chamber (Fig. 14), were trimmed periodically to eliminate excessively long stolons. All plants were watered with complete nutrient solutions until their growth had become well established, and complete vegetative coverage of the sand surface had been achieved. From that point on, control plants continued to receive complete solutions, while the other plants received solutions deficient in either nitrogen or iron.

Several weeks later, when moderate deficiency symptoms had developed, collection of various types of data began. Plants were again transported to NASA/JSC for spectral reflectance measurements using the Cary 14 laboratory spectrophotometer and the VISS field spectrometer system (Fig. 15). Overhead and oblique multiband photographs from 3 m and 6 m, respectively, were made at solar noon and during late afternoon. Only one camera, a Miranda Sensorex with a f 1.4 lens, was utilized for the photographs. Multiband photographs were accomplished by interchanging

Fig. 14. St. Augustine grass grown in sand culture using complete, nitrogen-deficient, and iron-deficient nutrient solutions.

Fig. 15. NASA's Visible-Infrared Spectrometer System (VISS) used to make outdoor reflectance measurements from St. Augustine grass plants grown in sand culture.

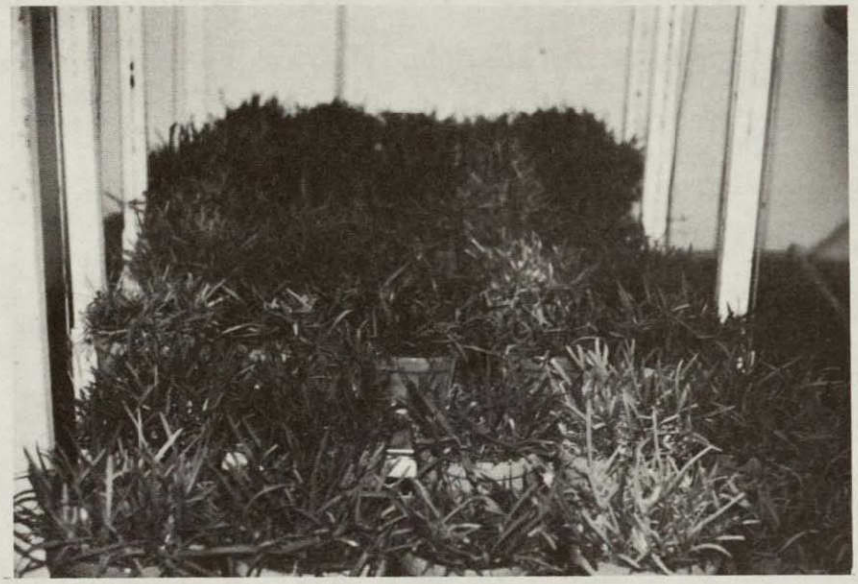

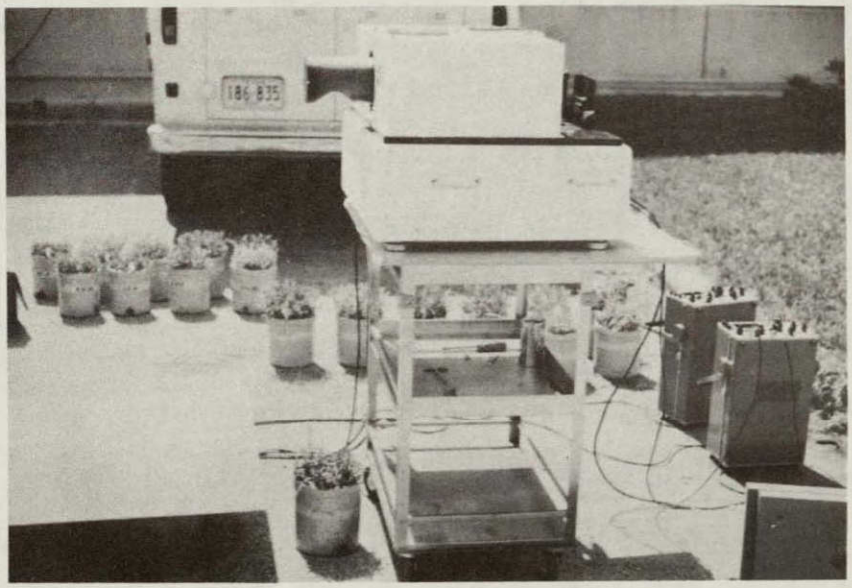

the various filters from one photograph to another, while taking care to prevent any movement of the camera or plants. These photographs were analyzed with the Spectral Data multispectral viewer and the Antech color density slicer at Weslaco, Texas. Color infrared photographs were also taken and then analyzed with the Antech density slicer and the Macbeth transmission densitometer.

In addition to the types of data collected from hydroponically grown grass, several additional types were obtained from plants grown in sand culture. An Exotech model 100 ERTS-band (Earth Resources Technology Satellite) radiometer was used to collect outdoor reflectance measurements on several different dates (Fig. 16). This instrument measures reflectance in four broad spectral bands. The ranges of bands 1, 2, 3, and 4 are 0.5-0.6 μm, 0.6-0.7 μm, 0.7-0.8 μm, and 0.8-1.1 μm, respectively. Reflectance values from a barium sulfate standard were compared to values from the targets to determine percent reflectance in each band. In order to restrict the field of view to the diameter of the crocks, measurements were taken with the tripod-mounted radiometer from

Fig. 16. ERTS (Earth Resources Technology Satellite)-band radiometer used to make outdoor reflectance measurements from St. Augustine grass plants grown in Sand culture.

a distance of about 50 cm and a look angle of 60-70° from horizontal. Measurements from each container were repeated three separate times on each date. Computer pattern recognition analysis was applied to the ERTS-band radiometer data using a statistical technique known as transformed divergence (70). This technique gives a measure of the dissimilarity of two distributions, and thus gives an indirect measure of the ability to discriminate between the two distributions. Transformed divergence values range between 0.0 and 2.0, with 2.0 representing maximum discrimination. Percent discrimination and transformed divergence values are logarithmically related, so that a transformed divergence value of 1.0 represents a percent discrimination of 84%, not 50%. Reflectance data from only two ERTS bands at a time were used for each analysis. Analyses were done to test the effectiveness of various 2-channel combinations for discrimination between different nutritional treatments of healthy and diseased grass.

Leaf transmittance measurements were also done using a transmissometer (24) in conjunction with the tripod-mounted ERTS-band radiometer (Fig. 17). Leaves exhibiting various severities of nutrient and/or

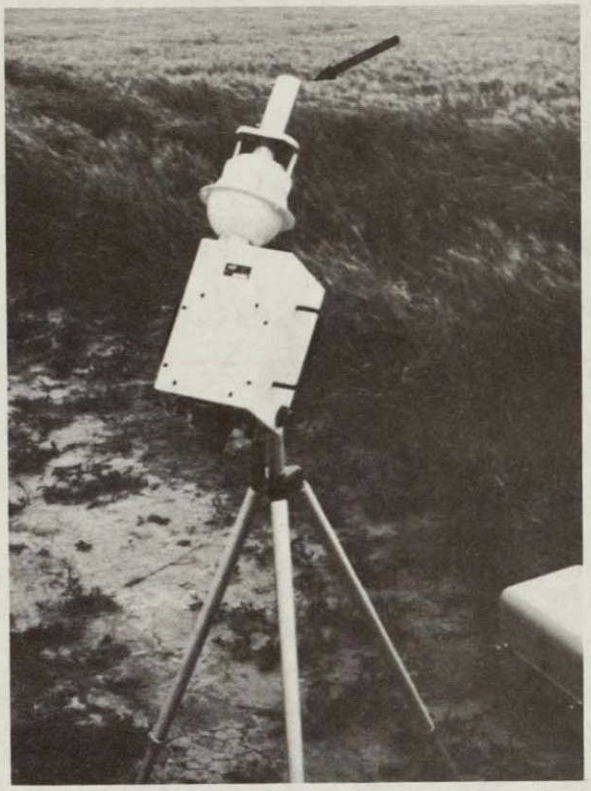

Fig. 17. ERTS-band radiometer equipped with a transmissometer attachment (arrow) used to measure transmittance of St. Augustine grass leaves.

virus symptoms were used for this purpose. The transmittance attachment consists of a collimator and 10 cm diameter integrating sphere coated with barium sulfate. The collimator is aimed directly at the sun to insure that the integrating sphere is irradiated normally. Radiation passes through the collimator and integrating sphere into the viewing optic of the radiometer where it is detected. A sample stage with variable slit widths separates the collimator and integrating sphere. To obtain hemispherical leaf transmittance, measurements are taken with and without a leaf placed over the stage slit. These two values are measured for all four bands by alternately placing the attachment over each of the four viewing optics. The two sets of values are then ratioed to obtain percent leaf transmission for each ERTS band.

Relative temperatures of each replication were measured in sunlight and shade on several dates with a Barnes PRT-5 infrared thermometer (Fig. 18) which detects radiation in the 6.5-20 μm region. With the instrument mounted on a tripod and aimed at a 45° angle, measurements were taken from a distance of about 1.5 m. Because of its narrow field of view

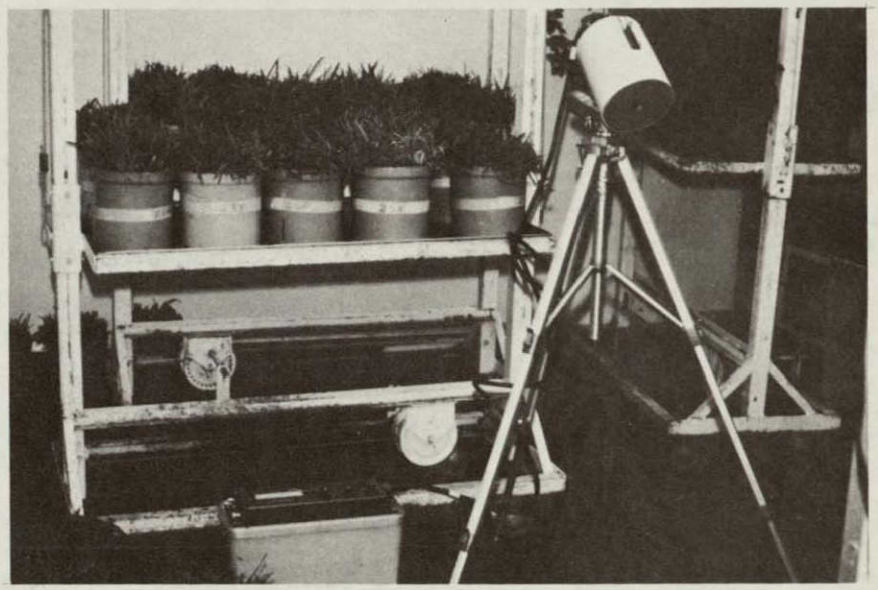

Fig. 18. Barnes PRT-5 infrared thermometer utilized to measure the canopy temperatures of St. Augustine grass plants grown in sand culture.

(2°), the instrument viewed only a small area within the grass canopy. Twenty measurements were taken at different points within each container, from which an average temperature was obtained. Data were not collected on cloudy or windy days in an effort to minimize effects of these conditions.

Following collection of these various types of data, the plants were harvested. Two five-gram samples of fresh leaves from each replication were used for chlorophyll determination. Total leaf area of each sample was measured using a Lambda model LI-3000 Portable Area Meter. To determine leaf area with this instrument, leaves are placed between two layers of transparent plastic which are then pulled slowly through the scanning head. The upper section of the scanning head contains a row of light emitting diodes, while the scanning head base contains a lens-photodiode sensing system which is sensitive to the light emitted from the diodes. As a leaf passes through the scanning head, it masks a certain number of the diodes, enabling the instrument to determine the leaf's width. The row of diodes is scanned one time for each mm of plastic (containing the leaves) pulled through the scanning head. Thus,

the leaf's total area (width x length) is accurately measured and recorded as cm^2 on the instrument's digital readout.

For chlorophyll analyses (6), individual samples were macerated with a mortar and pestle using a ml of 80% (V/V) aqueous acetone and a small amount of $MgCO_3$. The resulting slurry was filtered through Whatman No. 1 filter paper using a Buchner funnel. Residues were rinsed with additional 80% acetone. Each chlorophyll sample was then diluted to 50 ml with 80% acetone and throughly mixed. Optical density of each sample was determined at 0.652 μm using a Beckman model ACTA C III spectrophotometer. Chlorophyll content of each sample was calculated and expressed as mg chlorophyll/g tissue and mg chlorophyll/cm^2 tissue.

The remaining leaves from each treatment replication were weighed and oven-dried at 75°C for 48 hrs. After dry weight measurements were taken, percent moisture of each sample was determined. A quantitative measurement of the deficiency level of each dried sample was then made by the Agricultural Analytical Service.

Effects of Soil-Water Stress on Optical Properties of St. Augustine Grass

Soil-water stress is another factor commonly encountered under field conditions which can affect optical properties of plants. An experiment was conducted to determine the effects of soil-water stress on the optical properties of healthy and SAD-infected St. Augustine grass.

Three containers of healthy and three containers of diseased grass grown under greenhouse conditions were utilized for this experiment. The containers were 17 x 13 x 2 in (43 x 33 x 5 cm) plastic flats, and the growth medium consisted of a mixture of peatmoss and perlite. Prior to the experiment, plants were watered three times each week - once a week with Hoagland and Arnon's nutrient solution.

On the first day of the experiment, when all six containers were well-watered, various types of data were collected. Reflectance measurements were taken at midmorning using the ERTS-band radiometer. Measurements for all four bands were repeated three times with each container. Using transformed divergence analysis, these reflectance data were analyzed along with ERTS-band data from the nutritional defi-

ciency experiment. Water-stressed plants (healthy and diseased) were treated as separate categories in an effort to discriminate them from each other and from various nutrient treatments. Multiband and color infrared photographs were taken during early afternoon using the various film/filter combinations previously discussed. Photography was accomplished using the single Miranda Sensorex II. Multiband and color infrared photographs were qualitatively analyzed using the Spectral Data multispectral viewer and the Antech density slicer at Weslaco, Texas. Color infrared photographs were also analyzed quantitatively with the Macbeth transmission densitometer. Temperature measurements were made with the PRT-5 infrared thermometer. Average temperatures were calculated from twenty different measurements within each container of grass. These measurements were taken with the plants in complete shade, and again with the plants in full sunlight. To monitor plant water potential, sap pressures were determined with the pressure bomb apparatus (64) shown in (Fig. 19). Individual mature leaves which were used for these measurements were detached from the plants in full sunlight and immediately placed in the pressure bomb.

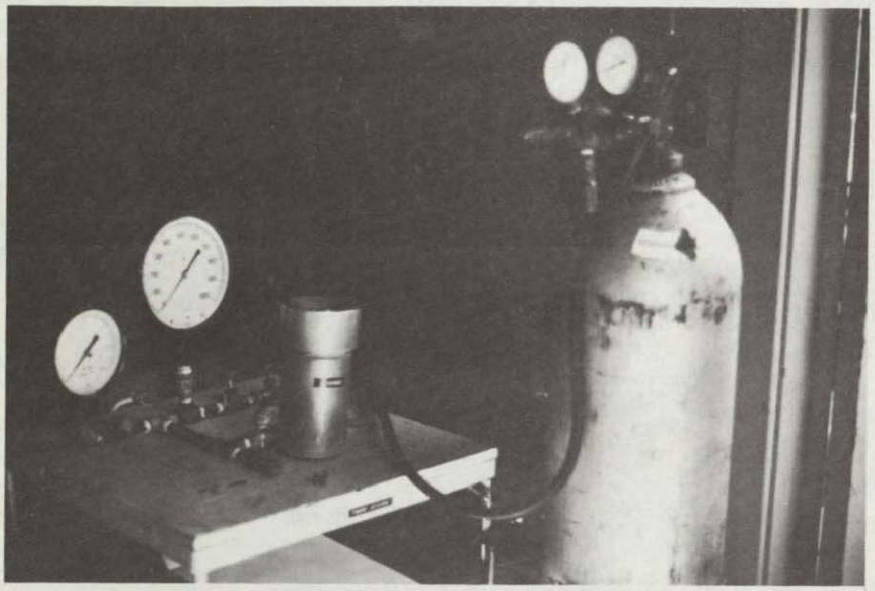

Fig. 19. Pressure bomb apparatus used to measure water potentials of water-stressed and nonstressed St. Augustine grass plants.

Average water potential was calculated for each plant on the basis of five leaf measurements. Fresh and dry weights of leaf samples were used to calculate the percent moisture in each plant. All of these different types of measurements were done within one day in efforts to minimize changes in water status for the entire set of data.

After the first day, one healthy and one diseased flat continued to receive water every two days. The other four flats (two healthy and two diseased) received no water for the remainder of the experiment. Three days later, when plants in the four stressed containers began to exhibit a moderate wilt, the various types of data mentioned above were again collected. Fig. 20 shows the wilting symptom which accompanied moderate to severe water stress. At the end of six days, the stressed plants were severely wilted, and a final set of data was collected.

Fig. 20. Containers of St. Augustine grass showing the wilting symptom (right) which resulted from moderate to severe water stress.

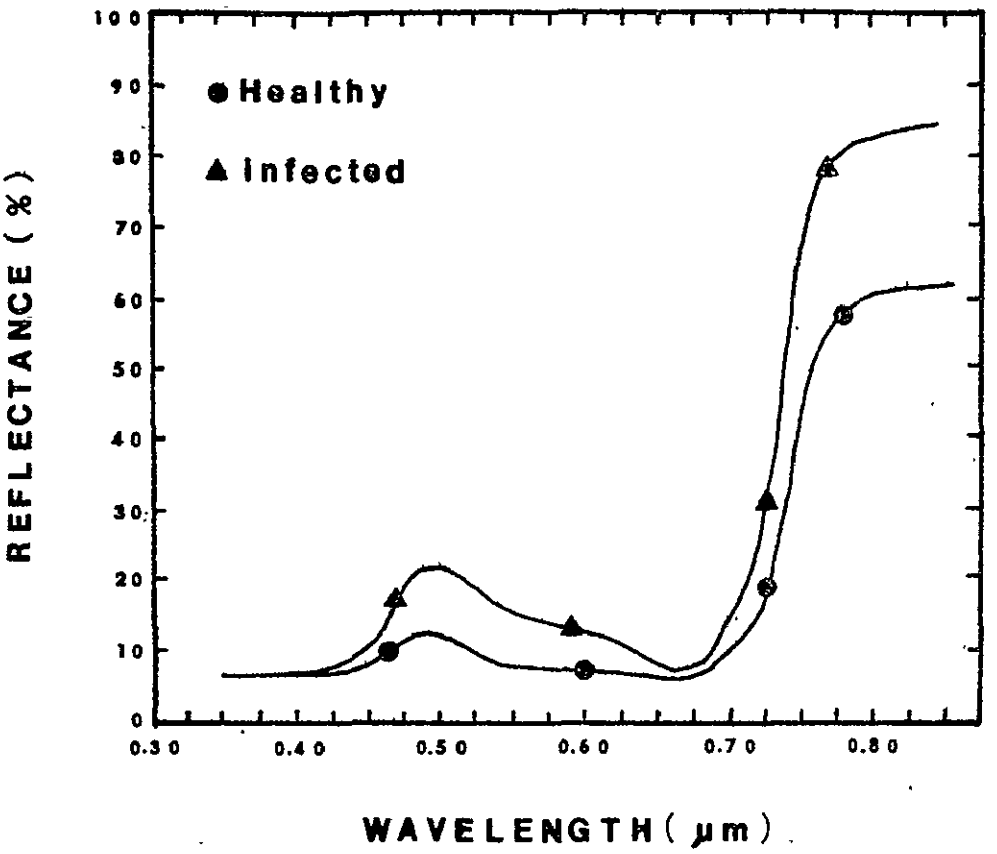

Fig. 21. Spectral reflectance curves of healthy and St. Augustine Decline-infected St. Augustine grass leaves determined with a Cary 14 spectrophotometer.

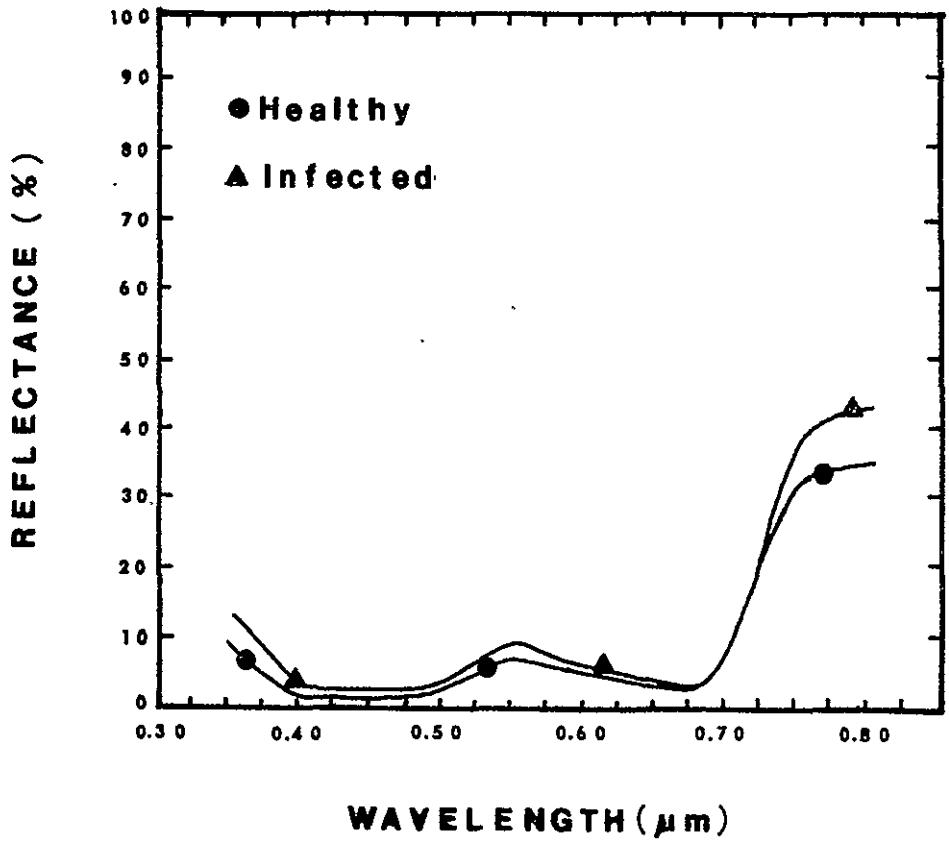

Fig. 22. Spectral reflectance curves of healthy and St. Augustine Decline-infected field plots of St. Augustine grass determined from EG & G radiometer data.

tion differences of up to 34% and 40% occurred in the blue (0.45-0.48 μm) and red (0.67-0.68 μm) regions, respectively (Fig. 23). Very little difference was observed in the yellow-green (0.55-0.56 μm) region.

Indoor and outdoor multiband photographs taken with red (25) and blue (47B) filters showed tonal differences between healthy and moderately to severely diseased grass. Use of polarizing filters in combination with red and blue filters enhanced these tonal differences. Photographs taken with the green (58) filter exhibited smaller tonal differences. Color enhancement of these density differences was accomplished with the I^2S system using multiband negatives of field plots. Analysis of two superimposed negatives (either the green and red or the green and blue) produced excellent tonal differentiation of healthy and infected grass (Fig. 24). General yellowing of diseased grass due to reduced chlorophyll levels could be seen in color photographs of the field plots (Fig. 25).

Tonal differences between healthy and SAD-infected grass were also apparent in color infrared photographs (Fig. 26-A). Qualitative density analysis using the Antech density slicing instrument enhanced

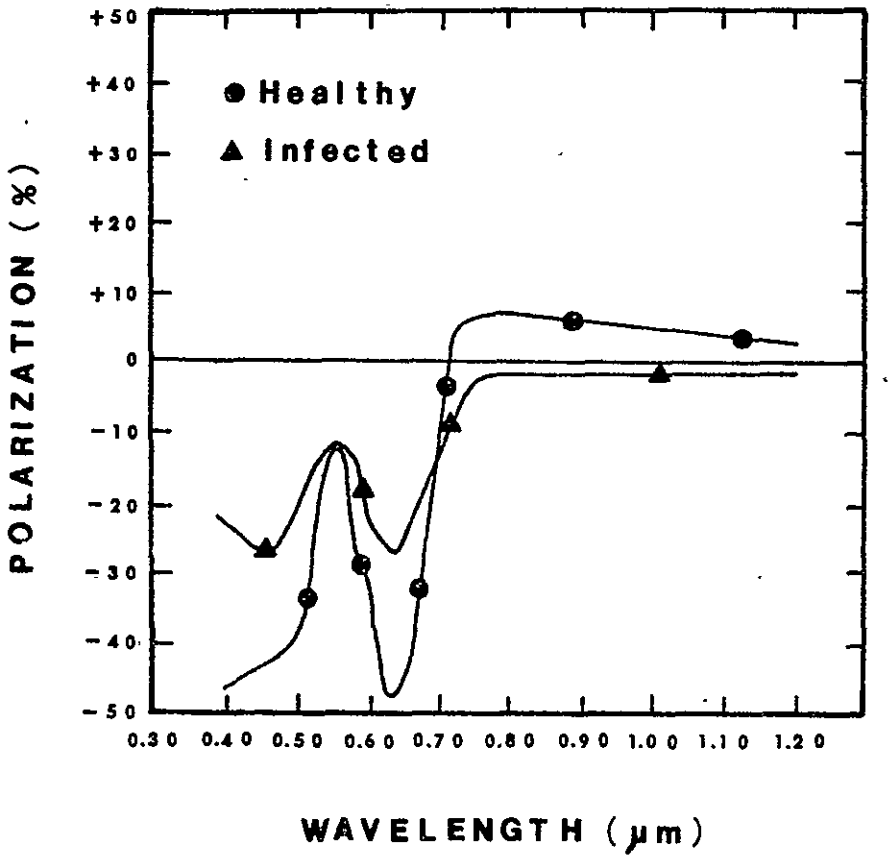

Fig. 23. Polarization differences between spectral reflectance curves of healthy and St. Augustine Decline-infected St. Augustine grass leaves measured with a Cary 14 spectrophotometer.

Fig. 24 (A,B). Density contouring and slici analysis of multiband photographs of St. Augustin grass field plots (H = healthy; I = St. Augustine Decline-infected). A) Combination of negatives m with red (25) and green (58) filters plus polariz B) Combination of negatives made with blue (47B) and green (58) filters plus polarizers.

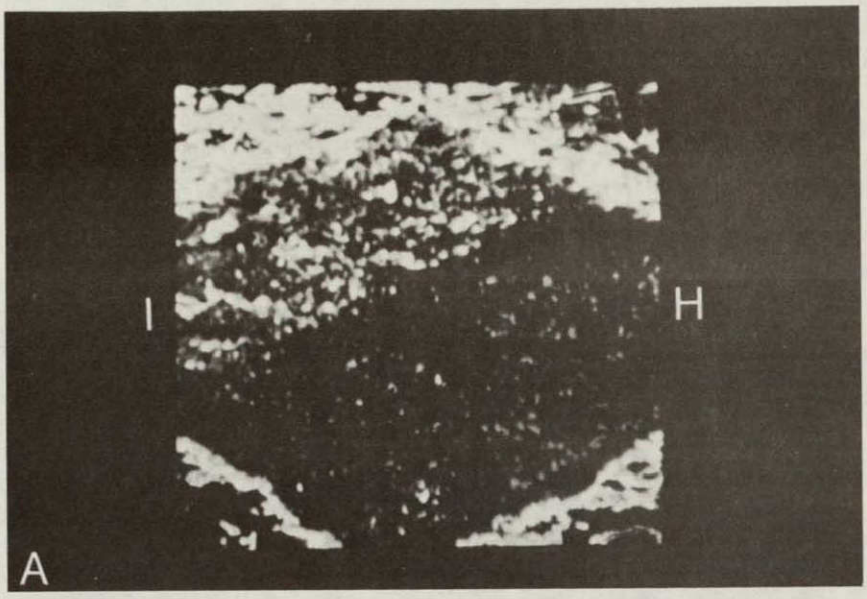

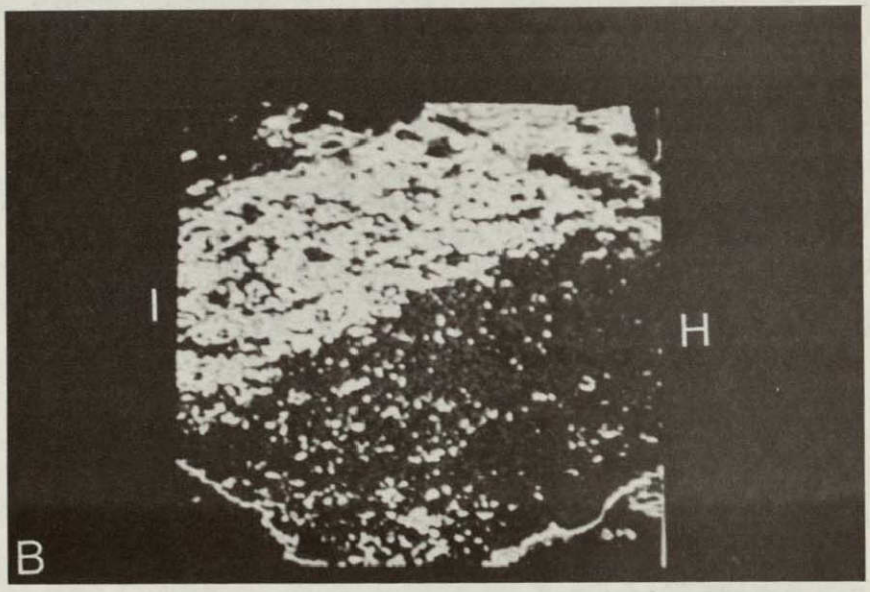

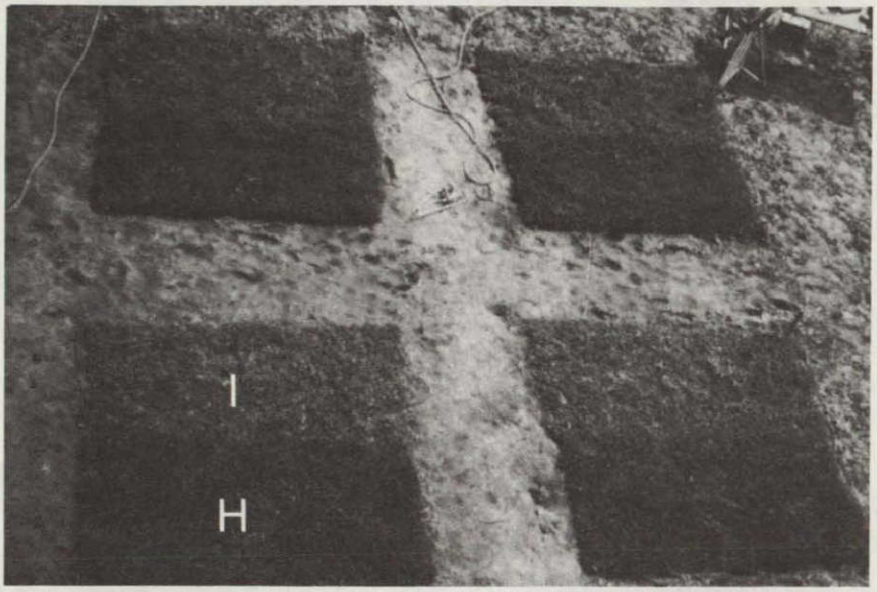

Fig. 25. Color photograph of four field plots showing healthy (H) and St. Augustine Decline-infected (I) grass.

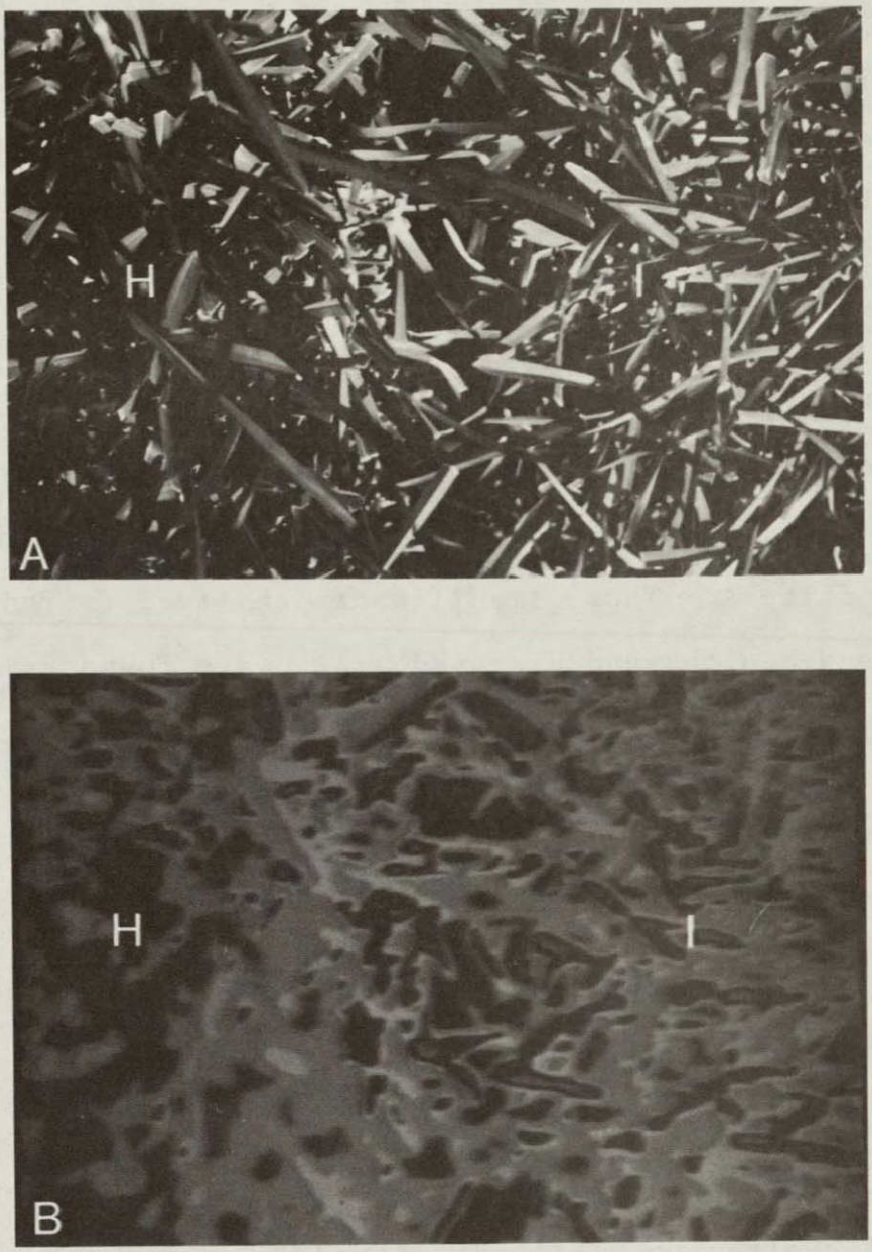

Fig. 26 (A,B). Photographs of healthy (H) and St. Augustine Decline-infected (I) grass. A) Color infrared photograph. B) Color enhancement of the same color infrared photograph using density slicing techniques.

these tonal differences (Fig. 26-B). Analysis using the Macbeth transmission densitometer provided quantitative measurements of color infrared film densities. Average optical count values for healthy grass were 1.50, 1.73, 2.27, and 0.91 using the visible, blue, green, and red filters, respectively. Average values for grass exhibiting moderate SAD symptoms were 1.25, 1.12, 1.68, and 0.82, respectively for the four filters. Thus, significant density differences between healthy and diseased grass were found using the visible, blue, and green filters. Much smaller differences were noted using the red filter.

Aerial Photography

Although several combinations of spectral bands were tested, qualitative analysis of multiband photographs using the Spectral Data multispectral viewer resulted in unsatisfactory density differentiation. Better results were achieved by analysis of only one band at a time utilizing the Antech density slicer. Using photographs taken from an altitude of 150 m, areas of heavy SAD infection were detected with all three filters plus minimum or maximum polarization (Fig. 27). Areas with slight to moderate

Fig. 27 (A-F). Density slicing analysis of aerial multiband photographs of St. Augustine grass lawns (Large arrows = SAD-infected areas; small arrows = noninfected areas with film densities similar to those of SAD-infected areas; S = shadow; T = tree; W = concrete walk). A) Red (25) filter plus minimum polarization. B) Red filter plus maximum polarization. C) Blue (47B) filter plus minimum polarization. D) Blue filter plus maximum polarization. E) Green (58) filter plus minimum polarization. F) Green filter plus maximum polarization.

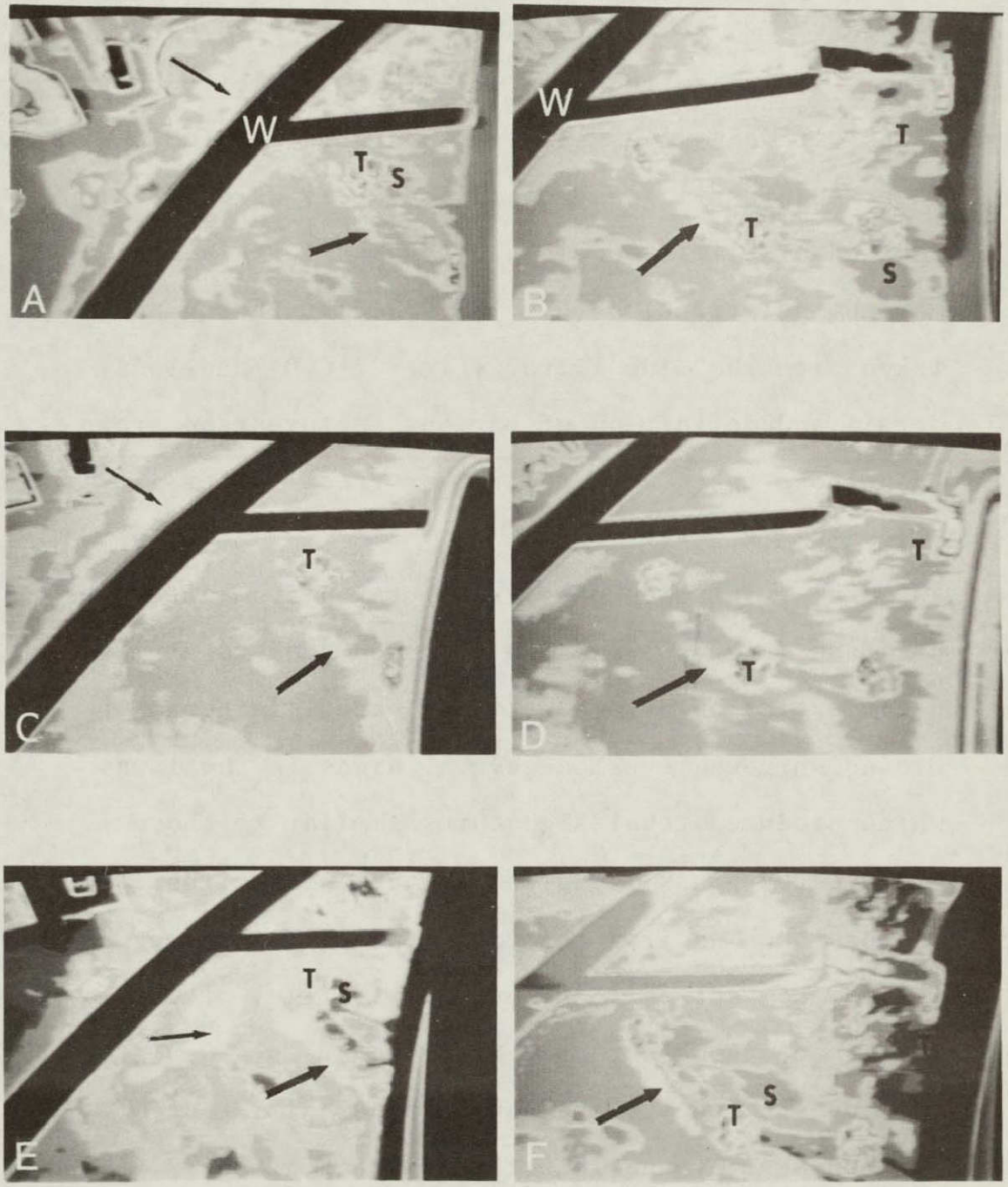

disease symptoms were difficult to detect with any consistency. In general, photographs taken with minimum polarization (Fig. 27-A,C,E) exhibited several areas with densities similar to densities of SAD-infected areas. These confusion areas were often reduced or eliminated in photographs taken with maximum polarization (Fig. 27-B,D,F). Photographs taken with the blue filter (Fig. 27-C,D) had less detail and definition of various features and areas than those taken with the red or green filters (Fig. 27-A,B,E,F).

Color infrared photographs taken from altitudes of 150 m (Fig. 28) and 300 m showed good tonal differentiation of moderate and severe infections. Ground surveys revealed several areas in the lawns which produced tonal signatures similar to those produced by grass in various stages of decline. Factors such as iron chlorosis and turf thinning due to dry, compact soil, pedestrian traffic, or close mowing accounted for most of these areas. Qualitative density analysis enhanced tonal differences between healthy and infected grass (Fig. 29). Quantitative analysis using the Macbeth transmission densitometer correlated well with ground truth in-

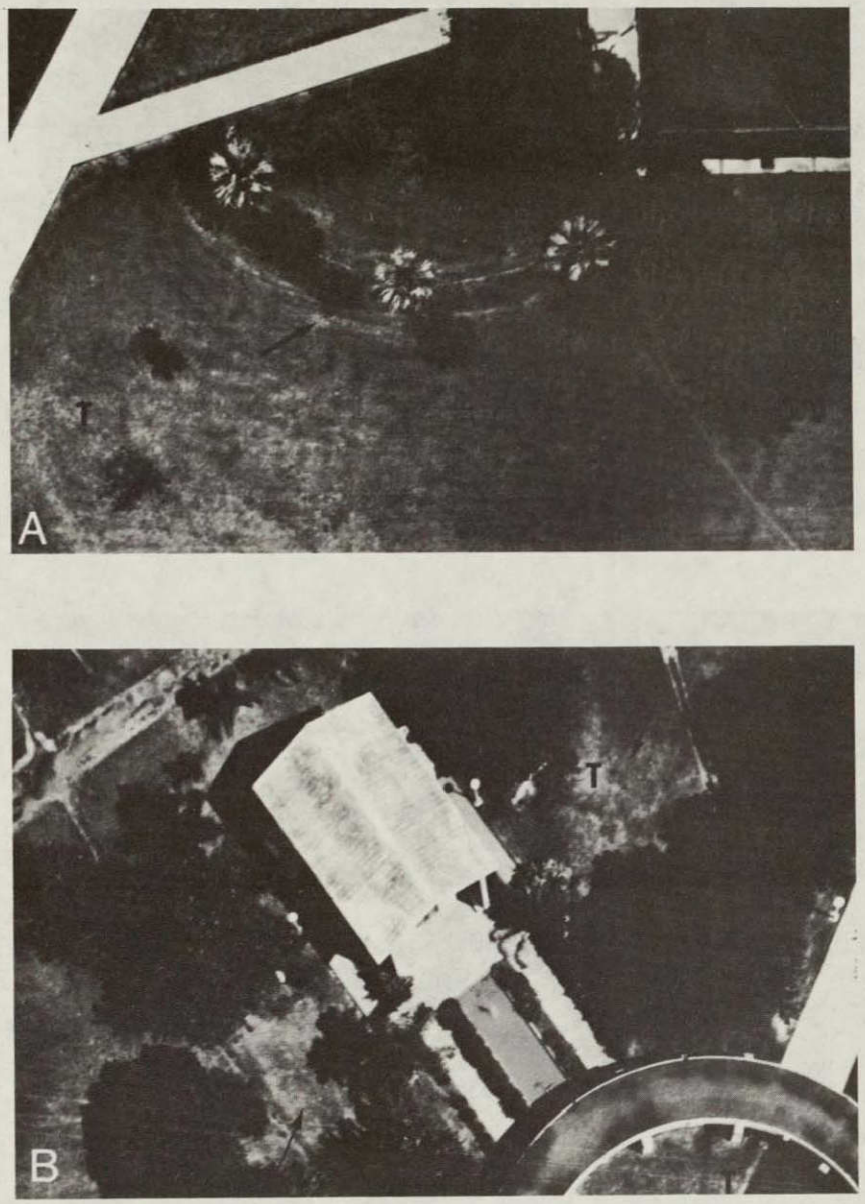

Fig. 28. Color infrared aerial photographs of St. Augustine grass lawns (Arrows = SAD-infected areas; T = areas where grass was thin because of dry, compacted soil, pedestrian traffic, or close mowing).

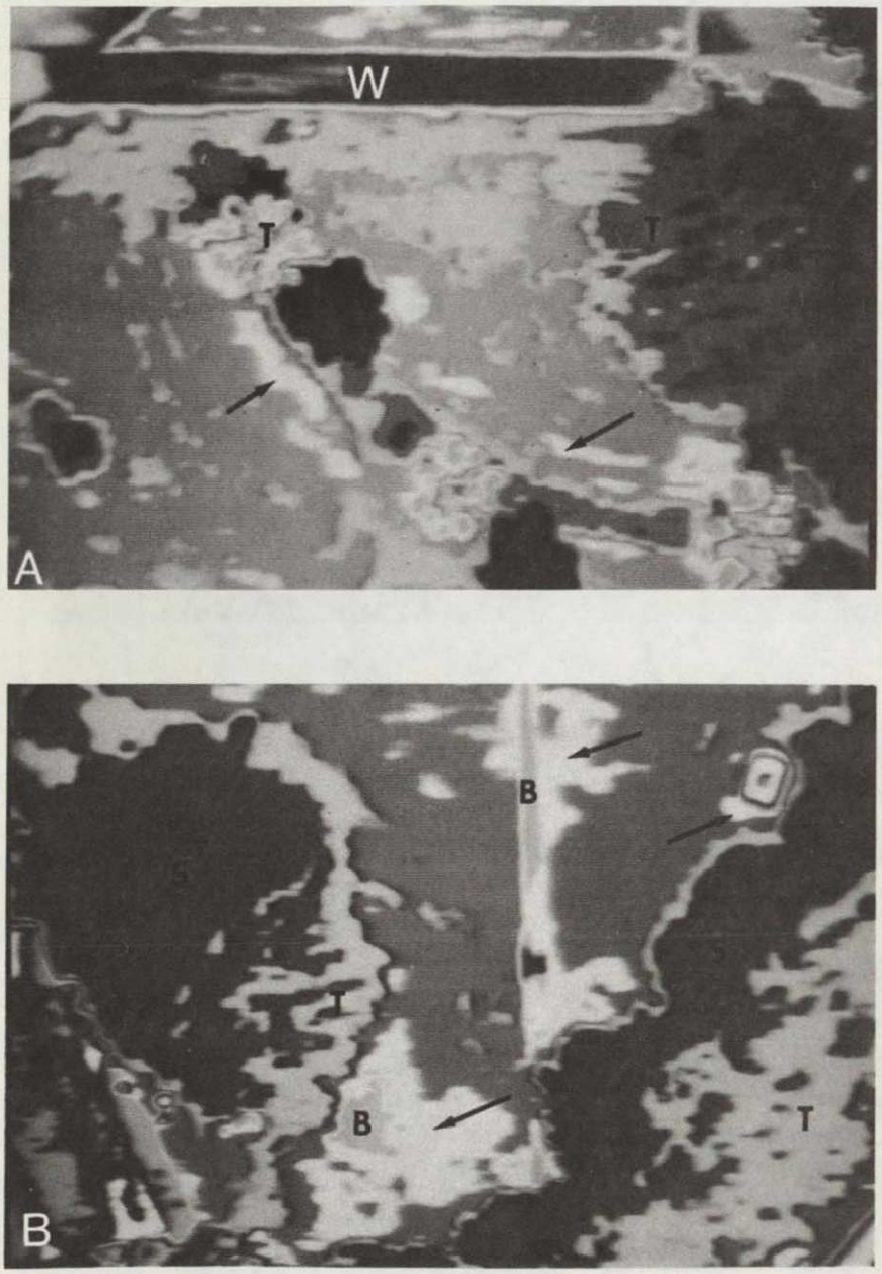

Fig. 29. Density slicing analysis of color infrared aerial photographs of St. Augustine grass lawns (Arrows = SAD-infected areas; B = bare soil; S = shadow; T = tree; W = concrete walk).

TABLE 1. Transmission densitometer measurements from areas on aerial color infrared photographs showing healthy and St. Augustine Decline-infected St. Augustine grass.

	Film density[a]			
Disease Intensity	V[b]	B	G	R
Healthy	1.16	2.00	1.98	0.47
Mild mottle	0.98	1.62	1.59	0.36
Green mottle	0.92	1.28	1.25	0.43
Chlorotic mottle	0.88	1.21	1.18	0.39
Chlorosis and stunting	0.80	1.03	1.01	0.40

[a]Average of five measurements.

[b]Abbreviations: V = visible filter; B = blue filter; G = green filter; R = red filter.

Fig. 30 Spectral reflectance curves of healthy control, nitrogen-deficient, and iron-deficient St. Augustine grass leaves determined with a Cary 14 spectrophotometer.

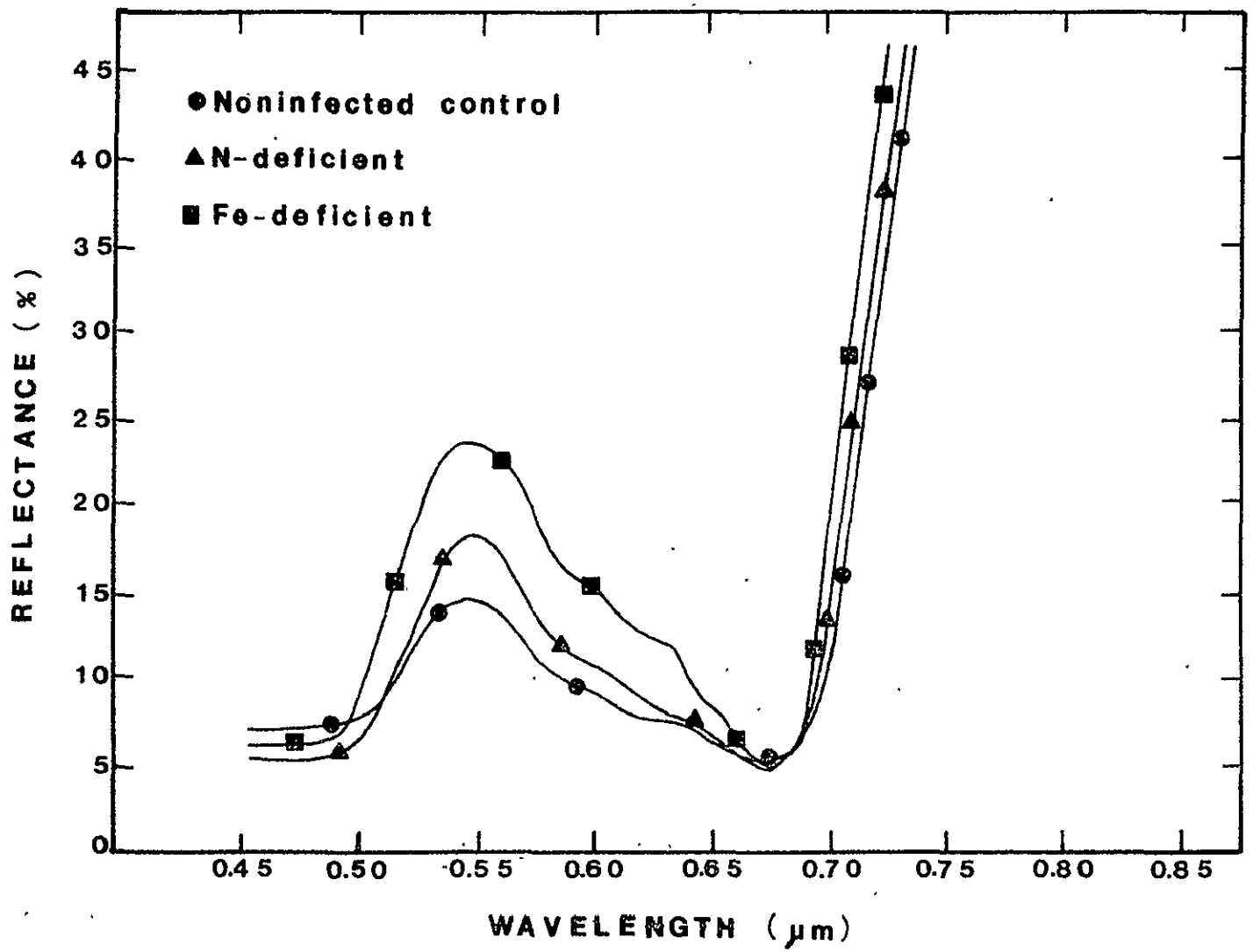
Noninfected control
N-deficient
Fe-deficient
REFLECTANCE (%)
0
5
10
15
20
25
30
35
40
45
0.45
0.50
0.55
0.60
0.65
0.70
0.75
0.80
0.85
WAVELENGTH (μm)

Fig. 31. Cary 14 spectral reflectance curves of St. Augustine grass leaves exhibiting various degrees of iron-deficiency symptoms.

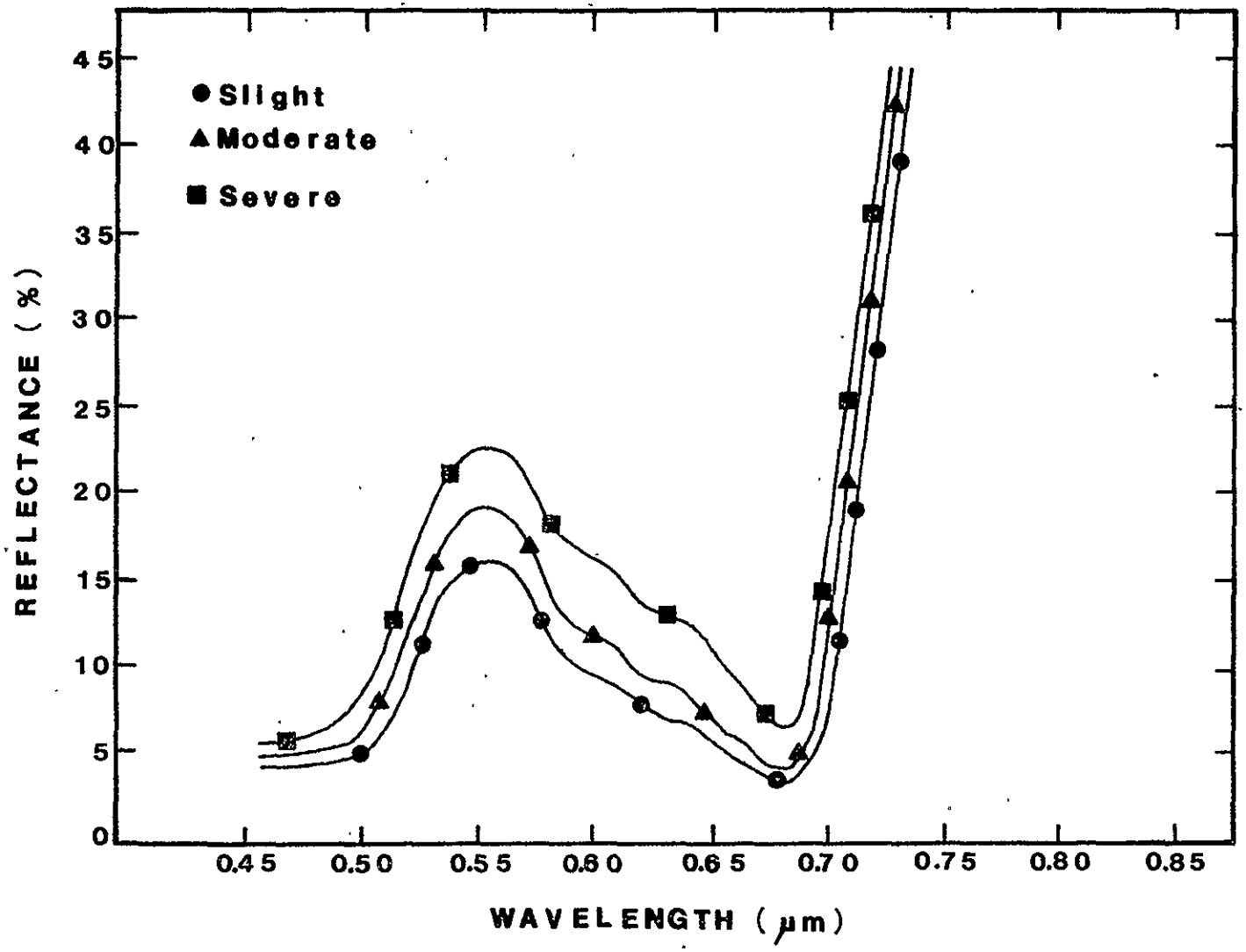
Slight
Moderate
Severe
REFLECTANCE (%)
45
40
35
30
25
20
15
10
5
0
0.45
0.50
0.55
0.60
0.65
0.70
0.75
0.80
0.85
WAVELENGTH (μm)

illustrates how reflectance at these wavelengths changed with increasing severity of iron deficiency symptoms. Nitrogen and iron deficiencies in combination with SAD produced even larger differences (Fig. 32). Table 2 summarizes reflectance values at specific wavelengths for the various treatments.

Photographs taken with the 4-camera multiband apparatus produced inconclusive results because of difficulties concerning analysis with the I^2S instrument. Registration (superimposition of two or more photographs) was impossible because of the parallax problems with the 4-camera apparatus used for close-up photography (4-5 m). Since the cameras are separated by a distance of about 0.5 m, objects (such as small containers of grass) at close range are viewed from a significantly different angle by each camera. This problem was eliminated in future experiments by using only one camera and changing filters between each exposure.

On the color infrared photography, noninfected control plants appear a dark red, while all other treatments appear light red or pink.

Elemental analysis of dried leaf samples provided quantitative measurements of deficiency

Fig. 32. Cary 14 spectral reflectance curves of SAD-infected St. Augustine grass leaves (control) and SAD-infected leaves deficient in nitrogen or iron.

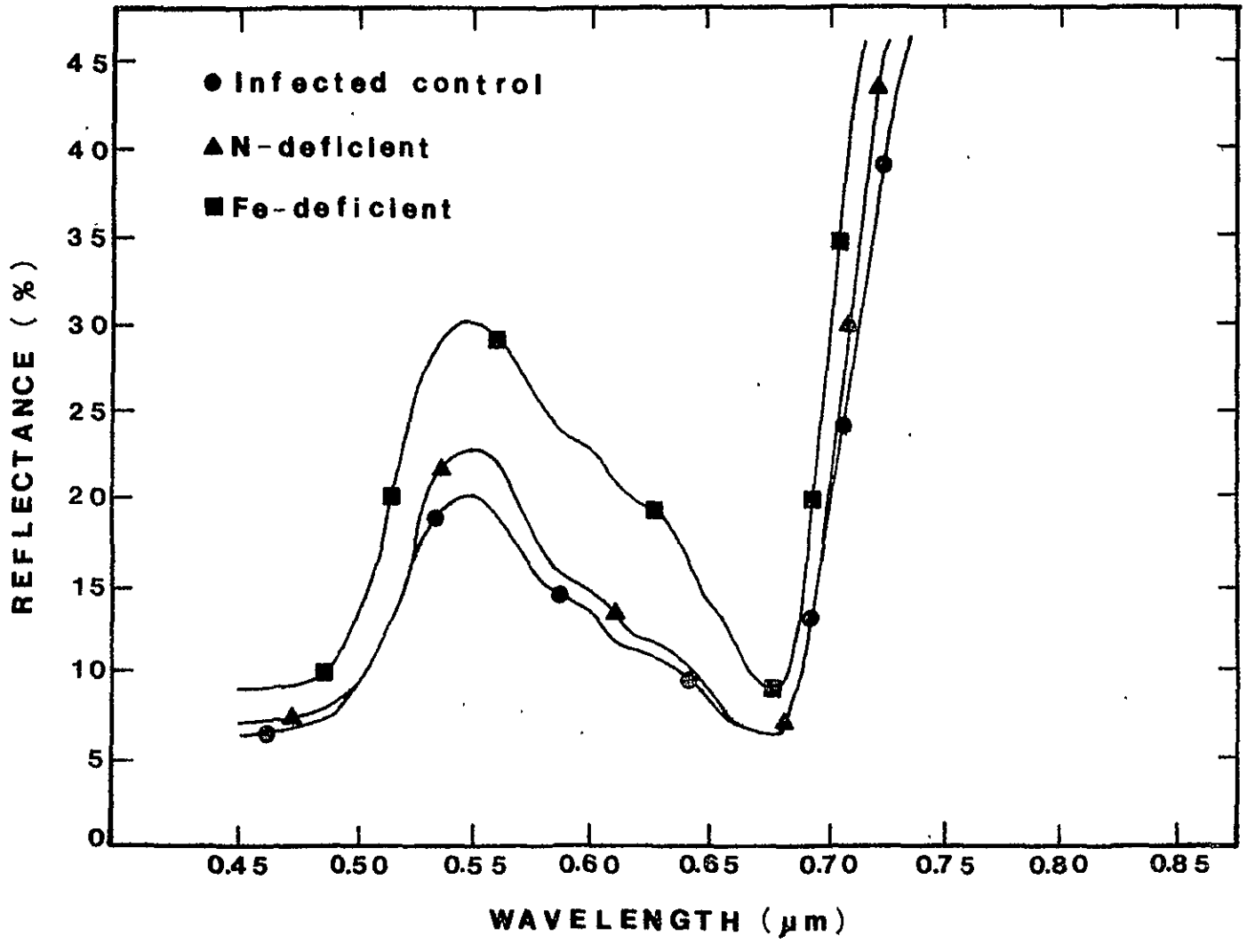
● Infected control
▲ N-deficient
■ Fe-deficient
REFLECTANCE (%)
0
5
10
15
20
25
30
35
40
45
0.45
0.50
0.55
0.60
0.65
0.70
0.75
0.80
0.85
WAVELENGTH (μm)

TABLE 2. Effects of nitrogen and iron deficiencies and St. Augustine Decline on visible reflectance of St. Augustine grass

	Reflectance (%) at selected wavelengths (μm)			
Treatment	0.55	0.60	0.63	0.65
NC[a]	14.5	9.5	8.0	6.5
IC	20.0	13.5	11.0	8.5
NN	18.0	10.5	8.5	6.0
IN	23.0	15.0	12.0	9.0
NFe	24.0	16.0	13.0	9.0
IFe	30.0	22.5	19.0	14.0

[a]Abbreviations: NC = noninfected control; IC = infected control; NN = noninfected, nitrogen-deficient; IN = infected, nitrogen-deficient; NFe = noninfected, iron-deficient; IFe = infected, iron-deficient.

levels resulting from the different treatments (Table 3).

Because most of the hydroponically grown plants consisted of only a few long stolons and relatively few leaves, VISS field spectrometer data were adversely affected by a high percentage of background reflectance which varied from container to container.

A second group of experiments were done using plants grown in sand culture. This was done because plants grown in sand culture provided targets which simulated natural grass canopies more closely than did hydroponically grown plants. Cary 14 measurements from plants grown in sand culture produced reflectance curves very similar to those presented for hydroponically grown plants in Fig. 30 (p. 85) and Fig. 32 (p. 90).

VISS reflectance data in the visible region (Figs. 33 and 34) corresponded to Cary 14 data concerning relative peak heights of noninfected and infected deficiency treatments. VISS measurements also provided information about infrared (0.75-2.5 μm) reflectance of the various treatments. In general, nitrogen and iron-deficient plants had about a 10% lower reflectance in this range. The only distinc-

TABLE 3. Elemental analysis of noninfected and St. Augustine Decline-infected nutrient treatments of St. Augustine grass

Treatment	Elemental content[a]	
	Nitrogen (%)	Iron (ppm)
NC[b]	3.49	143
IC	3.47	128
NN	1.64	--
IN	1.76	--
NFe	--	64.1
IFe	--	65.8

[a]Average of four replications.

[b]Abbreviations: NC = noninfected control; IC = infected control; NN = noninfected, nitrogen deficient; IN = infected, nitrogen-deficient; NFe = noninfected, iron-deficient; IFe = infected, iron-deficient.

Fig. 33. Spectral reflectance curves of healthy control, nitrogen-deficient, and iron-deficient St. Augustine grass determined with NASA's Visible-Infrared Spectrometer System.

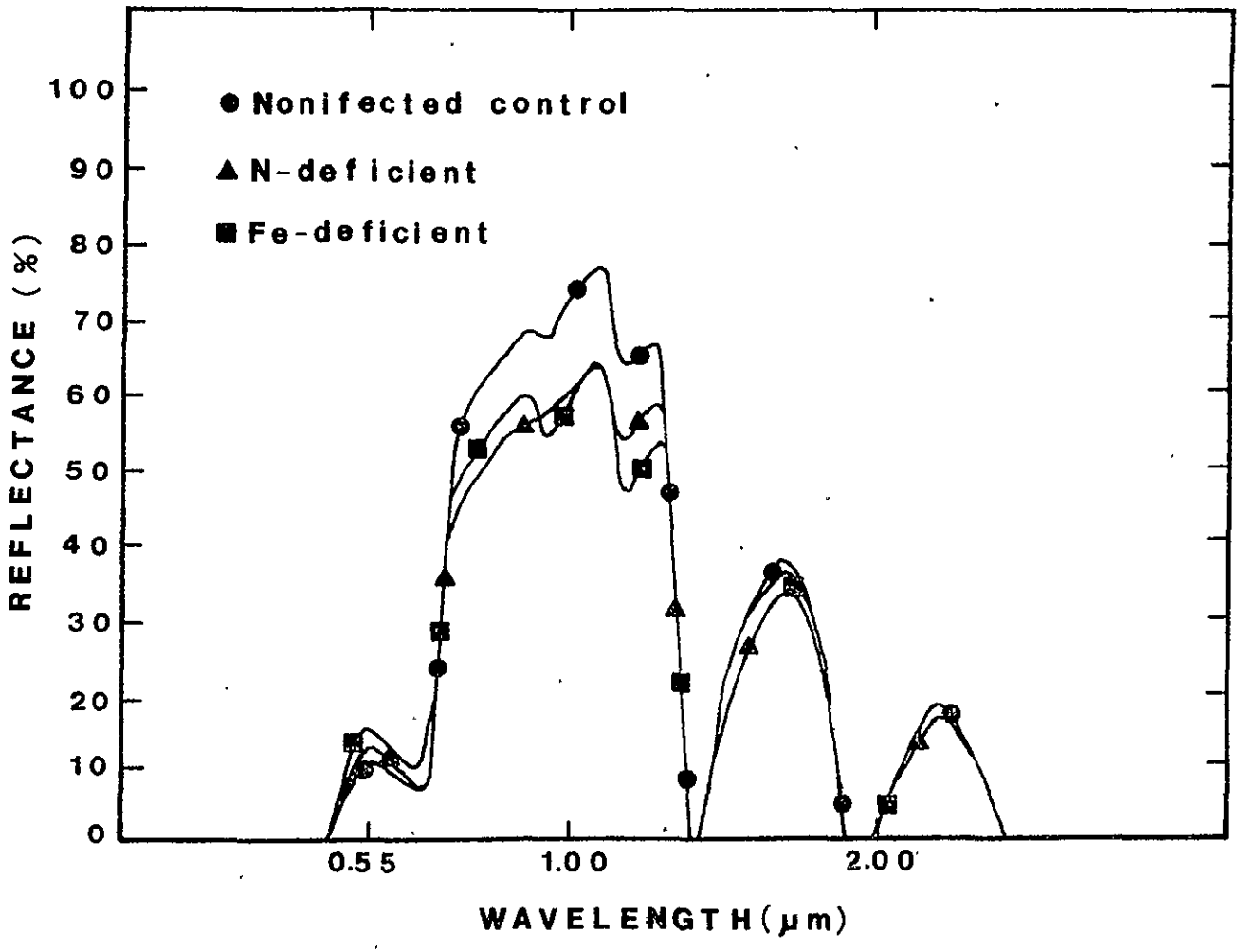
Nonifected control
N-deficient
Fe-deficient
REFLECTANCE (%)
100
90
80
70
60
50
40
30
20
10
0
0.55
1.00
2.00
WAVELENGTH (μm)

Fig. 34. VISS spectral reflectance curves of SAD-infected St. Augustine grass (control) and SAD-infected grass deficient in nitrogen or iron.

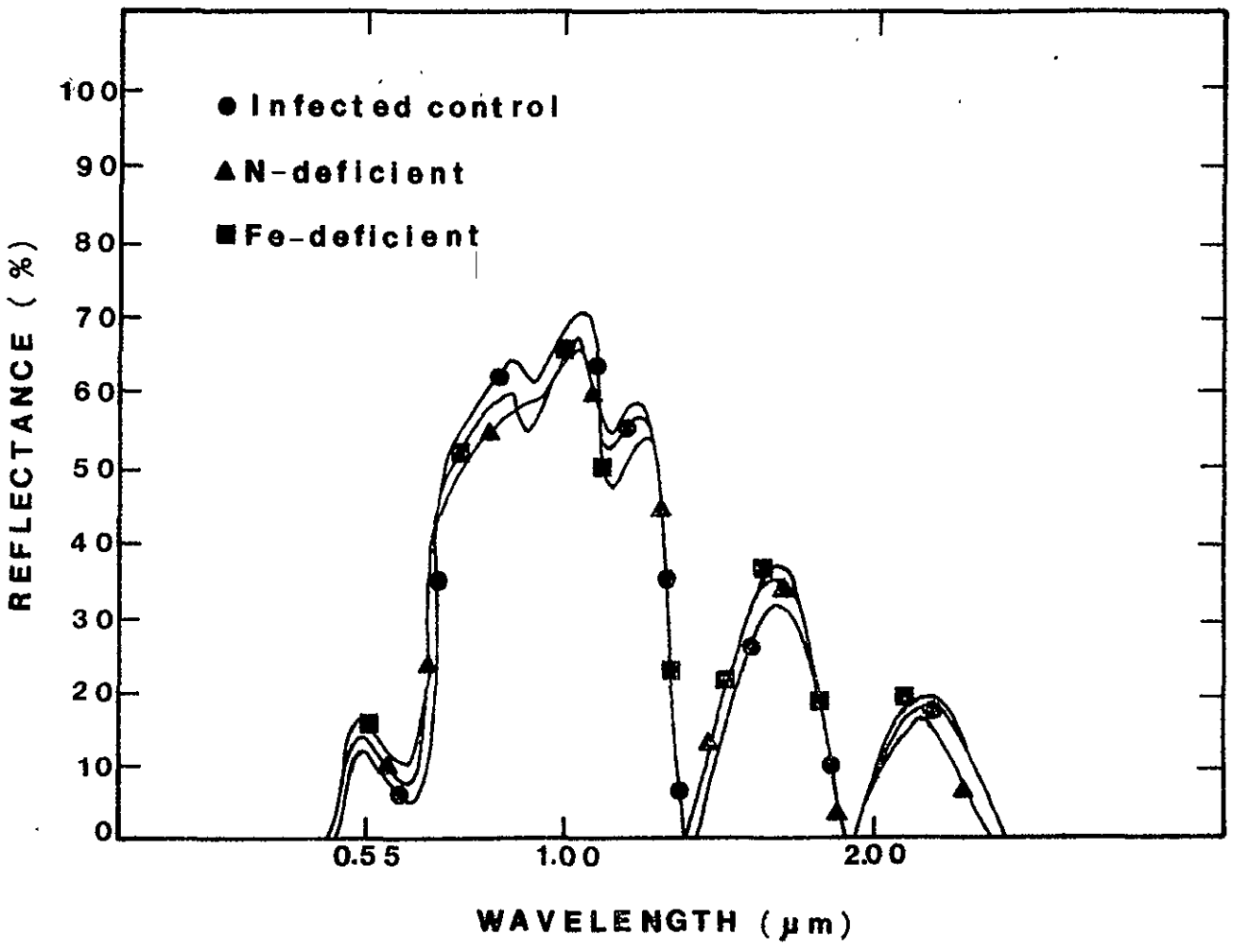
● Infected control
▲ N-deficient
■ Fe-deficient
REFLECTANCE (%)
100
90
80
70
60
50
40
30
20
10
0
0.55
1.00
2.00
WAVELENGTH (μm)

tive differences in reflectance patterns occurred at 0.9 and 1.1 μm. At these two wavelengths, iron-deficient plants indicated almost complete absence of the absorption band at 0.9 μm, with a much smaller reduction at 1.1 μm. In general, deficiencies caused a higher visible reflectance and a lower infrared reflectance. SAD also caused an increased visible reflectance; and although infrared reflectance was usually reduced, this reduction was variable and smaller than that observed for nutritional deficiencies.

Qualitative density analysis of multiband photographs using the Antech density slicer resulted in good differentiation of most treatments from noninfected controls. Best detail and differentiation were obtained in photographs taken during the afternoon with a red filter and polarizer. In density sliced photographs, noninfected controls exhibited a dark red color, while SAD and deficiency symptoms appeared as yellow, blue, and pink colorations (Fig. 35-B). Photographs taken at noon and during the afternoon with a blue filter and polarizer also showed some treatment differentiation (Fig. 35-C,D). Analysis of the same photographs utilizing the

Fig. 35 (A-F). Density slicing analysis (A-D) and multispectral viewer analysis (E,F) of multiband photographs taken of St. Augustine grass at noon and during the afternoon using maximum polarization. (1 = Healthy grass; 2 = Moderate St. Augustine Decline (SAD) infection; 3 = Severe SAD infection; 4 = Nitrogen deficiency; 5 = Nitrogen deficiency plus moderate SAD infection; 6 = Nitrogen deficiency plus severe SAD infection; 7 = Iron deficiency; 8 = Iron deficiency plus moderate SAD infection; 9 = Iron deficiency plus severe SAD infection). A) Red (25) filter at noon. B) Red filter during the afternoon. C) Blue (47B) filter at noon. D) Blue filter during the afternoon. E) Red filter at noon. F) Red filter during the afternoon.

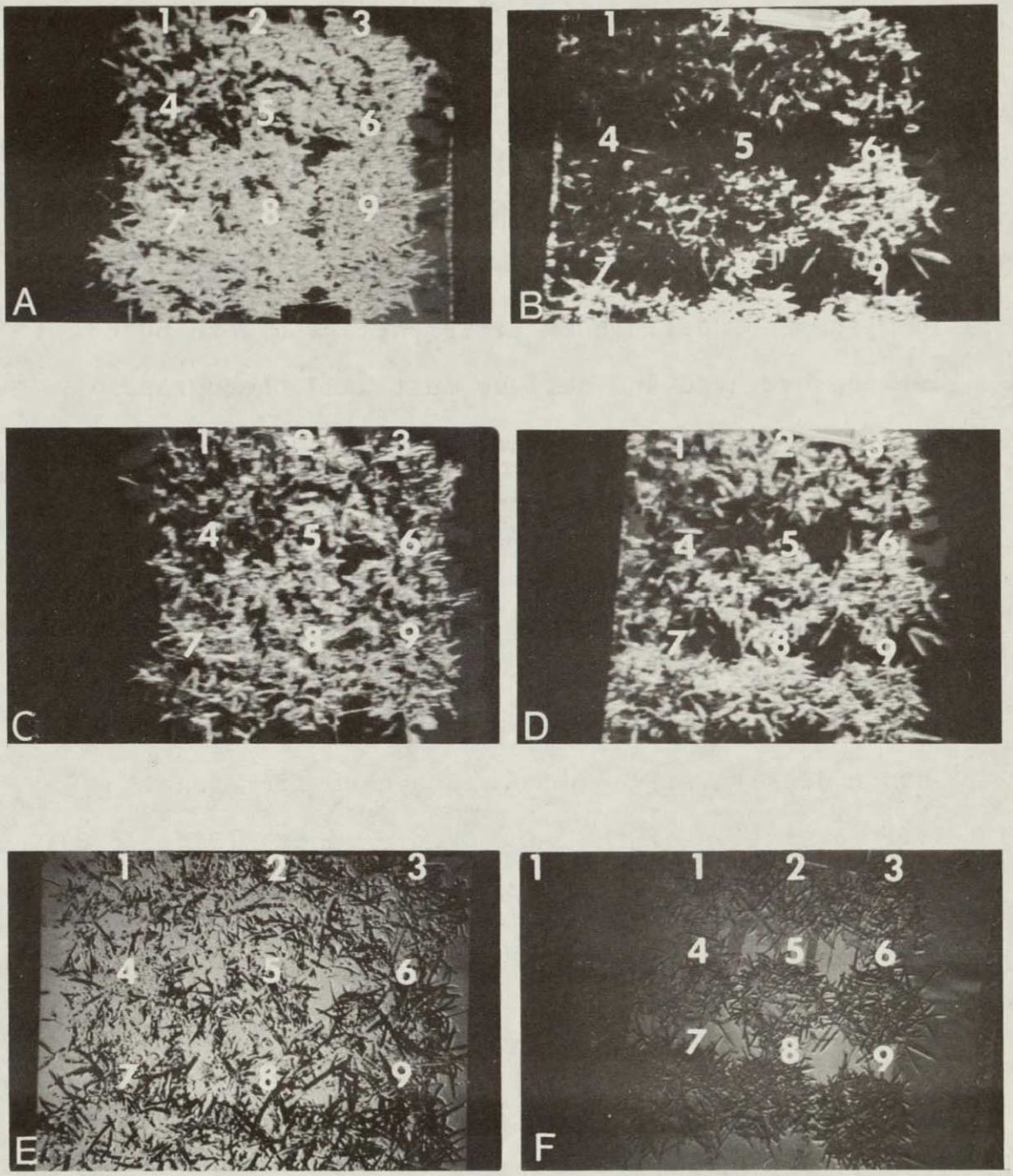

Spectral Data multispectral viewer produced poorer differentiation among the treatments (Fig. 35-E,F). Noninfected controls could be differentiated from the other treatments, but plants with various degrees of disease and deficiency symptoms were not easily distinquished from one another. No significant differences in disease or deficiency differentiation were noted between overhead and oblique multiband photographs.

Color infrared photographs also showed good separation of the various treatments from noninfected controls (Fig. 36-A). As expected, noninfected control plants appeared as a dark red color, while disease and deficiency symptoms produced lighter tones. Color enhancement of color infrared photographs using the Antech density slicer produced even better tonal differentiation of the various treatments (Fig. 36-B). Quantitative measurements with the Macbeth transmission densitometer also showed good differentiation (Table 4). Density measurements of noninfected control plants using visible, blue, and green filters were substantially higher than those of noninfected nitrogen and iron-deficient plants. Increases in disease severity also resulted in decreased density values for all

Fig. 36 (A,B). Photographs of nutrient treatments of noninfected and SAD-infected St. Augustine grass (1 = Healthy grass; 2 = Moderate SAD infection; 3 = Severe SAD infection; 4 = Nitrogen deficiency; 5 = Nitrogen deficiency plus moderate SAD infection; 6 = Nitrogen deficiency plus severe SAD infection; 7 = Iron deficiency; 8 = Iron deficiency plus moderate SAD infection; 9 = Iron deficiency plus severe SAD infection). A) Color infrared photograph. B) Density slicing analysis of the same color infrared photograph.

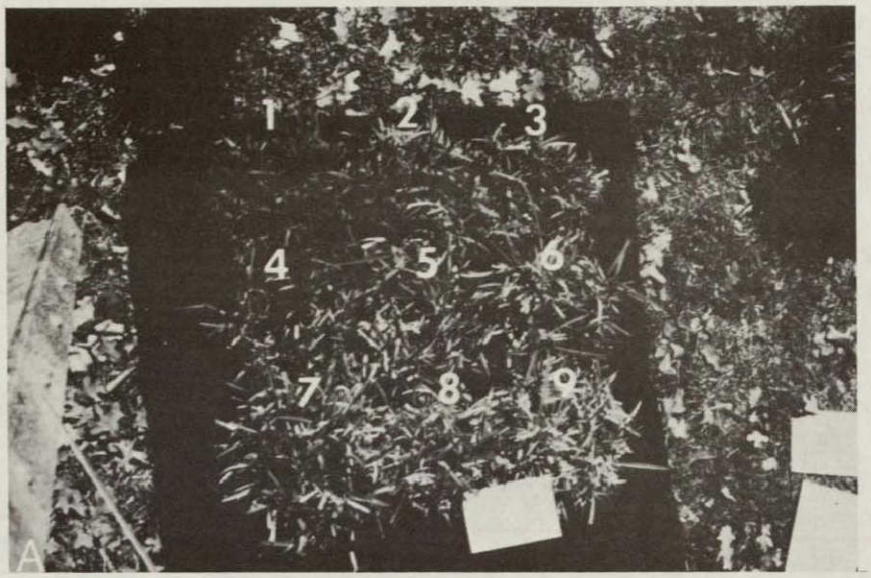

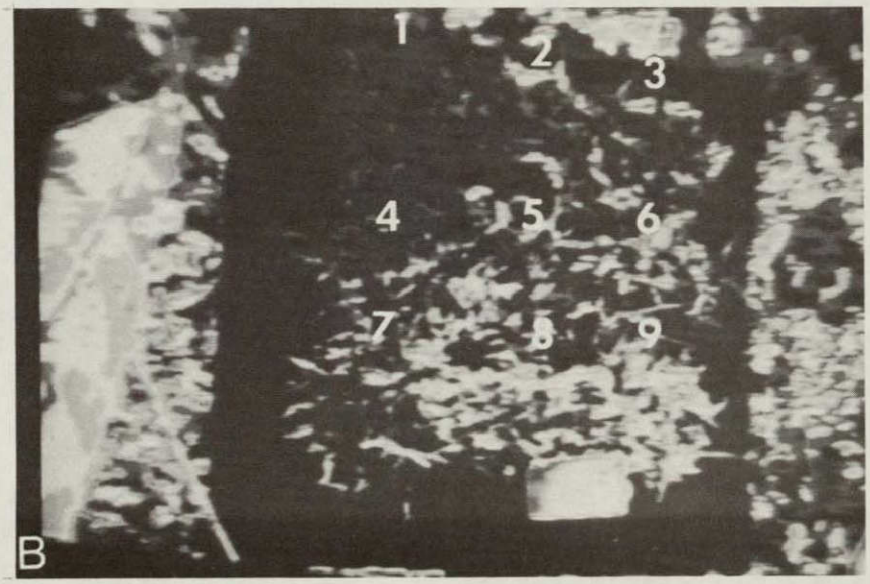

TABLE 4. Transmission densitometer measurements from color infrared photograph showing noninfected and St. Augustine Decline-infected nutrient treatments of St. Augustine grass

Treatment	Film density[a]			
	V[b]	B	G	R
NC	1.57	1.58	1.97	1.15
IC1	1.24	1.11	1.46	1.00
IC2	1.09	0.97	1.17	1.01
NN	1.25	1.10	1.35	1.14
IN1	1.05	0.91	1.16	0.96
IN2	0.98	0.81	1.02	1.02
NFe	1.21	1.02	1.36	1.03
IFe1	0.98	0.82	1.08	0.88
IFe2	0.80	0.67	0.82	0.89

[a]Average of four measurements.

[b]Abbreviations: V = visible filter; B = blue filter; G = green filter;

TABLE 4. [b]Abbreviations (continued)

R = red filter; NC = noninfected control; IC1 = moderately infected control; IC2 = severely infected control; NN = noninfected, nitrogen-deficient; IN1 = moderately infected, nitrogen-deficient; IN2 = severely infected, nitrogen-deficient; NFe = noninfected, iron-deficient; IFe1 = moderately infected, iron-deficient; IFe2 = severely infected, iron-deficient.

nutrient treatments. Poorer differentiation was obtained from measurements made with the red filter.

An example of ERTS-band reflectance data, from one of three dates, is presented in Fig. 37. Reflectance in bands 1 and 2 was lowest for noninfected controls. SAD-infected controls exhibited higher reflectance, while noninfected and infected nitrogen-deficient plants had the highest values. Infected control and iron-deficient plants had higher reflectance values in bands 1 and 2 than noninfected ones. Very small differences among treatments occurred in band 2, with noninfected, iron-deficient plants exhibiting slightly higher values than other treatments. For band 4, a somewhat reversed situation was evident, in which nitrogen-deficient plants exhibited the least reflectance. Noninfected control and iron-deficient plants had higher values than infected ones. For different dates some variability occurred between noninfected and infected plants receiving the same nutrient treatment; however, reflectance patterns as influenced by nutrient treatments alone remained consistent.

Results from computer pattern recognition analysis are summarized in Table 5. Good discrimination was

Fig. 37. ERTS-band reflectance values for nutrient treatments of noninfected and SAD-infected St. Augustine grass leaves (NC = noninfected control; IC = infected control; NN = noninfected, nitrogen-deficient; IN = infected, nitrogen-deficient; NFe = noninfected, iron-deficient; IFe = infected, iron-deficient).

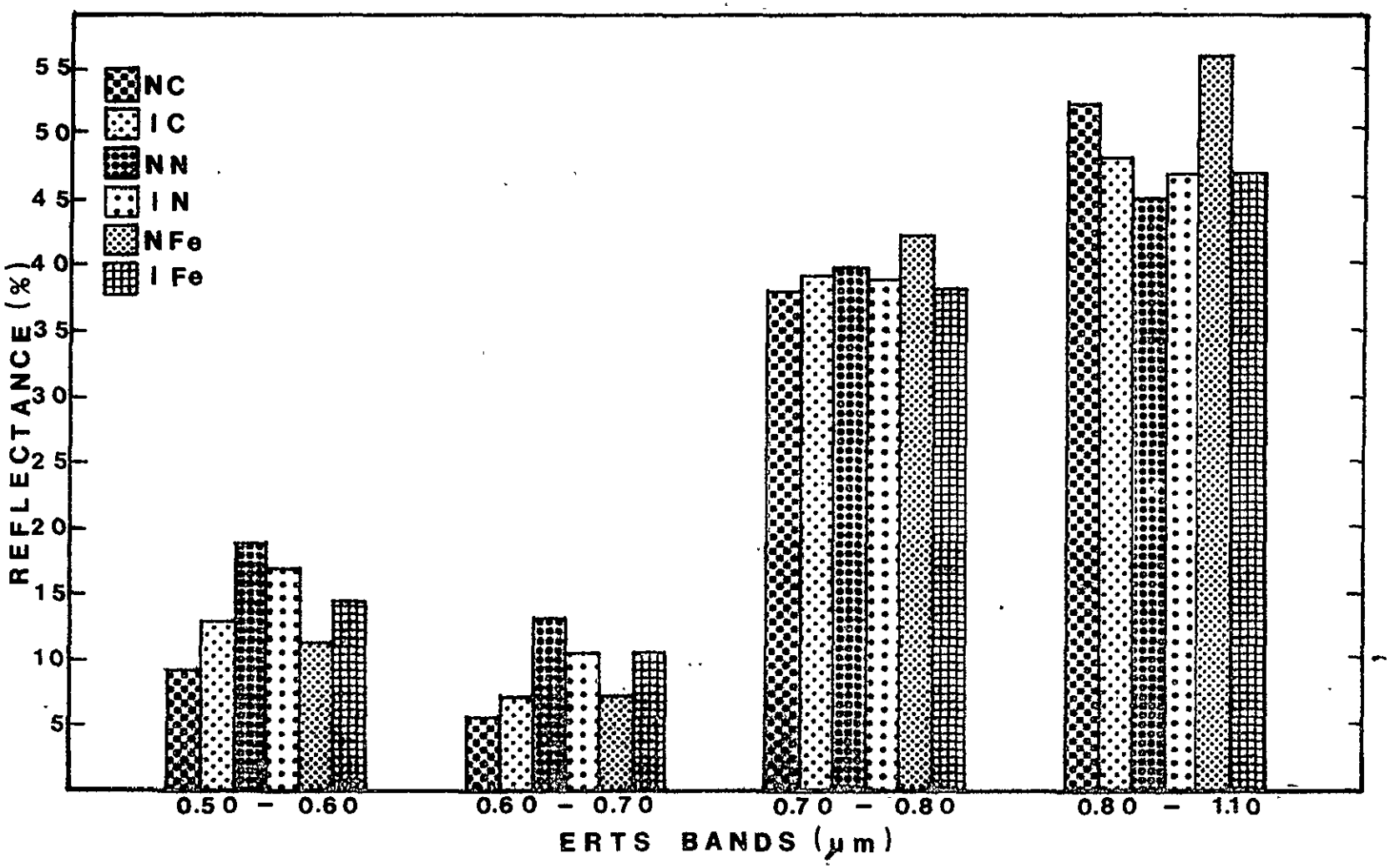
NC
IC
NN
IN
NFe
IFe
REFLECTANCE (%)
5
10
15
20
25
30
35
40
45
50
55
0.50 – 0.60
0.60 – 0.70
0.70 – 0.80
0.80 – 1.10
ERTS BANDS (μm)

TABLE 5. Transformed divergence analysis of ERTS-band reflectance data from noninfected and St. Augustine Decline (SAD)-infected nutrient treatments of St. Augustine grass

ERTS-Band Combination	Date	Transformed divergence (Dt)[a]						
		NC/IC[b]	NC/NN	NC/NFe	IC/IN	IC/IFe	IC/NN	IC/NFe
1 + 4	5/16	1.53	1.91	2.00	2.00	1.99	1.48	2.00
1 + 4	5/31	1.74	2.00	1.59	2.00	1.96	1.83	1.56
1 + 4	7/28	1.89	2.00	1.51	1.66	1.06	1.97	1.98
1 + 4	Mean	1.72	1.97	1.70	1.89	1.67	1.76	1.85
2 + 4	5/16	1.85	2.00	1.97	1.99	1.52	1.47	1.63
2 + 4	5/31	1.55	2.00	1.91	2.00	1.96	2.00	2.00
2 + 4	7/28	1.36	2.00	1.42	1.99	1.32	2.00	1.33
2 + 4	Mean	1.59	2.00	1.77	1.99	1.60	1.82	1.65
2 + 3	5/16	1.66	2.00	1.96	1.01	1.14	1.78	1.60

TABLE 5. Continued.

ERTS-Band Combination	Date	Transformed divergence (D_t)[a]						
		NC/IC[b]	NC/NN	NC/NFe	IC/IN	IC/IFe	IC/NN	IC/NFe
2 + 3	5/31	1.24	2.00	1.93	1.94	1.88	2.00	1.48
2 + 3	7/28	2.00	2.00	1.67	2.00	2.00	2.00	2.00
2 + 3	Mean	1.63	2.00	1.85	1.65	1.67	1.93	1.69

[a]D_t is a statistical technique which determines the dissimilarity of two distributions and therefore gives an indirect measure of the ability to discriminate between them. Values range from 0.0 to 2.0, with 2.0 representing maximum discrimination. Percent discrimination and D_t values are logarithmically related, so that a D_t of 1.0 represents 84% discrimination, not 50%.

[b]Abbreviations: NC = noninfected control; IC = infected control; NN = noninfected, nitrogen-deficient; IN = infected, nitrogen-deficient; NFe = noninfected, iron-deficient; IFe = infected, iron-deficient.

achieved for most treatment pairs using all three band combinations. Although transformed divergence (D_t) values for each treatment pair varied for different dates and band combinations, best overall results were achieved with band combinations 1 + 4 and 2 + 3. For example, the D_t for infected controls/infected, iron-deficient plants was the lowest (1.67) for all treatment pairs tested with bands 1 and 4. However, this value still represents a 96% discrimination ability. Overall results indicated that noninfected control plants could be adequately distinguished from infected controls and from noninfected deficiency treatments. Infected controls could also be distinguished from noninfected and infected deficiency treatments.

Leaf transmittance data obtained with the ERTS-band radiometer revealed that largest differences among treatments occurred in band 1 (0.5-0.6 μm) (Fig. 38). Transmittance values, which were lowest for noninfected control leaves, increased for noninfected nitrogen and iron-deficient leaves. Infected, nutrient-deficient leaves exhibited highest transmittance values in these two bands. Relatively small differences were observed among the various treatments using band 3 (0.7-0.8 μm). Fig. 39 illustrates how transmittance varied with in-

Fig. 38. ERTS-band transmittance values for nutrient treatments of noninfected and SAD-infected St. Augustine grass leaves (NC = noninfected control; IC = infected control; NN = noninfected, nitrogen-deficient, IN = infected, nitrogen-deficient; NFe = noninfected, iron-deficient; IFe = infected, iron-deficient).

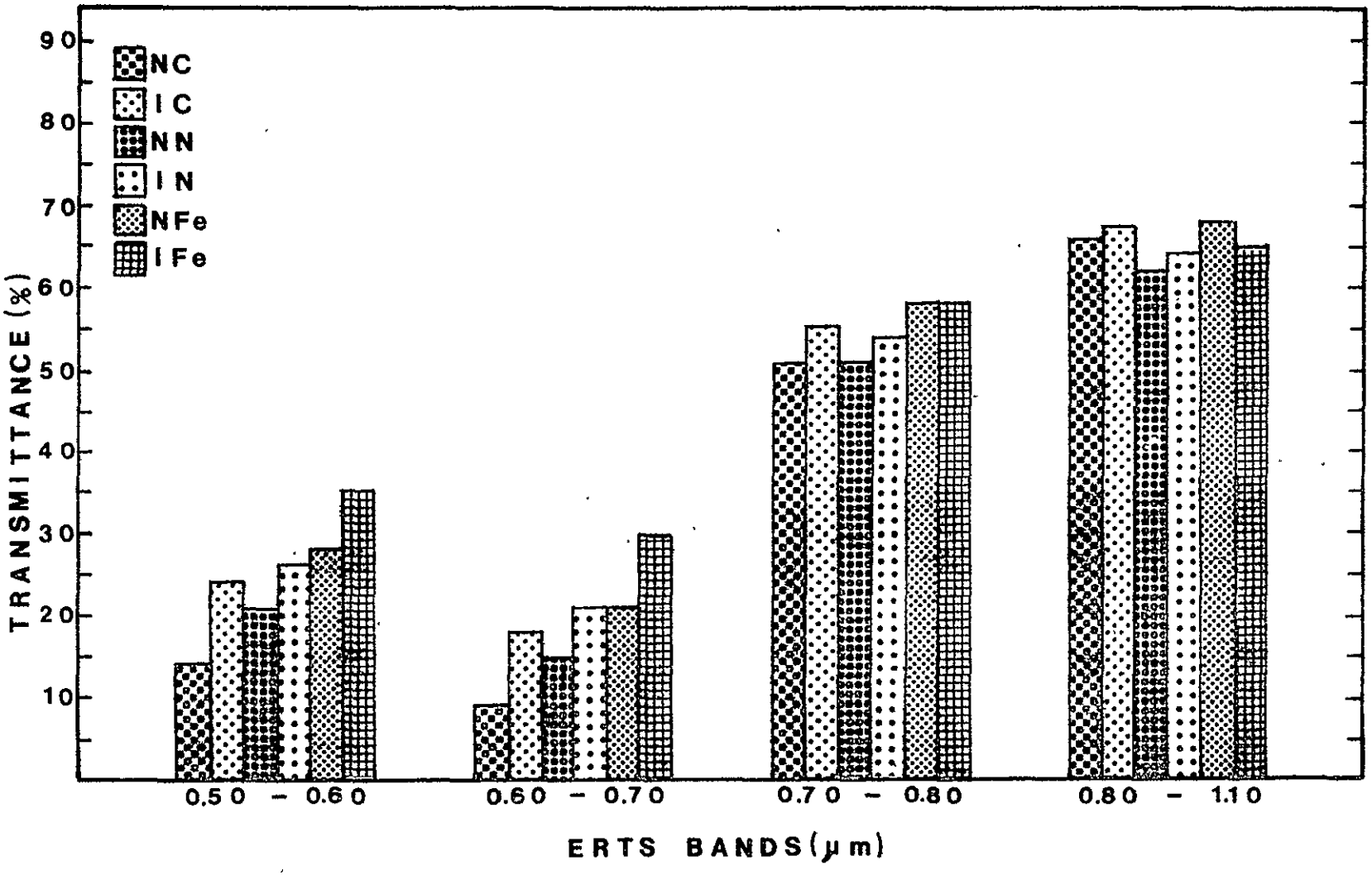
NC
IC
NN
IN
NFe
IFe
TRANSMITTANCE (%)
90
80
70
60
50
40
30
20
10
0.50 - 0.60
0.60 - 0.70
0.70 - 0.80
0.80 - 1.10
ERTS BANDS(μm)

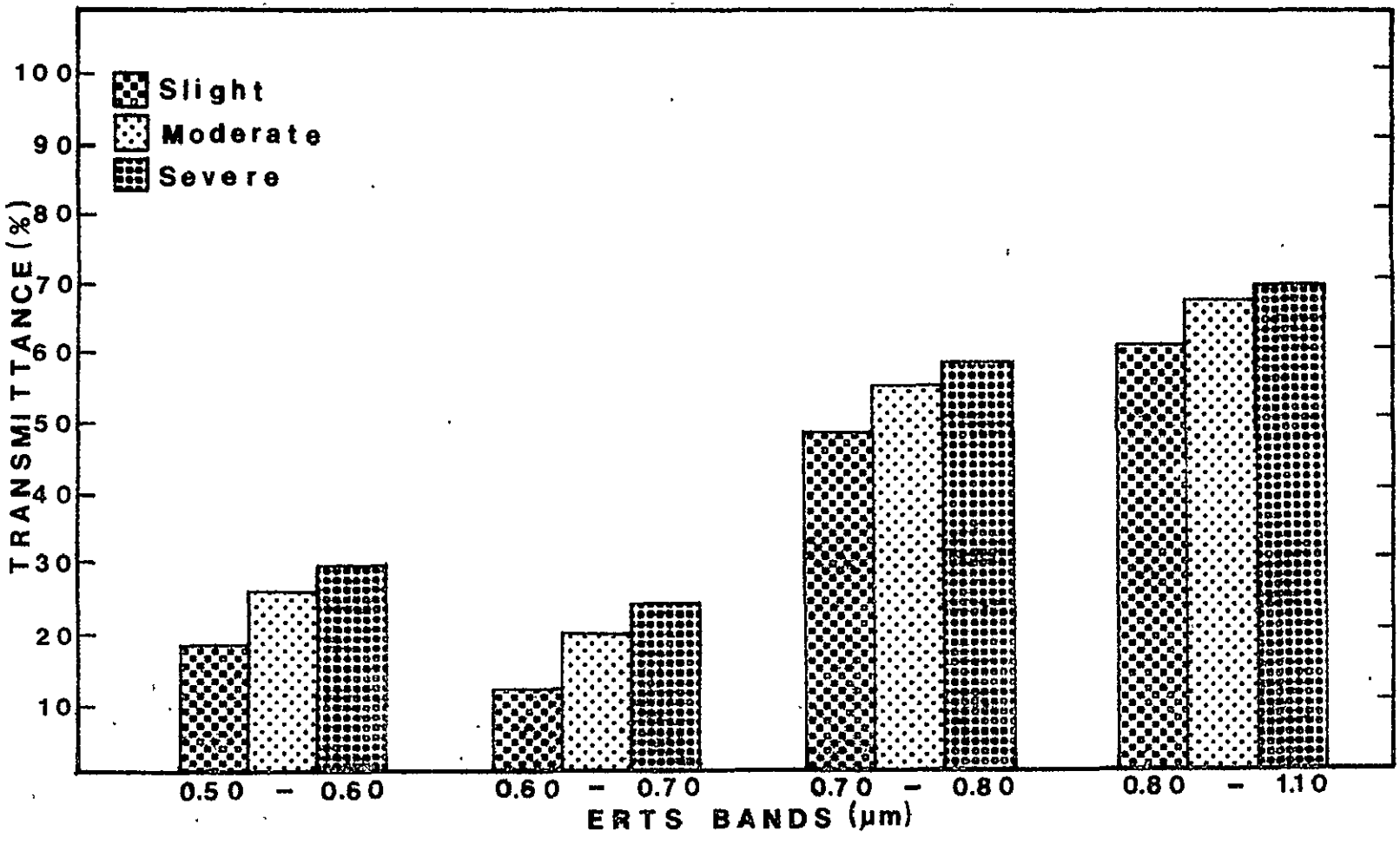

Fig. 39. ERTS-band transmittance values for St. Augustine grass leaves exhibiting different intensities of St. Augustine Decline symptoms.

creased disease intensity. For all bands, transmittance increased as symptom severity increased.

Canopy temperatures of the various treatments proved to be quite variable from one date to another because of changes in ambient air temperature, cloud cover, wind, and water status of the plants. Figure 40 illustrates the results from one set of temperature data recorded in sunlight at an ambient air temperature of 28°C. Although relative temperature patterns among treatments were not consistent for every data set, some general characteristics were evident from data gathered on several different dates. Nitrogen-deficient plants had the highest canopy temperatures, averaging about 1.5°C warmer than control plants. Iron-deficient plants were usually around 0.5°C cooler than controls, but the reverse was true for some dates. In general, infected replications of each nutrient treatment had slightly higher (0.5-0.8°C) temperatures than noninfected ones. Although temperatures of shaded plants were lower, relative differences and patterns among treatments were similar to those shown from data taken in full sunlight.

The average chlorophyll, moisture, and deficient-element content of each treatment is summarized in

Fig. 40. Temperature measurements for nutrient treatments of noninfected and SAD-infected St. Augustine grass taken in sunlight and an ambient air temperature of 28°C (NC = noninfected control; IC = infected control; NN = noninfected, nitrogen-deficient, IN = infected, nitrogen-deficient; NFe = noninfected, iron-deficient; IFe = infected, iron-deficient).

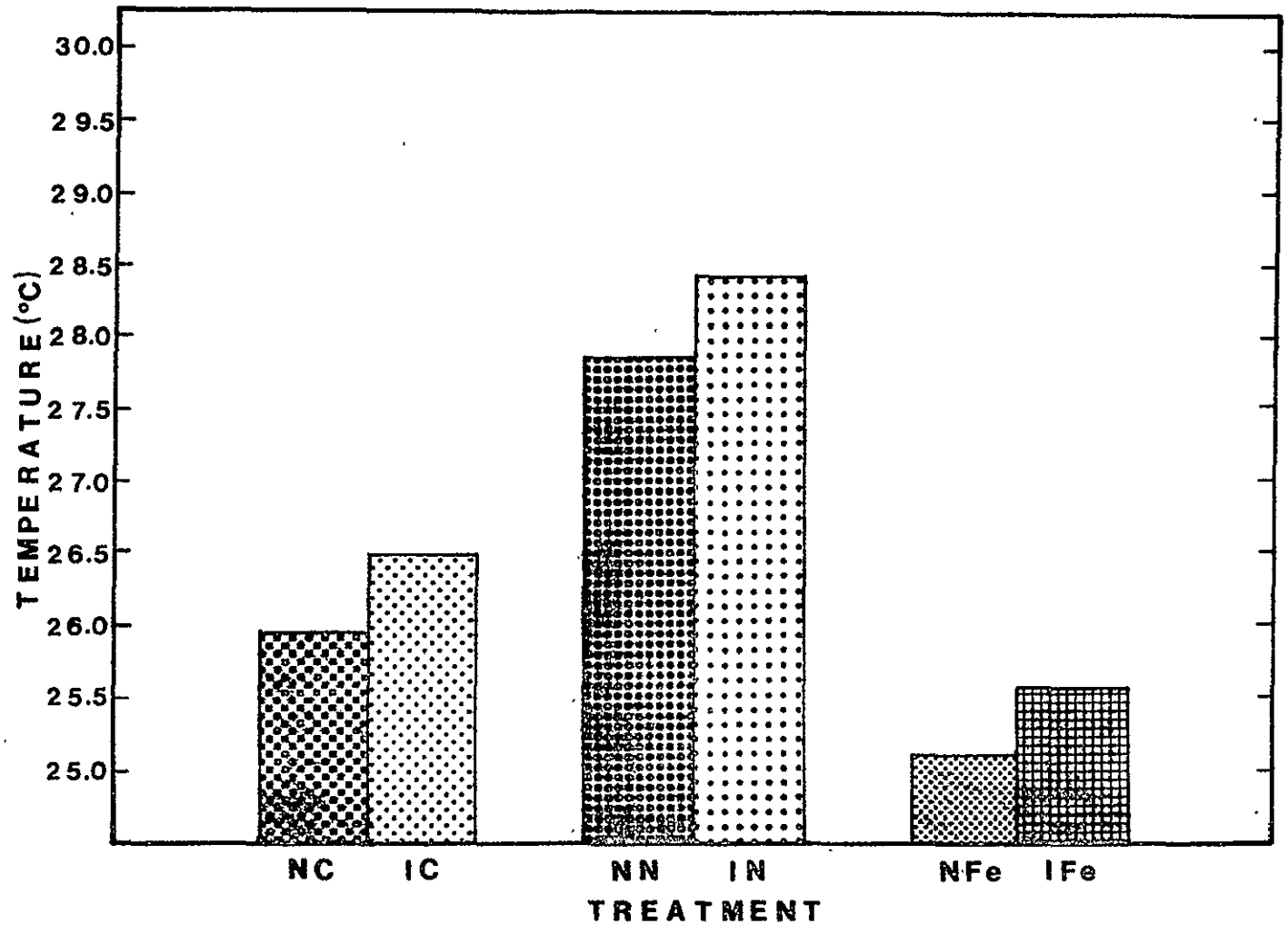
30.0
29.5
29.0
28.5
28.0
27.5
27.0
26.5
26.0
25.5
25.0
TEMPERATURE (°C)
NC
IC
NN
IN
NFe
IFe
TREATMENT

Table 6. Total chlorophyll content, as compared to control plants, was lower for nitrogen and iron-deficient plants. Deficient plants infected with SAD Virus contained even smaller amounts of chlorophyll. Elemental analysis revealed that oven-dried leaf tissue from control plants contained more than twice as much nitrogen as tissue from nitrogen-deficient plants. Similar results were shown concerning the iron content of control and iron-deficient plants. Control plants and iron-deficient plants contained similar amounts of moisture (79-80%), while nitrogen-deficient plants contained significantly less (73-74%).

TABLE 6. Elemental, chlorophyll, and moisture content of noninfected and St. Augustine Decline-infected nutrient treatments of St. Augustine grass

Treatment	Moisture content[c]	Chlorophyll content[a]		Elemental content[b]	
	(%)	mg/g	mg/cm^2	Nitrogen (%)	Iron (ppm)
NC[d]	80.0	1.60	0.023	2.67	205
IC	79.8	1.29	0.018	2.15	186
NN	73.5	0.96	0.015	1.05	--
IN	74.0	0.76	0.012	1.22	--
NFe	79.3	0.87	0.011	--	92
IFe	79.6	0.70	0.010	--	88

[a,b,c]Average of four replications.

[d]Abbreviations: NC = noninfected control; IC = infected control; NN = noninfected, nitrogen-deficient; IN = infected, nitrogen-deficient; NFe = noninfected, iron-deficient; IFe = infected, iron-deficient.

Effects of Soil-Water Stress on Optical Properties of St. Augustine Grass

Water potentials, % moisture, and temperatures of each stress level are shown in Table 7. When fully watered, plants had water potentials of -14.0 to -16.1 bars. Moisture contents ranged from 77-81%. Temperatures measured with plants in sunlight showed variability among plants (33.8-38.6°C), even though they had all been fully watered two days earlier. However, temperatures recorded with plants in shade were similar, ranging from 30.3 to 30.7°C. Because of factors such as ambient air temperature, it is difficult to compare temperature values measured on different dates. Therefore, measurements were made from fully watered control plants on each date for comparison with stressed plants.

At moderate stress levels, stressed plants had water potentials ranging from -16.6 to -21.6 bars and moisture contents of 76 to 74%. Sunlight and shade temperature ranges were 37.7-39.7°C and 28.0-28.4°C, respectively (Table 7). Noninfected and infected control plants both had moisture contents of 78% and water potentials of -16.0 and -15.5 bars, respectively. Sunlight and shade temperatures

TABLE 7. Water potential, moisture content, and temperature of noninfected and St. Augustine Decline (SAD)-infected water stress treatments of St. Augustine grass

Treatment	Water potential[a] (bars)	Moisture[b] (%)	Temperature (°C)[c] Sun	Shade
Fully watered				
NC[d]	-15.7	79	33.8	30.3
N1	-16.1	77	38.5	30.7
N2	-14.5	81	36.5	30.3
IC	-14.0	81	34.6	30.3
I1	-15.2	80	37.5	30.4
I2	-15.9	78	38.6	30.6
Moderate stress				
NC	-16.0	78	32.4	26.4
N1	-20.1	74	39.7	28.0
N2	-19.9	75	37.7	28.3
IC	-15.5	78	33.3	25.9
I1	-21.6	74	39.6	28.4
I2	-16.6	76	38.8	28.4

TABLE 7. Continued.

Treatment	Water potential[a] (bars)	Moisture[b] (%)	Temperature (°C)[c] Sun	Shade
Severe stress				
NC[d]	-15.5	78	33.4	31.0
N1	-29.8	60	40.8	33.2
N2	-27.0	64	38.5	34.1
IC	-15.4	79	34.0	30.4
I1	-25.6	67	40.7	33.4
I2	-30.4	58	41.1	34.2

[a]Mean values from pressure bomb measurements of five leaves.

[b]Determined from fresh and oven-dried weights of leaf samples using the following formula:

$$\% \text{ moisture} = \frac{\text{fresh weight-dry weight}}{\text{fresh weight}} \times 100$$

[c]Mean values of twenty readings made with a portable infrared thermometer.

[d]Abbreviations: NC = noninfected, fully watered control; N1 = noninfected, water stress replication #1; N2 = noninfected, water stress replication #2; IC = infected, fully-watered control; I1 = infected, water stress replication #1; I2 = infected, water stress replication #2.

of the noninfected control were 32.4 and 26.4°C, respectively, while those for the infected control were 33.3 and 25.9°C.

At severe stress levels, water potentials of stressed plants fell to values of -25.6 to -30.4 bars, as compared to those of control plants which remained around -15.5 bars (Table 7). Moisture contents of stressed plants ranged from 67 to 58%, and sunlight and shade temperatures were 38.5-41.1°C and 33.2-34.2°C, respectively. Noninfected and infected control plants exhibited sunlight temperatures of 33.4 and 34.0°C and shade temperatures of 31.0 and 30.4°C, respectively.

Results from qualitative density analysis of multiband photographs using the Antech density slicer are shown in Figs. 41 and 42. Photographs made at the beginning of the experiment (Fig. 41-A,B,C) showed good differentiation of noninfected and infected plants using a red, blue, or green filter plus maximum polarization. One of the noninfected plants (N1) exhibited a slightly different density than the other two noninfected plants. This plant had a lower water potential and moisture content at this time than the other two plants (Table 7).

Fig. 41 (A-F). Density slicing analysis of multi-band photographs of noninfected and SAD-infected, fully watered (A-C) and moderately moisture-stressed (D-F) St. Augustine grass taken with maximum polarization (NC = noninfected, fully watered control; N1 = non-infected water stress replication #1; N2 = noninfected, water stress replication #2; IC = infected, fully-watered control; I1 = infected water stress replication #1; I2 = infected water stress replication #2). A,D) Red (25) filter. B,E) Blue (47B) filter. C,F) Green (58) filter.

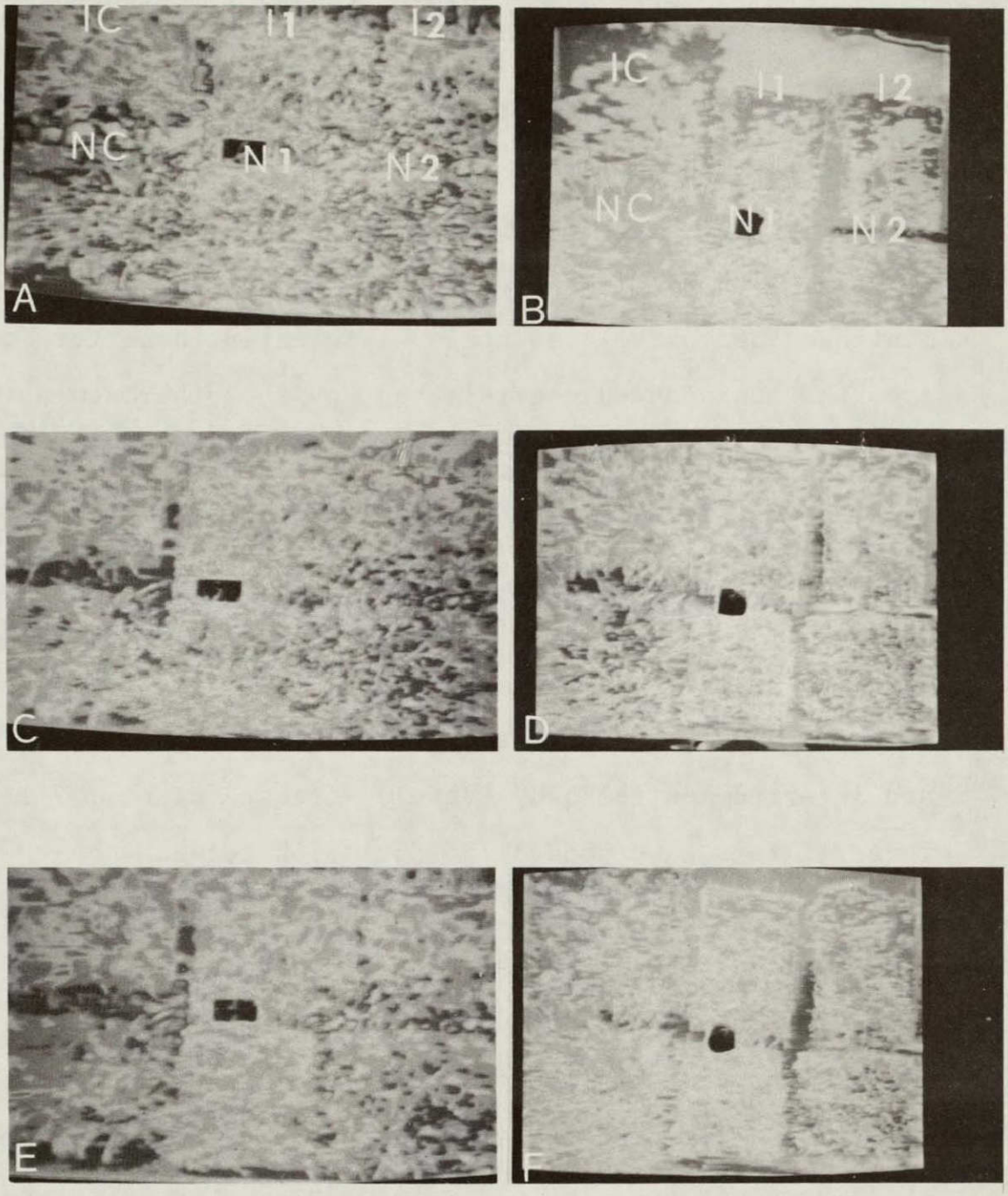

Fig. 41-D,E,F shows noninfected and infected control and moderately stressed plants. Photographs taken with red (Fig. 41-D) and green (Fig. 41-F) filters gave best differentiation between noninfected and infected control plants and between control and water-stressed plants. The same noninfected, stressed plant mentioned above (N1) was again differentiated better from the noninfected control than was the other noninfected, stressed plant. Density changes resulting from moisture stress were more difficult to determine for SAD-infected plants because disease symptoms caused these plants to have lower film densities to begin with (Fig. 41-A,C,B).

Fig. 42 shows oblique photographs of noninfected and infected control and severely stressed plants. All three filters gave good differentiation between noninfected and infected control plants and between control and stressed plants. Density differences between noninfected control and noninfected stressed plants were clearly apparent. Although differences between infected control and infected stress plants were also present, these were not as easy to distinguish. Severely stressed noninfected and infected plants looked very similar. Wilting and reduced leaf area resulting from water

Fig. 42 (A-C). Density slicing analysis of oblique multiband photographs of noninfected and SAD-infected, fully watered and severely moisture-stressed St. Augustine grass taken with maximum polarization (NC = noninfected, fully watered control; N1 = noninfected water stress replication #1; N2 = noninfected, water stress replication #2; IC = infected, fully-watered control; I1 = infected water stress replication #1; I2 = infected water stress replication #2). A) Red (25) filter. B) Blue (47B) filter. C) Green (58) filter.

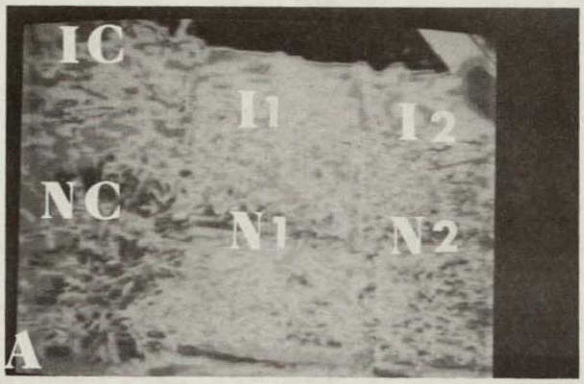

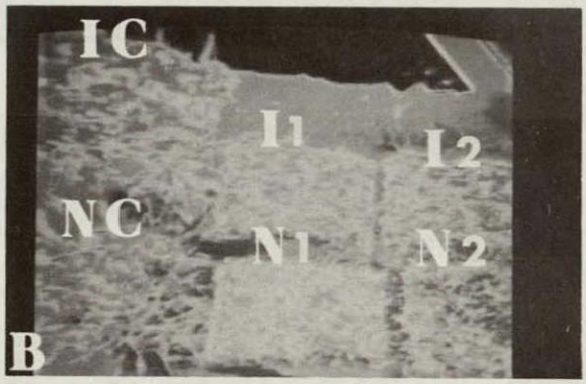

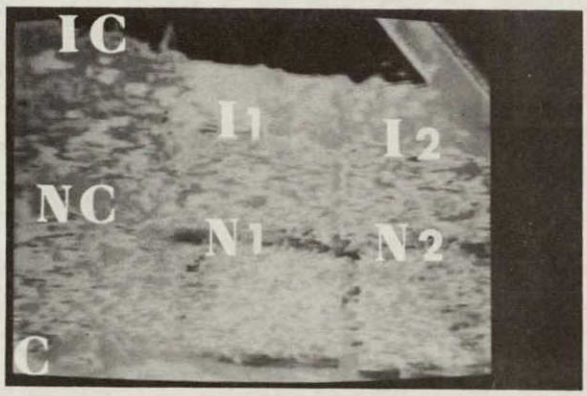

stress caused noticeable differences in the size and shape of canopies of control and stressed plants.

Fig. 43 shows color infrared photographs of the plants at the beginning of the experiment (Fig. 43-A) and at the end of the experiment when they were under severe stress (Fig. 43-B). Because infected plants exhibited only moderate disease symptoms without extensive chlorosis, density differences between noninfected and SAD-infected controls were not extreme. However, striking tonal differences did occur between control and stressed plants. Stress-induced tonal differences masked the differences originally noted between noninfected and infected plants.

Using density slicing techniques, tonal differences in color infrared photographs were enhanced to reveal significant density differences between noninfected and infected control plants and between control and stressed plants (Fig. 44). These differences were similar to those seen in multiband photographs of the same plants (Fig. 43).

Transmission densitometer measurements from color infrared photographs (Table 8) showed small differences between noninfected and infected control plants and between control and moderately stressed plants. Large

Fig. 43 (A,B). Color infrared photographs of non-infected and SAD-infected, fully watered and moisture-stressed St. Augustine grass (NC = noninfected, fully watered control; N1 = noninfected water stress replication #1; N2 = noninfected water stress replication #2; IC = infected, fully watered control; I1 = infected water stress replication #1; I2 = infected water stress replication #2). A) All plants fully watered. B) NC, IC fully watered and N1, N2, I1, I2 severely stressed.

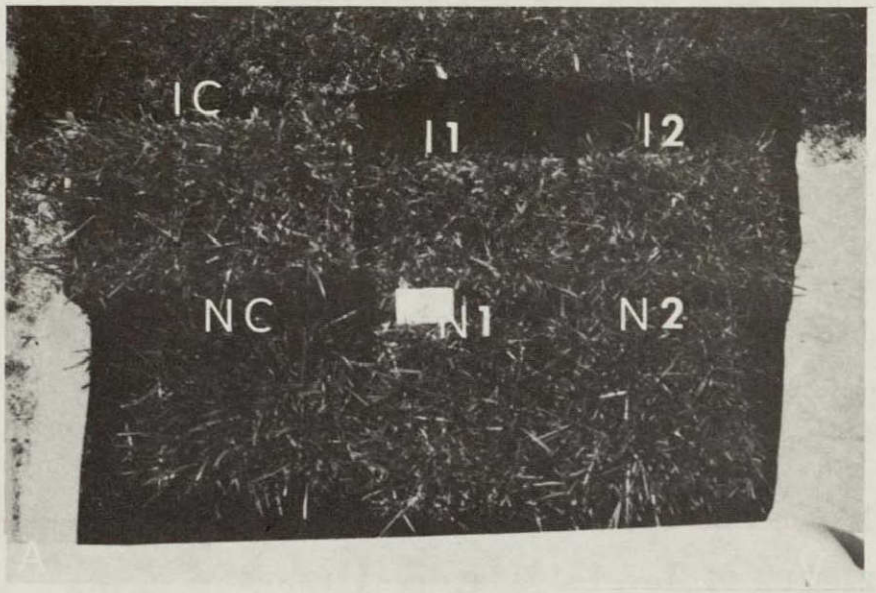

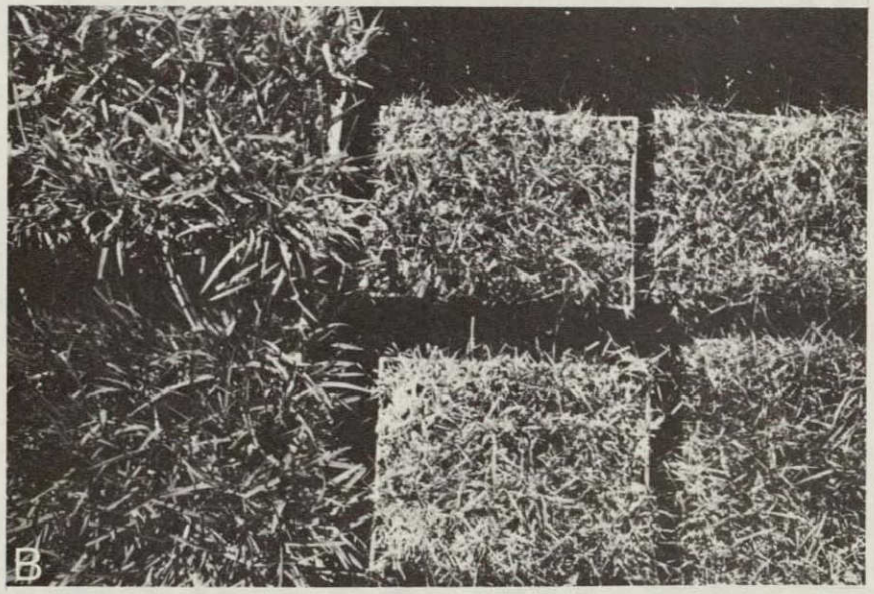

Fig. 44 (A,B). Density slicing analysis of color infrared photographs of noninfected and SAD-infected fully watered and moisture stressed St. Augustine grass (NC = noninfected, fully watered control; N1 = noninfected water stress replication #1; N2 = noninfected water stress replication #2; IC = infected, fully watered control; I1 = infected water stress replication #1; I2 = infected water stress replication #2). A) All plants fully watered. B) NC, IC fully watered and N1, N2, I1, I2 severely water-stressed.

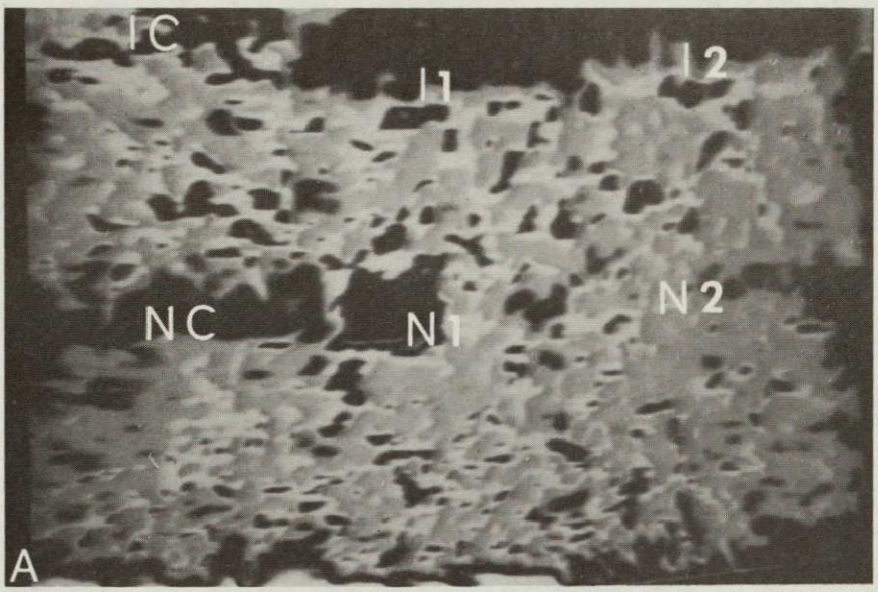

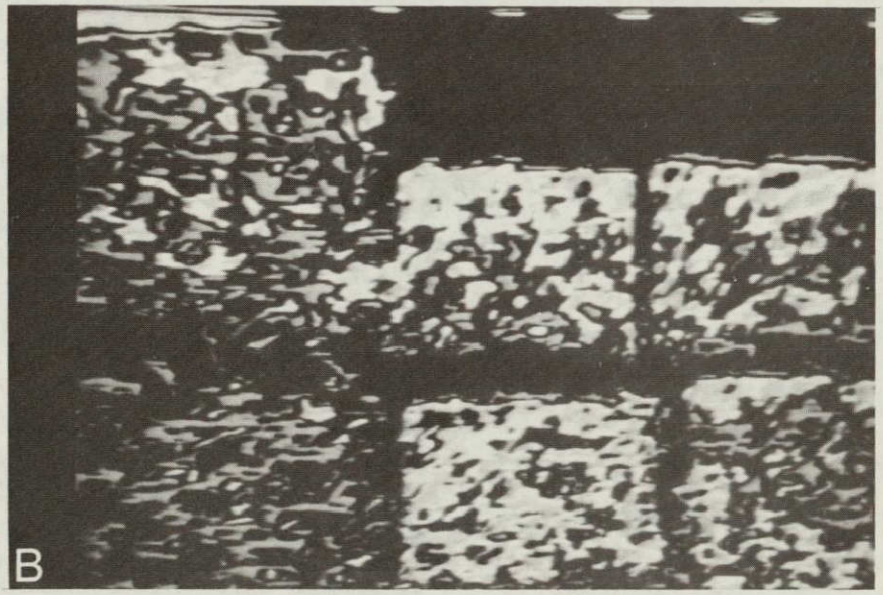

TABLE 8. Transmission densitometer measurements from color infrared photographs of noninfected and SAD-infected, fully watered and moisture-stressed St. Augustine grass

	Film Density[a]			
Treatment	V[b]	B	G	R
Fully watered				
NC	1.40	1.36	1.85	0.96
N1	1.37	1.34	1.79	0.97
N2	1.40	1.37	1.83	0.96
IC	1.33	1.21	1.69	0.94
I1	1.33	1.26	1.71	0.94
I2	1.35	1.30	1.77	0.95
Moderate stress				
NC	1.52	1.32	1.79	1.25
N1	1.36	1.19	1.55	1.20
N2	1.50	1.33	1.70	1.31
IC	1.48	1.29	1.65	1.23
I1	1.42	1.24	1.58	1.30
I2	1.46	1.27	1.64	1.28

density differences were found between control and severely infected plants using visible, blue, and green filters. Smaller, inconsistent differences were revealed with the red filter.

ERTS-band reflectance data from control and severely stressed plants are presented in Fig. 45. In bands 1 and 2, the infected control plant exhibited slightly higher reflectance than the noninfected control. All stressed plants had higher reflectance values in these two bands than both controls. A reverse pattern was evident in band 3, and more so in band 4. The noninfected control had a higher reflectance than the infected control, and both control plants exhibited higher reflectances than any of the stressed plants.

ERTS-band reflectance data from control and severely stressed plants were used in combination with previously discussed ERTS-band data from the nutritional deficiency experiment to do a transformed divergence analysis (Table 9). All three channel combinations tested were effective in distinguishing noninfected and infected stressed plants from noninfected and infected control plants and nutrient-deficient plants. A high % discrimination was also shown

Fig. 45. ERTS-band reflectance measurements from noninfected and St. Augustine Decline (SAD)-infected fully watered and moisture-stressed St. Augustine grass (NC = noninfected, fully watered control; N1 = noninfected water stress replication #1; N2 = noninfected, water stress replication #2, IC = infected, fully-watered control; I1 = infected water stress replication #1; I2 = infected water stress replication #2).

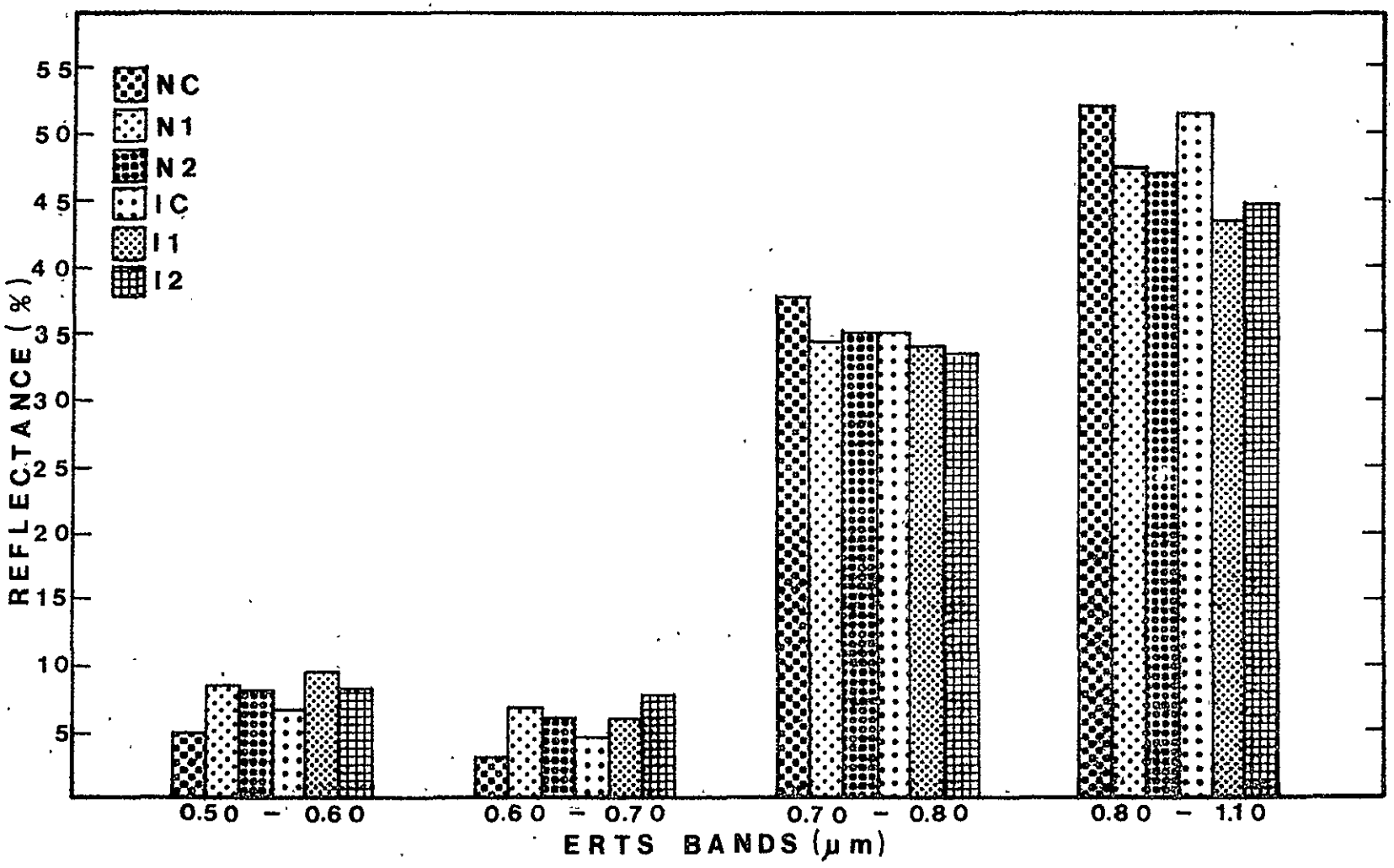
NC
N1
N2
IC
I1
I2
REFLECTANCE (%)
55
50
45
40
35
30
25
20
15
10
5
0.50 – 0.60
0.60 – 0.70
0.70 – 0.80
0.80 – 1.10
ERTS BANDS (μm)

TABLE 9. Transformed divergence analysis of ERTS-band reflectance data from moisture-stressed noninfected and St. Augustine Decline (SAD)-infected St. Augustine grass and noninfected and SAD-infected nutrient treatments

Bands combinations	Transformed divergence (D_t)[a]						
	NC[b]	IC	NN	IN	NFe	IFe	NS/IS
1 + 4							1.89
NS	2.00	1.41	2.00	2.00	2.00	1.54	
IS	2.00	1.72	1.99	2.00	2.00	1.21	
2 + 4							1.93
NS	2.00	1.99	2.00	1.88	2.00	1.04	
IS	2.00	1.49	2.00	1.96	2.00	2.00	
2 + 3							1.98
NS	1.97	2.00	2.00	2.00	1.97	1.45	
IS	1.97	2.00	1.73	2.00	1.93	2.00	

[a] D_t is a statistical technique which determines the dissimilarity of two distributions and therefore gives an indirect measure of the ability to discriminate between them. Values range from 0.0 to 2.0, with 2.0 representing maximum discrimination. Percent discrimination and D_t values are logarithmically related, so that a D_t of 1.0 represents 84% discrimination, not 50%.

TABLE 9. Continued.

[b]Abbreviations: NC = noninfected, fully watered; IC = infected, fully watered; NN = noninfected, nitrogen-deficient; IN = infected, nitrogen-deficient; NFe = noninfected, iron-deficient; IFe = infected, iron-deficient; NS = noninfected, water-stressed; IS = infected, water-stressed.

between noninfected and infected stressed plants. 85% or higher discrimination ability was indicated for all treatment pairs evaluated with the three ERTS-band combinations.

DISCUSSION AND CONCLUSIONS

Laboratory and field measurements revealed that all of the stress factors studied (St. Augustine Decline, nitrogen and iron deficiencies, and water stress) caused an increased reflectance of visible wavelengths (Figs. 21, 30, 31, 37, 45), (p. 68, 85, 87, 108, 138). Visible reflectance, which is affected by a wide array of physiological problems (49), is primarily governed by absorption from chlorophyll and other pigments so that a reduction in pigment content results in higher visible reflectance (31, 49, 61). In this study, nitrogen and iron deficiencies and SAD caused a reduction in the chlorophyll content of St. Augustine grass leaves (Table 6), (p. 119). Reduction in chlorophyll content and corresponding increase in reflectance of visible wavelengths has been shown for nitrogen (1, 52, 74, 73) and iron (35) deficiencies. Water stress has also been reported to cause increases in visible reflectance (49, 75).

Laboratory and field measurements of changes in infrared reflectance were not as consistent as those for visible reflectance. Some variability may have resulted from differences in disease and nutritional

deficiency development or from differences in measurement techniques. Cary 14 reflectance measurements from single layers of leaves placed in metal sample holders indicated an increased near infrared reflectance for SAD-infected grass (Fig. 21), (p. 68). EG & G field measurements from field plots with thick canopies indicated similar, but smaller differences (Fig. 22), (p. 69).

On the other hand, VISS measurements from container-grown grass having thinner canopies showed a slightly lower near infrared reflectance for infected plants and plants deficient in nitrogen or iron (Figs. 33, 34), (p. 95,97). Previous reports have also shown that plant diseases (15, 19, 47, 51, 63), nitrogen deficiency (1, 74) and iron deficiency (35) can cause lower than normal near infrared reflectance. VISS reflectance curves also indicated differences between treatments at minor water absorption bands located around 0.9 and 1.1 μm. The band at 0.9 μm was almost absent for nitrogen-deficient plants. Reflectance in this region is governed by water content and cellular arrangement (57). Although nitrogen-deficient plants exhibited lower water contents than control plants,

cellular changes within the leaves may have also contributed to this change. Iron-deficient plants, which exhibited the largest absorption at 0.9 and 1.1 μm, had water contents similar to controls. Gausman and his co-workers (35) reported that iron-deficient sorghum leaves reflected less near infrared radiation because they were thinner than healthy leaves and had a smaller number of mesophyll cells. ERTS-band radiometer data gave variable results from one date to another concerning effects of SAD and nutritional deficiencies on near infrared reflectance (Fig. 37, (p. 108). Reflectance values in band 3 (0.70-0.80 μm) were similar for all treatments, but SAD-infection and nitrogen-deficiency generally resulted in reduced reflectance values for channel 4 (0.80-1.10 μm).

Severely water-stressed plants exhibited lower reflectance in ERTS bands 3 and 4 (Fig. 45), (p. 138). Reduced reflectance may have been due primarily to reduction in leaf area from wilting, rather than a reduced infrared reflectance of individual leaves (49). Although some investigators have reported lower infrared reflectance from water-stressed leaves (20, 49), most have found the reverse situation

(increased reflectance) to be more typical (23, 52, 59, 74, 75).

Transmittance measurements with the ERTS radiometer indicated that SAD caused an increased transmittance in all bands (Fig. 39), (p. 114). Nutrient deficiencies also resulted in higher transmittance (Fig. 38), (p. 113) in bands 1, 2 and 3 with more variable results in band 4. Increased transmittance of visible wavelengths is related to chlorophyll reduction (reduced absorption of visible wavelengths) (3), while changes in near infrared reflectance are usually related to cellular structure and water content (57). Safir and his colleagues (62) attributed increased visible transmittance of corn leaves infected with Helminthosporium maydis (Nisikado and Miyake) Race T to reduced chlorophyll levels. Nitrogen (1) and iron (35) deficiencies have also been shown to cause increased visible and near infrared transmittance.

Polarization measurements with the Cary 14 spectrophotometer indicated that blue and red wavelengths reflected from healthy grass leaves were more highly polarized than those reflected from SAD-infected leaves (Fig. 3), (p. 5). The degree of polarization of reflected light is greatest for wavelengths which

are strongly absorbed by leaves (30). Because of the large polarization differences indicated by Cary 14 data, polarizing filters were used in conjunction with blue, green and red filters and black and white plus X type film to make multiband photos of healthy and infected field plots. Qualitative density analysis of the photographs using the I^2S density contouring and slicing instrument produced excellent differentiation of healthy and diseased grass (Fig. 24), (p. 73). Tonal differences could also be seen in photos taken without polarizers, but use of polarizers made these differences more apparent.

In aerial multiband photographs, polarization did not prove to be very useful for enhancement of disease detection in a direct sense. Severely diseased areas could be detected with and without using polarizing filters. However, another advantage of polarizers was noted. Several photographs taken with minimum polarization revealed certain noninfected areas in the lawn which exhibited film densities similar to those of SAD-infected grass (Fig. 27-A, C, E), (p. 78). In photographs of the same locations using maximum polarization, these confusion areas could be differentiated from infected grass (Fig. 27-B, D, F), (p. 78).

Ground surveys revealed that these areas consisted primarily of sparse, slightly yellowed turf resulting from dry, compacted soil, pedestrian traffic, and close mowing.

Aerial imagery was analyzed using the Antech density slicer, which is only capable of analyzing one photograph at a time. Better information may have been obtained with a density slicing instrument (such as the I^2S) capable of analyzing several superimposed photographs taken with different filters.

Ground-based multiband photographs demonstrated that illumination angle and look angle are important factors when dealing with polarization. Fig. 35 (p. 100) illustrates differences in tonal qualities resulting from two different sun angles. Although at both sun angles noninfected control plants could be differentiated from infected plants and plants deficient in nitrogen or iron, better differentiation among treatments was obtained at low sun angles. Working with grass turf, Coulson (21) has shown that low illumination angles result in increased polarization of reflected light at 0.492 μm. Look angle has also been shown by Coulson and his co-workers (22) to be a critical factor. With a fixed illumination angle, polarization of wavelengths

0.492 and 0.643 μm reached maximum at a look angle of 35° from nadir. In one instance, Coulson and his co-workers obtained a difference between indoor and outdoor polarization data even though factors such as illumination and look angles remained constant. They suggested this variability could be due to the fact that different grass samples were used for the two measurements, and also that the degree of polarization may depend upon factors such as blade density, differential growth patterns, blade orientation, etc. Some of these factors may also explain why better polarization effects were not seen in aerial multiband photographs. Multiband photographs taken from directly overhead and from a 45° look angle using a blue filter are shown in Fig. 41-E (p. 125) and Fig. 42-B (p. 128). Better differentiation of healthy and SAD-infected plants was obtained in the oblique photograph.

Noninfected, moderately and severely water-stressed plants were differentiated from noninfected control plants in multiband photos (Figs. 41, 42), (p. 125, 128). Water stress of SAD-infected plants was more difficult to discern because these plants had an above normal visible reflectance associated with SAD alone. Water stress exhibited a masking effect because non-

infected, stressed plants could not be differentiated from infected, stressed plants. Since spectral reflectance measurements had indicated that SAD, nutritional deficiencies, and water stress all have similar effects on visible reflectance, it is not surprising that these factors had similar tonal characteristics using the three visible bands employed for multiband photography. All of the stress factors could be differentiated from healthy grass, but differentiation of the factors from one another was not possible.

Although most disease symptoms can be detected in color photographs, color infrared film produces tonal contrasts which are more readily detected by the human eye (49). Loss of redness does not always denote a reduction in near infrared reflectance. Because the film has three emulsion layers which are sensitive to green, red, and near infrared wavelengths, visible reflectance plays a major role in formation of the various tonal colors (49). SAD, water stress, and nitrogen and iron deficiencies were shown to cause variations in the normal visible and infrared reflectance of St. Augustine grass. Ground-based and aerial photography also demonstrated that these stress factors could be detected with color infrared film (Figs. 26,

28, 29, 36, 43, 44), (p. 75, 80, 81, 103, 131, 133). Detection of a few plant virus diseases (7, 8, 15, 17), water stress (51, 74), and iron deficiency (35) using infrared photography has also been reported.

Moderate to severe SAD symptoms could be readily detected in aerial color infrared photographs by visual inspection (Fig. 28), (p. 80) and by density slicing techniques (Fig. 29), (p. 81). Areas of sparse grass coverage or yellowed grass due to poor nutrition or drought stress had tonal signatures similar to those of infected areas. Transmission densitometer measurements were made only for areas where a disease rating could be obtained from ground survey information. Density measurements using the visible, blue, and green densitometer filters indicated that differences in visible reflectance between healthy and diseased grass had significant effects on film density (Table 1), (p. 83). Although healthy grass exhibited higher densities in the red band than diseased grass, the differences were not as large as in the other bands. This analysis revealed density differences for disease symptoms which were not detectable by visual inspection. However, since this technique was sensitive enough to detect small variations due to factors in the lawn

other than SAD, consistent detection of mild disease symptoms was not possible.

Densitometer measurements also revealed that nitrogen and iron deficiencies produced tonal signatures similar to those caused by SAD (Table 4), (p. 104). Gausman and his colleagues (35) found film densities for iron-deficient sorghum to be reduced using visible, blue, green, and red filters. Largest differences occurred with the green filter. Gardenas and Gausman (16) found that chlorophyll content of barley (Hordeum sativum (L.) Pers.) cultivars was directly related to color infrared film density using a visible or green filter.

No significant density differences were found for water-stressed grass until plants became wilted and severely stressed (49). Severe stress caused significantly smaller density values for measurements made with the green filter (Table 8), (p. 134). Smaller, but definite, reductions occurred with visible and blue filters. Measurements made with the red filter indicated a small increase over controls for all but one stressed plant.

Densitometric values varied greatly on different dates because of differences in film emulsions and

exposures. Density measurements from closeup, ground-based photographs may have been affected to some extent by shadows within the plant canopies, which were avoided as much as possible. Analysis with a scanning microdensitometer would have given much more detailed and conclusive density measurements for all of the color infrared photographs, especially aerial photos.

Color infrared photography appeared to be as efficient as multiband techniques for disease detection, and may have some advantages over multiband photography in that it requires only one camera and one film/filter combination. Information can be obtained from color infrared film by direct observation and/or densitometric analysis, whereas multiband photography requires more elaborate types of analysis. Results from color enhancement and density slicing techniques employed for multiband photography analysis are often tedious and difficult to duplicate.

Working with St. Augustine grass and St. Augustine Decline presented some unique problems concerning photographic interpretation of diseased areas. A grass turf consists of a continuous and, in most cases, a relatively uniform vegetative canopy. Diseased grass may be interspersed within this continuous canopy in

irregular patterns, so that a diseased area can consist of varying amounts of healthy and infected leaves. In addition to this, early stages of SAD are manifested as a relatively inconspicuous mottling symptom which, depending upon environmental and cultural conditions, may persist for several weeks or months.

Although PRT-5 temperature data from different dates gave variable temperature rankings for some treatments, a few general patterns remained consistent. Nitrogen-deficient plants had higher temperatures (1.5°C) than control plants (Fig. 40), (p. 117). Al-Abbas et. al. (1) have also reported that nitrogen-deficient corn leaves had 0.9°C higher temperatures than healthy leaves. Leaf temperature is dependent upon factors such as ambient air temperature, wind velocity, the plant's water status, and the amount of incident radiation (71, 79). Therefore, meaningful comparison of absolute values from different dates is difficult when dealing with uncontrolled environmental conditions. Only relative differences among treatments from any one set of measurements are meaningful. On some dates iron-deficient plants had slightly lower temperatures than control plants, but these results were variable.

In general, SAD-infected treatments were slightly warmer (0.5-0.8°C) than noninfected ones.

Temperature measurements with the PRT-5 were more sensitive to initial moisture stress stages than were visible and infrared reflectance measurements. Moderately stressed plants were 5.3-7.3°C and 1.9-2.5°C warmer than nonstressed plants in the sun and shade, respectively (Table 7), (p. 121). Severely stressed plants were 5.1-7.4°C warmer than healthy plants while in sunlight and 3.0-3.8°C warmer while in shade. Bartholic and his co-workers (9) measured temperatures of irrigated and water-stressed cotton using an aerial thermal scanner. They found a maximum difference of 6°C between watered cotton with a water potential of -13 bars and stressed cotton with a water potential of -24 bars.

Transformed divergence analysis of ERTS-band reflectance data using various 2-band combinations indicated that an 85-100% discrimination ability existed between any two of the various noninfected and infected treatments tested (Tables 5, 9), (p. 109, 139). This suggests that all of these factors could be distinguished from each other if they appeared together in the same scene. Use of more than two bands might improve dis-

crimination ability even more. If functional, this technique would have definite advantages over photographic techniques. As previously mentioned, healthy grass could be distinguished from all of the stress treatments tested using multiband or color infrared photography; however, these methods provided no discrimination among the different stress treatments. Transformed divergence analysis indicated that such problems could possibly be solved using this technique.

In conclusion, results from this study show that SAD can be detected using aerial multiband or color infrared photography. Because surveys involving commercial St. Augustine grass would involve small acreages, low altitude photography could be used in an effort to detect small areas of disease. Since most commercially grown turf grass is grown under optimum cultural conditions (proper watering, fertilization, mowing, etc.), few of the stress factors mentioned earlier would be expected to be present to complicate disease detection.

Preliminary results indicate that thermal sensing may also have some practical use in grass turf management. Tests using an aerial thermal scanner need to be performed to determine the effectiveness of temperature monitoring for detection of water stress, diseases, and nutritional deficiencies.

A classification technique based on transformed divergence analysis appears to have great potential not only for solving problems involved in this study, but for applications in many remote sensing programs involving plant pathology and related fields. This type of computerized analysis could be done using data collected by a multispectral scanner employing several spectral bands. Modern scanning devices can almost approximate the high degree of resolution achieved with photographic techniques (41), and small differences in resolution capabilities would be overshadowed by increased discrimination capabilities.

LITERATURE CITED

1. AL-ABBAS, A. H., R. BARR, J. D. HALL, F. L. CRANE, and M. F. BAUMGARDNER. 1974. Spectra of normal and nutrient-deficient maize leaves. Agron. J. 66:16-20.

2. ALLEN, L. H., and K. W. BROWN. 1965. Shortwave radiation in a corn crop. Agron. J. 57:575-580.

3. ALLEN, L. H., C. S. YOCUM, and E. R. LEMON. 1964. Photosynthesis under field conditions. VII. Radiant energy exchanges within a corn canopy and implications in water use efficiency. Agron. J. 56:253-259.

4. ALLEN, W. A., H. W. GAUSMAN, A. J. RICHARDSON, and J. R. THOMAS. 1969. Interaction of isotropic light with a compact plant leaf. J. Opt. Soc. Am. 59:1376-1379.

5. ALLEN, W. A., and A. J. RICHARDSON. 1968. Interaction of light with a plant canopy. J. Opt. Soc. Am. 58:253-259.

6. ARNON, D. I. 1949. Copper enxymes in isolated chloroplasts. Polyphenoloxidase in Beta vulgaris. Plant Phys. 24:1-15.

7. AUSMUS, BEVERLY S., and J. W. HILTY. 1971. Reflectance studies of healthy, Maize Dwarf Virus-infected, and Helminthosporium maydis-infected corn leaves. Rem. Sens. Environ. 2:77-81.

8. AUSMUS, BEVERLY S., and J. W. HILTY. 1972. Aerial detection of Maize Dwarf Mosaic-diseased corn. Phytopathology 62:1070-1074.

9. BARTHOLIC, J. F., L. N. NAMKEN, and C. L. WIEGAND. 1972. Aerial thermal scanner to determine temperatures of soils and of crop canopies differing in water stress. Agron. J. 64:603-608.

10. BAUER, M. E., P. H. SWAIN, R. P. MROCZYNSKI, P. E. ANUTA, and R. B. MACDONALD. 1971. Detection

of southern corn leaf blight by remote sensing techniques. Pages 693-699 in 7th Int. Symp. on Remote Sensing of Environment, Willow Run Laboratories, Univ. of Michigan, Ann Arbor.

11. BAWDEN, F. C. 1933. Infrared photography and plant virus diseases. Nature 132:168.

12. BILLINGS, W. D., and J. J. MORRIS. 1951. Reflectance of visible and infrared radiation from leaves. Am. J. Bot. 38:327-331.

13. BRENCHLEY, G. H., and C. V. DADD. 1962. Potato blight recording by aerial photography. N.A.A.S. Quarterly Review (London) 57:21-25.

14. BRODRICK, H. T., B. GILBERTSON, and M. H. KREITZER. 1971. Detecting avocado Phytophthora root rot. Citrus J. 449:9-13.

15. BURNS, E. E., M. J. STARZYK, and D. L. LYNCH. 1969. Detection of plant virus symptoms with infrared photography. Trans. Ill. State Acad. Sci. 62:102-105.

16. CARDENAS R., and H. W. GAUSMAN. 1973. Relation of light reflectance of six barley lines with chlorophyll assays and optical film densities. Agron. J. 65:518-519.

17. CARDENAS, R., C. E. THOMAS, and H. W. GAUSMAN. 1972. Photographic pre-visual detection of Watermelon Mosaic Virus in cucumber. J. Rio Grande Hortic. Soc. 26:73-75.

18. COFFMAN, B. 1971. Corn blight from 11 miles up. Farm J. 95:32-33.

19. COLWELL, R. N. 1956. Determining the prevalence of cereal crop disease by aerial photography. Hilgardia 26:223-286.

20. COLWELL, R. N. 1963. Basic matter and energy relationships in remote sensing. Photog. Eng. 29:761-799.

21. COULSON, K. L. 1966. Effects of reflection properties of natural surfaces in aerial reconnaissance. Appl. Opt. 5:905-917.

22. COULSON, K. L., G. M. B. BOURICIUS, and E. L. GRAY. 1965. Effects of surface reflection on radiation emerging from the top of a planetary atmosphere. General Electric Space Sciences Lab., Rep. R65D64 for Goddard Space Flight Center, NASA. 148 p.

23. DADYKIN, V. P., and V. P. BEDENKO. 1961. The connection of the optical properties of plant leaves with soil moisture. Dokl. Acad. Sci. (USSR) 134:212-214.

24. DE WITT, D., and B. ROBINSON. 1975. Exotech/ERTS-band transmissometer. LARS Information Note 052075. Lab. for Applic. of Remote Sensing, Purdue Univ., West Lafayette, Indiana. 15 p.

25. DUNCAN, W. G., R. S. LOOMIS, W. A. WILLIAMS, and R. HANAU. 1967. A model for simulating photosynthesis in plant communities. Hilgardia 38:181-205.

26. EDWARDS, G. J., and E. P. DU CHARME. 1974. Attempt at previsual diagnosis of Citrus Young Tree Decline by use of a remote sensing infrared thermometer. Plant Dis. Rep. 58:793-796.

27. EDWARDS, G. J., E. P. DU CHARME, G. G. NORMAN, and M. COHEN. 1973. Instrumentation methods and photographic techniques for detection of citrus trees affected with Young Tree Decline. Fla. State Hortic. Soc. 86:104-107.

28. EDWARDS, G. J., T. SCHEHL, E. P. DU CHARME. 1975. Multispectral sensing of Citrus Young Tree Decline. Photogram. Eng. 41:653-657.

29. GATES, D. M. 1967. Remote sensing for the biologist. Bioscience 17:303-307.

30. GATES, D. M. 1970. Physical and physiological properties of plants. Pages 224-252 in J. R. Shay, ed. Remote sensing with special

reference to agriculture and forestry. Nat. Acad. Sci., Wash., D. C. 424 p.

31. GATES, D. M., H. J. KEEGAN, J. C. SHLETER, and V. R. WEIDNER. 1965. Spectral properties of plants. Appl. Opt. 4:11-20.

32. GATES, D. M., and W. TANTRAPORN. 1952. The reflectivity of deciduous trees and herbacious plants in the infrared to 25 microns. Science 115: 613-616.

33. GAUSMAN, H. W., W. A. ALLEN, and R. CARDENAS. 1969. Reflectance of cotton leaves and their structure. Rem. Sens. Environ. 1:19-22.

34. GAUSMAN, H. W., W. A. ALLEN, and R. CARDENAS. 1970. Detection of foot rot disease of grapefruit trees with infrared color film. J. Rio Grande Hortic. Soc. 24:36-42.

35. GAUSMAN, H. W., R. CARDENAS, and A. H. GERBERMANN. 1974. Plant size, etc., and aerial films. Photogram. Eng. 40:61-67.

36. GAUSMAN, H. W., D. E. ESCOBAR, and R. R. RODRIGUEZ. 1972. Using reflectance measurements on squash plants to discriminate among nutrient deficiencies. Agron. Abstr. p. 30.

37. HILL, J. H., A. H. EPSTEIN, M. R. MCLAUGHLIN, and R. F. NYVALL. 1972. Aerial detection of Tobacco Ringspot Virus-infected soybean plants. Plant Dis. Rep. 57:471-472.

38. HOAGLAND, D. R., and D. I. ARNON. 1938. The water-culture method for growing plants without soil. Calif. Agric. Exp. Stn. Circ. 347. 39 p.

39. HOFFER, R. M., and C. J. JOHANNSEN. 1969. Ecological potentials in spectral signature analysis. Pages 1-16 in P. L. Johnson, ed. Remote sensing in ecology. Univ. of Georgia Press, Athens. 244 p.

40. HOLT, E. C., W. W. ALLEN, and M. H. FERGUSON. 1964. Turfgrass maintenance costs in Texas. Tex. Agric. Exp. Stn. Bull. B-1027. 19 p.

41. HOLTER, M. R. 1970. Imaging with nonphotographic sensors. Pages 73-163 in J. R. Shay, ed. Remote sensing with special reference to agriculture and forestry. Nat. Acad. Sci., Wash., D.C. 424 p.

42. HORN, G. C., A. E. DUDECK, and R. W. TOLER. 1973. "Floratam" St. Augustine grass. Fla. Agric. Exp. Stn. Circ. S-224. 13 p.

43. HORWITZ, W. 1975. Official Methods of Analysis, 12th ed. Assoc. Official Analyt. Chemists, Wash., D.C. p. 15 and 22.

44. HOWARD, J. A. 1966. Spectral energy relations of isobilateral leaves. Austral. J. Bot. 19: 757-766.

45. JACKSON, H. R., and V. R. WALLEN. 1975. Microdensitometer measurements of sequential aerial photographs of field beans infected with bacterial blight. Photopathology 65:961-968.

46. JACKSON, R. 1964. Detection of plant disease by infrared. J. Biolog. Photog. Assoc. 32:45-58.

47. KEEGAN, H. J., J. C. SHLETER, W. A. HALL, and GLADYS M. HAAS. 1956. Spectrophotometric and calorimetric record of diseased and rust resisting cereal crops. Nat. Bur. Stds. Rep 4591. U.S. Dep. Commerce, Wash., D.C. 128 p.

48. KLESHNIN, A. F. and I. A. SHUL'GIN. 1959. The optical properties of plant leaves. Dokl. Acad. Sci. (USSR) 125:108-110.

49. KNIPLING, E. B. 1967. Physical and physiological basis for differences in reflectance of healthy and diseased plants. Workshop on Infrared Color Photography in the Plant Sciences, Winter Haven, Fla. 24 p.

50. LEE, T. A. 1973. Isolation, purification and characterization of the virus causing St. Augustine Decline. Ph. D. Thesis, Texas A & M Univ., College Station, Texas. 64 p.

51. MANZER, F. E., and G. R. COOPER. 1967. Aerial photographic methods of potato disease detection. Main Agric. Exp. Stn. Bull. 646. 14 p.

52. MCCLELLAN, W. D., J. P. MEINER, and D. G. ORR. 1963. Spectral reflectance studies on plants. Pages 403-413 in 2nd Symp. Remote Sensing of Environment, Inst. Sci. Tech., Univ. of Michigan, Ann Arbor.

53. MCCOY, N. L., R. W. TOLER, and J. AMADOR. 1969. St. Augustine Decline (SAD)-A virus disease of St. Augustine grass. Plant Dis. Rep. 53:955-958.

54. MESTRE, H. 1935. The absorption of radiation by leaves and algae. Cold Springs Harbor Symp. Quant. Biol. 3:191-209.

55. MEYER, M. R., and L. CALPOUZOS. 1968. Detection of crop diseases. Photogram. Eng. 34:554-557.

56. MOSS, R. H., and W. E. LOOMIS. 1952. Absorption spectra of leaves. I. The visible spectrum. Plant Physiol. 27:370-391.

57. MYERS, V. I. 1970. Soil, water, and plant relations. Pages 253-283 in J. R. Shay, ed. Remote sensing with special reference to agriculture and forestry. Nat. Acad. Sci., Wash., D.C. 424 p.

58. MYERS, V. I., and W. A. ALLEN. 1968. Electrooptical remote sensing methods as nondestructive testing and measuring techniques in agriculture. Appl. Opt. 7:1819-1838.

59. MYERS, V. I., C. L. WIEGAND, M. D. HELLMAN, and J. K. THOMAS. 1966. Pages 801-813 in Proc. 4th Symp. Remote Sensing of Environment, Inst. Sci. Tech, Univ. of Michigan, Ann Arbor.

60. NORMAN, G. G., and N. L. FRITZ. 1965. Infrared photography as an indicator of disease and decline in citrus trees. Proc. Fla. State Hortic. Soc. 78:59-63.

61. RABIDEAU, G. S., C. S. FRENCH, and A. S. HOLT. 1946. The absorption and reflection spectra of leaves, chloroplast suspensions and chloroplast fragments as measured in an ultrabright sphere. Am. J. Bot. 33:769-777.

62. SAFIR, G. R., G. H. SVITS, and A. H. ELLINGBOE. 1972. Spectral reflectance and transmittance of corn leaves infected with Helminthosporium maydis. Photopathology 62:1210-1213.

63. SAKAMATO, G. M., and R. H. SHAW. 1967. Light distribution in field soybean canopies. Agron. J. 59:7-9.

64. SCHOLANDER, P. F., H. T. HAMMEL, EDDA BRADSTREET, and E. A. HEMMINGSEN. 1965. Sap pressure in vascular plants. Science 148:339-346.

65. SCOTT, D., P. H. MENALDA, and R. W. BROUGHAM. 1968. Spectral analysis of radiation transmitted and reflected by different vegetations. N. Z. J. Bot. 6:427-449.

66. SEIBERT, J. 1969. Plant disease losses and market potential of control chemicals. Pages Q1-Q3 in Proc. 1st Ann. Tex. Conf. Insect, Plant Disease, Weed, and Brush Control, Texas A & M Univ., College Station.

67. SHULL, C. A. 1929. A spectrophotometric study of reflection of light from leaf surfaces. Bot. Gazette 87:583-607.

68. SINCLAIR, T. R., M. M. SCHREIBER, and R. M. HOFFER. 1973. Diffuse reflectance hypothesis for the pathway of solar radiation through leaves. Agron. J. 65:276-283.

69. STANHILL, G., M. FUCHS, M. ROBINSON, and D. SHIMSHI. 1973. The effect of irrigation on solar reflectance from wheat crops. Pages 29-41 in The Radiative and Aerodynamic Properties of Agricultural Crops and Natural Vegetation Assoc., Final Rep. of Res.

70. SWAIN, P. H.; and R. C. KING. 1973. Two effective feature selection criteria for multispectral remote sensing. LARS Information Note 042673. Lab. for Applic. of Remote Sensing, Purdue Univ., West Lafayette, Indiana. 15 p.

71. TANNER, C. B. 1963. Plant temperatures. Agron. J. 55:210-211.

72. TAUBENHAUS, J. J., W. N. EZEKIEL, and C. B. NEBLETTE. 1929. Airplane photography in the study of cotton root rot. Phytopathology 19:1025-1029.

73. THOMAS, J. R., F. I. MYERS, M. D. HEILMAN, and C. L. WIEGAND. 1966. Factors affecting light reflectance of cotton. Pages 304-312 in 4th Symp. Remote Sensing of Environment, Inst. Sci. Tech., Univ. of Michigan, Ann Arbor.

74. THOMAS, J. R., L. N. NAMKEN, G. F. OERTHER, and R. G. BROWN. 1971. Estimating leaf water content by reflectance measurements. Agron. J. 63:845-847.

75. THOMAS, J. R., and G. F. OERTHER. 1972. Estimating nitrogen content of sweet pepper leaves by reflectance measurements. Agron J. 64:11-13.

76. THOMAS, J. R., C. L. WIEGAND, and V. I. MYERS. 1967. Reflectance of cotton leaves and relation to yield. Agron J. 59:551-554.

77. UNITED STATES DEPARTMENT OF AGRICULTURE. 1965. Losses in agriculture. U. S. Dept. Agric. Handb. 291. 120 p.

78. WEST, D. F. 1959. Aerial surveys for better crops. Crops and Soils 11:17-18.

79. WIEGAND, C. L., and L. N. NAMKEN. 1966. Influences of plant moisture stress, solar radiation, and air temperature on cotton leaf temperature. Agron. J. 58:582-586.

The REMOTE SENSING CENTER was established by authority of the Board of Directors of the Texas A&M University System on February 27, 1968. The CENTER is a consortium of four colleges of the University; Agriculture, Engineering, Geosciences, and Science. This unique organization concentrates on the development and utilization of remote sensing techniques and technology for a broad range of applications to the betterment of mankind.